東京大學

地震研究所彙報

第25號　第1~4册

昭和22年1～12月

目　次

論文及報告　頁

1. 津浪による灣水の振動（英文）……高橋龍太郎　1
2. 海底の變動に因る津浪の成生(第三報)一次元的浪源(英文)…高橋龍太郎　5
3. 地磁氣および地電流變化の關係を論ずる一方法(英文)……力武常次　9
4. 津浪の浪源について(英文)……表俊一郎　15
5. 德島縣椿泊灣の津浪(英文)……力武常次・村内必典　21
6. 筑波山に於ける土地傾斜變化の觀測(其の三)(英文)……萩原尊禮　27
7. 鹿兒島縣肝屬郡垂水町唉花平產蛍青石の產出狀態(英文)……森本良平　33
8. 地面の波狀運動に對する光學的說明の可能性(英文)……佐藤泰夫　37
9. A. W. Lee の方法による脈動の研究(英文)……岸上冬彥・池上良平　43
10. 1946年12月12日南海地震に際しての角柱轉倒の研究 英文）池上良平・岸上冬彥　49
11. 强振動計(英文)……那須信治　57
12. 地震による建物の損傷について(英文)……金井清　61
13. 有珠火山の最近の活動(I)（英文）……水上武　65
14. 有珠火山の最近の活動(II)（英文）……水上武　71
15. 1947年の能生谷村及び根知村の地辷り(英文)……佐久間修三　77
16. 津浪の局部的現象(其一)(英文)……那須信治・白井俊明　81
17. 南海道大地震前後における室戸岬の地殼變動(英文)……永田武・岡田悖　85

所　報

本彙報ハ年4回（但シ第1號ヨリ第6號マデハ不定期ニ，第7號ハ3冊トシテ發行セリ），彙報別冊ハ不定期ニ發行ス．

本彙報掲載ノ論文及ビ報告ノ内容ニ關シテハ著者ノミニ其責任アルモノトス．

本彙報ニ關スル照會通信ハ東京大學地震研究所長ヘ宛テラレタシ．

The Bulletin is published quarterly. (Vols. I-VI were published at irregular intervals and Vol. VII consisted of three parts.)
Supplementary Volume is published at irregular inteval.

The authors of the papers alone are responsible for the statements and opinions contained in their respective papers.

All communications relating to this Bulletin should be addressed to the Director of the Earthquake Research Institute, Tokyo University.

1. Motion of the Bay Water caused by Seismic Sea Waves.

By Ryutaro TAKAHASI,

Earthquake Research Institute.

(Read Dec. 17, 1946.—Received June 30, 1948.)

It is well known[1] that when a bay, of which the depth is $h(x)$, the breadth $b(x)$, the length l, is subjected to the disturbance $\zeta = f(t)$ at its mouth $x = 0$, the elevation of the sea surface $\zeta(x, t)$ in the bay is given by

$$\zeta = gb(0)h(0)\sum_{s=1}^{\infty}\left(\frac{d\chi_s}{dx}\right)_0 \frac{\chi_s}{\lambda_s}\int_0^t f(\tau)\sin\lambda_s(t-\tau)d\tau\,, \tag{1}$$

where χ_s's are normalized normal functions satisfying the equations:

$$\frac{d}{dx}\left[b(x)h(x)\frac{d\chi_s}{dx}\right]+\frac{\lambda_s^2}{g}b(x)\chi_s = 0, \tag{2}$$

$$\chi_s = 0 \qquad \text{at} \quad x = 0\,, \tag{3}$$

$$d\chi_s/dx = 0 \qquad \text{at} \quad x = l\,, \tag{4}$$

and

$$\int_0^l b(x)\chi_s^2 dx = 1\,. \tag{5}$$

In the case of a bay having a uniform depth H and breadth B, we have

$$\chi_s = \sqrt{2/Bl}\sin\left(s-\frac{1}{2}\right)\frac{\pi}{l}x\,, \qquad \lambda_s = \frac{\sqrt{gH}}{l}\left(s-\frac{1}{2}\right)\pi\,, \tag{6}$$

so that

$$\zeta = \frac{2c}{l}\sum_{s=1}^{\infty}\sin\left(s-\frac{1}{2}\right)\frac{\pi x}{l}\int_0^t f(\tau)\sin c\left(s-\frac{1}{2}\right)\frac{\pi}{l}(t-\tau)d\tau\,, \tag{7}$$

where $c = \sqrt{gH}$. Writing that $t' = ct/l$, $\tau' = c\tau/l$, we have

1) *Bull. Earthq. Res. Inst. Suppl. Vol.* 1 (1934), 182.

$$\zeta = 2\sum_{s=1}^{\infty} \sin\left(s-\frac{1}{2}\right)\frac{\pi x}{l}\int_0^{t'} f(l\tau'/c)\sin\left(s-\frac{1}{2}\right)\pi(t'-\tau')d\tau' \qquad (7')$$

$$= \frac{2}{l}\sum_{s=1}^{\infty} \sin\left(s-\frac{1}{2}\right)\frac{\pi x}{l}\int_0^{tc} f(t-\xi/c)\sin\left(s-\frac{1}{2}\right)\frac{\pi\xi}{l}d\xi\,. \qquad (7'')$$

Since we assume that $f(t)$ vanishes when $t<0$, the upper limit of the integral in (7″) may be replaced by ∞. Now devide the range of integration $0\sim\infty$ into $0\sim l$, $l\sim 2l$, $2l\sim 3l$, ... and change the variable ξ to ξ', $2l-\xi'$, $2l+\xi'$, ... respectively. Then, noting that

$$f(x) = \frac{2}{l}\sum_{s=1}^{\infty} \sin\left(s-\frac{1}{2}\right)\frac{\pi x}{l}\int_0^{l} f(\xi)\sin\left(s-\frac{1}{2}\right)\frac{\pi\xi}{l}d\xi, \qquad (8)$$

because $\sqrt{2/Bl}\sin\left(s-\frac{1}{2}\right)\pi x/l$ is a normal function, we obtain the following expression:

$$\zeta = f(t-x/c)-f(t-2l/c-x/c)+f(t-4l/c-x/c)$$
$$+f(t-2l/c+x/c)-f(t-4l/c+x/c)+ \qquad (9)$$

The same expression will be obtained more easily by the method of operational calculus. It can easily be seen from the above expression that ζ is composed of the direct wave and the waves reflected at the head and mouth of the bay. The coefficients of reflection are 1 and -1 in this case. When they are respectively α, $(-1<\alpha<0)$ at the mouth and β, $(1>\beta>0)$ at the head of the bay owing to such causes as the scattering of the energy, the friction at the bottom, etc., we have the following expression instead of (9):

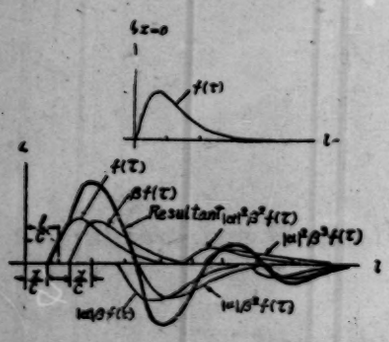

Fig. 1. $\zeta(t)$ at the mouth of the bay (above) and $\zeta(t)$ at any place in the bay (below), which is composed of the direct wave and reflected waves.

$$\zeta = \sum_{n=0}^{\infty} \alpha^n\beta^n[f(t-2nl/c-x/c)$$
$$+\beta f(t-2\overline{n+1}\,l/c+x/c)] \quad (10)$$

It can be seen from (10) that in the bay there develop oscillations of the period $4l/c$ and their harmonics of odd orders, irrespective of the shape of $f(t)$.

It will be worthy of notice that from (10) we can deduce the following important relations:

$$\Phi(t)\equiv\zeta(t)-\alpha\beta\zeta(t-2l/c)\equiv f(t-x/c)+\beta f(t-2l/c+x/c), \tag{11}$$

and

$$f(t)=\sum_{n=0}^{\infty}(-1)^n\beta^n\Phi(t-2n\overline{l-x}/c+x/c). \tag{12}$$

By means of this expression, we can calculate the original shape of the seismic sea waves from the observation made at any point in the bay, provided that α and β are known. In most cases β is nearly equal to unity. As for α, it depends on the shape of the bay, but we can estimate it from the period-amplitude diagram of the record of the seismic sea waves. Assuming, for the sake of simplicity, that $\beta=1$, $x=l$, and $f=e^{ipt}$, we have

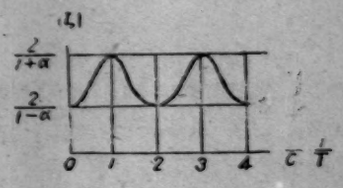

Fig. 2. Theoretical period-amplitude diagram, from which α may be estimated.

$$|\zeta|=2/\sqrt{(1-\alpha)^2\cos^2 pl/c+(1+\alpha)^2\sin^2 pl/c}\,, \tag{13}$$

so that the ratio $|\zeta|_{\max}/|\zeta|_{\min.}$ is equal to $(1-\alpha)/(1+\alpha)$.

2. On Seismic Sea Waves caused by Deformations of the Sea Bottom. The 3rd Report. The One-dimensional Source.

By Ryutaro TAKAHASI,

Earthquake Research Institute.

(Read Mar. 18, 1947.—Received June 30, 1948.)

Travel-times of the seismic sea waves, observed at various tide guage stations in the case of the Nankai Earthquake on Dec. 21, 1946, suggest a belt-like source elongated in the direction EW. The present paper deals with the seismic sea waves that will be generated from such an elongated source as can be regarded one-dimensional. As in the previous papers[1], we take the origin of the coordinates at the undisturbed sea surface, x-axis horizontally and z-axis vertically downwards. The depression of the sea surface ζ and the velocity of depression of the sea bottom η are assumed to be functions of x and t only. Denoting by ϕ the velocity potential, we have

$$\frac{\partial^2\phi}{\partial x^2}+\frac{\partial^2\phi}{\partial z^2}=0, \tag{1}$$

and

$$\left[\frac{\partial\phi}{\partial t}+2\mu\phi\right]_{z=\zeta}=g\zeta, \tag{2}$$

where μ is the coefficient of fictitious viscosity. As the boundary condition, we have at the sea bottom, where $z=H$,

$$\left(\frac{\partial\phi}{\partial z}\right)_{z=H}=\eta(x,t)\equiv f(x)\cdot\chi(t), \tag{3}$$

where $\eta(x,t)$ is assumed to be separable into space and time factors. From these expressions we can easily obtain the formal solution as follows:

$$\zeta=\frac{1}{4\pi^2}\int_{-\infty}^{\infty}d\alpha\int_{-\infty}^{\infty}\chi(\tau)e^{i\alpha(t-\tau)}d\tau\int_{-\infty}^{\infty}Gdk\int_{-\infty}^{\infty}f(\lambda)e^{ik(x-\lambda)}d\lambda, \tag{4}$$

1) *Bull. Earthq. Res. Inst.*, **20** (1943), 375; **23** (1946), 23.

where

$$G = -(\alpha i+2\mu)/[(\alpha^2-2\mu\alpha i)\cosh kH-gk\sinh kH]. \tag{5}$$

The change of order of the integration being allowed, we integrate first with respect to α. Since G has poles at $\alpha = i\mu \pm \gamma$, we get, just in the same way as in the lst paper,

$$\left.\begin{aligned}\int_{-\infty}^{\infty} G e^{i\alpha(t-\tau)}d\alpha &= 2\pi[\mu\sin\gamma(t-\tau)+\gamma\cos\gamma(t-\tau)]e^{-\mu(t-\tau)}/\gamma\cosh kH \\ &\qquad \text{if} \quad (t-\tau)>0, \\ &= 0 \qquad \text{if} \quad (t-\tau)<0,\end{aligned}\right\} \tag{6}$$

where

$$\gamma = \sqrt{gk\tanh kH-\mu^2}\,. \tag{7}$$

Therefore in the limit of $\mu \to 0$, we have

$$\zeta = \frac{1}{2\pi}\int_{-\infty}^{\infty}\frac{dk}{\gamma\cosh kH}\int_{-\infty}^{t}\chi(\tau)\gamma\cos\gamma(t-\tau)d\tau\int_{-\infty}^{\infty}f(\lambda)e^{ik(x-\lambda)}d\lambda \tag{8}$$

Next we will execute the integration with respect to τ. We assume that

$$\left.\begin{aligned}\chi(t) &= 0 \qquad t<0, \quad t>T, \\ &= 1/T \qquad 0<t<T,\end{aligned}\right\} \tag{9}$$

that is, the deformation of the sea bottom is assumed to grow uniformly and simultaneously at each point and attain to the final amount $f(x)$ at $t = T$. We have then

$$\left.\begin{aligned}\int_{-\infty}^{t}\chi(\tau)\gamma\cos\gamma(t-\tau)d\tau &= -\frac{1}{T}\sin\gamma(t-\tau)\Big|_0^T \quad \text{if} \quad t>T\,, \\ &= -\frac{1}{T}\sin\gamma(t-\tau)\Big|_0^T \quad \text{if} \quad t<T\,.\end{aligned}\right\} \tag{10}$$

Therefore, if we write

$$\xi(t) \equiv \frac{1}{2\pi}\int_{-\infty}^{\infty}\frac{\sin\gamma t}{\gamma\cosh kH}dk\int_{-\infty}^{\infty}f(\lambda)e^{ik(x-\lambda)}d\lambda \tag{11}$$

we have simply

$$\left.\begin{aligned}\zeta &= [\xi(t)-\xi(t-T)]/T \qquad t>T \\ &= [\xi(t)-\xi(0)]/T \qquad t<T\end{aligned}\right\} \tag{12}$$

Therefore we can put with $\xi(t)$ in place of ζ. In the case of $T \to 0$, that is, when the deformation occur instantaneously, we have obviously $\zeta = \partial\xi/\partial t$.

Now changing variables from k, λ, x, H to m, s, ρ, h, by the relations

$$m = ka, \quad \lambda = sa, \quad x = \rho a, \quad H = ha \tag{13}$$

where a is a parameter expressing the width of the deformed area, we have

$$\xi(t) = \frac{1}{2\pi}\int_{-\infty}^{\infty} \frac{\sin \gamma t}{\gamma \cosh mh} dm \int_{-\infty}^{\infty} f(s) e^{im(\rho - s)} ds \tag{14}$$

$$\gamma = \sqrt{(gm \tanh mh)/a} \tag{15}$$

In most cases of seismic sea waves, deformed area measures several hundred km in width, whereas the sea is only a few km deep, so we have $h \ll 1$. In such cases, $\gamma \fallingdotseq mc/a$, $c = \sqrt{gH}$; then we obtain

$$\xi(t) = \frac{a}{2\pi c}\int_{-\infty}^{\infty} \sin m\frac{ct}{a} e^{im(\rho - s)} \frac{dm}{m} \int_{-\infty}^{\infty} f(s) ds \tag{16}$$

$$= \frac{a}{2c}\int_{\rho - ct/a}^{\rho + ct/a} f(s) ds, \tag{17}$$

in virtue of the integral formula:

$$\left.\begin{aligned} \frac{1}{\pi}\int_{-\infty}^{\infty} \sin \rho x \cdot e^{i\sigma x} \frac{dx}{x} &= 0 \qquad |\sigma/\rho| > 1 \\ &= 1 \qquad |\sigma/\rho| < 1. \end{aligned}\right\} \tag{18}$$

By means of (17), $\xi(t)$ can be calculated easily for any $f(x)$. In the case of $T \to 0$, since $\zeta = \partial\xi/\partial t$, we have

$$\zeta(t) = \frac{1}{2} f(\rho + ct/a) + \frac{1}{2} f(\rho - ct/a). \tag{19}$$

In the case when T is finite, we can obtain $\zeta(t)$ from (12).

Now if

$$f(s) = 0 \quad \text{when} \quad s > 1 \quad \text{or} \quad s < -1, \tag{20}$$

we have from (17)

when $\rho > 1$, $\xi(t) = \dfrac{a}{2c}\int_{-1}^{1} f(s)ds$ if $ct/a > (\rho+1)$,

$= \dfrac{a}{2c}\int_{\rho-ct/a}^{1} f(s)ds$ if $(\rho+1) > ct/a > (\rho-1)$,

$= 0$ if $ct/a < (\rho-1)$,

and when

$1 > \rho > 0$, $\xi(t) = \dfrac{a}{2c}\int_{-1}^{1} f(s)ds$ if $ct/a > (\rho+1)$,

$= \dfrac{a}{2c}\int_{\rho-ct/a}^{1} f(s)ds$ if $(\rho+1) > ct/a > (1-\rho)$,

$= \dfrac{a}{2c}\int_{\rho-ct/a}^{\rho+ct/a} f(s)ds$ if $ct/a < (1-\rho)$.

ρ can be considered positive without loss of generality. As examples, wave forms for the two cases:

a) $f(s) = L$ $|s| < 1$, $f(s) = 0$ $|s| > 1$, $T = a/2c$;

b) $f(s) = L\sin \pi s$ $|s| < 1$, $f(s) = 0$ $|s| > 1$, $T = a/2c$;

are shown in Figs. 1. and 2.

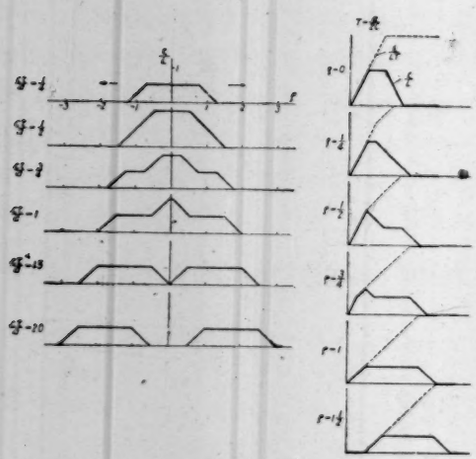

Fig. 1. Shape of seismic sea waves when the deformation is $f(\rho) = L$, $|\rho| < 1$.

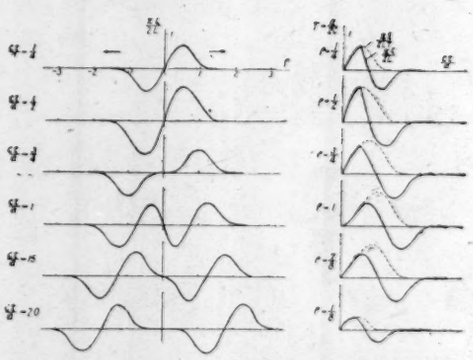

Fig. 2. Shape of seismic sea waves when the deformation is $f(\rho) = L\sin \pi\rho$, $|\rho| < 1$.

3. *A Method for Studying the Relations between the Changes in Geomagnetism and Earth Current.*

By Tsuneji RIKITAKE,

Earthquake Research Institute.

(Read Mar. 16, 1948.—Received June 20, 1948.)

It was often reported that anomalous changes in earth current occured before earthquakes sometimes. As is well known, however, changes in earth current are in the main caused by changes in the earth's magnetic field originated outside the earth. Consequently, it is difficult to abstract change only related to the earthquake itself. Hence, it is desirable to eliminate changes due to those of geomagnetic field of external origin. T. Yosimatu[1] proposed the "Difference method". He measured earth potential with two systems having respectively long and short electrode-distances. Subtracting, then, the values multiplied by a suitable constant from the other values, he assumed that the changes of large scale were approximately eliminated leaving only local or regional changes. According to him, the changes thus observed have some relations to earthquake occurrences.

Meanwhile, the writer[2] studied a method for discussing the relations between geomagnetic field and earth current in the case of periodic variation. That method will be extended to the case of non-periodic variation in this paper intending to apply to the elimination of the geomagnetic effects of external origin.

When we neglect displacement current, electric and magnetic quantities in earth are connected by the relation

$$\mathrm{rot}\,\vec{H} = 4\pi\vec{i}, \tag{1}$$

$$\mathrm{rot}\,\vec{E} = -\frac{\partial\vec{B}}{\partial t}, \tag{2}$$

where $\vec{H}$, $\vec{B}$, $\vec{E}$, and $\vec{i}$ denote respectively magnetic field, magnetic induc-

1) T. Yosimatu, *Journ. Meteorol. Soc. Japan* **15** (1937), 145.
2) T. Rikitake, *Bull Earthq. Res. Inst.* **24** (1946), 1.

tion, electric field and electric current-density. Between these quantities we have the next relations

$$\vec{i} = (\sigma)\vec{E}^{3)}, \tag{3}$$

$$\vec{B} = (\mu)\vec{H}, \tag{4}$$

and

$$\operatorname{div}\vec{B} = 0, \tag{5}$$

where σ and μ denote respectively electrical conductivity and magnetic permeability which are in general tensor quantities. From (1) and (3) we have

$$E = \frac{(\rho)}{4\pi}\operatorname{rot}\vec{H} \tag{6}$$

where ρ denotes electrical resistivity being defined by $(\sigma)(\rho) = 1$. Substituting (6) and (4) in (2), we obtain

$$\operatorname{rot}\{(\rho)\operatorname{rot}\vec{H}\} = -4\pi(\mu)p\vec{H} \tag{7}$$

where we write p in place of $\partial/\partial t$. When one of the principal axes of ρ and μ coincides with z-axis that is perpendicular to the earth's surface, the components of the direction of the principal axes satisfy[4)]

$$\left.\begin{aligned} \frac{d^2H_x}{dz^2} &= \frac{4\pi\mu_{xx}p}{\rho_{yy}}H_x, \\ \frac{d^2H_y}{dz^2} &= \frac{4\pi\mu_{yy}p}{\rho_{xx}}H_y, \\ pH_z &= 0, \end{aligned}\right\} \tag{8}$$

where it is assumed that the magnetic field depends only on z. Thus solving (8), we have

$$\left.\begin{aligned} H_x(t) &= H_{ox}(t)e^{-\sqrt{\frac{4\pi\mu_{xx}p}{\rho_{yy}}}z}, \\ H_y(t) &= H_{oy}(t)e^{-\sqrt{\frac{4\pi\mu_{yy}p}{\rho_{xx}}}z}, \end{aligned}\right\} \tag{9}$$

where $\vec{H}_0$ is the magnetic field at the surface $z = 0$.

As to the electric field, we have from (6) and (9)

3) ( ) denotes tensor quantity.

4) It is assumed that the principal axes of ρ and μ are the same

$$\left.\begin{aligned} E_x(t) &= \sqrt{\frac{\rho_{xx}\mu_{yy}p}{4\pi}}e^{-\sqrt{\frac{4\pi\mu_{yy}p}{\rho_{xx}}}z}H_{oy}(t)\,, \\ E_y(t) &= -\sqrt{\frac{\rho_{yy}\mu_{xx}p}{4\pi}}e^{-\sqrt{\frac{4\pi\mu_{xx}p}{\rho_{yy}}}z}H_{ox}(t)\,. \end{aligned}\right\} \tag{10}$$

Solving these operational equations, we obtain

$$\left.\begin{aligned} E_x(t) &= \frac{d}{dt}\int_0^t H_{oy}(t-u)h_x(u)du\,, \\ E_y(t) &= -\frac{d}{dt}\int_0^t H_{oy}(t-u)h_y(u)du\,, \end{aligned}\right\} \tag{11}$$

where
$$h(t) = \frac{\sqrt{\rho\mu}}{2\pi}t^{-\frac{1}{2}}\,e^{-\frac{\pi\mu z^2}{\rho t}}\,. \tag{12}$$

Thus we can obtain the changes in earth potential due to those of the eaath's magnetic field at the surface expressed by $\vec{H}=0$ $(t<0)$ and $\vec{H}=\vec{H}o\,(t)$ $(t>0)$.

In order to get the expression for $z=0$, we divide the integration into two parts, say $\int_0^\delta$ and $\int_\delta^t$, where δ is so small that the rate of the change in the magnetic field can be regarded as constant during the interval $0\sim\delta$. Hence it becomes

$$\begin{aligned} &\frac{d}{dt}\int_0^\delta H_{oy}(t-u)h_x(u)du \\ &\quad= H'_{oy}(t)\int_0^\delta h_x(u)du \\ &\quad= H'_{oy}(t)\sqrt{\frac{\rho_{xx}\mu_{yy}}{\pi}}a_x\int_{a_x/\sqrt{\delta}}^\infty (e^{-v^2}/v^2)dv \\ &\quad= H'_{oy}(t)\frac{\sqrt{\rho_{xx}\mu_{yy}}}{\pi}\left\{\sqrt{\delta}\,e^{-a_x^2/\delta}-2a_x\int_{a_x/\sqrt{\delta}}^\infty e^{-v^2}dv\right\} \end{aligned}$$

where

$$a_x^{\,2} = \frac{\pi\mu_{yy}z^2}{\rho_{xx}}\,.$$

Thus making $z \to 0$, we have

$$\lim_{z\to 0}\frac{d}{dt}\int_0^{\delta} H_{oy}(t-u)h_x(u)du = \frac{\sqrt{\rho_{xx}\mu_{yy}}}{\pi}\sqrt{\delta}\,H'_{oy}(t),$$

$$\lim_{z\to 0}\frac{d}{dt}\int_{\delta}^{t} H_{oy}(t-u)h_x(u) = \lim_{z\to 0}\int_{\delta}^{t} H'_{oy}(t-u)h_x(u)du$$

$$= \frac{\sqrt{\rho_{xx}\mu_{yy}}}{2\pi}\int_{\delta}^{t} H'_{oy}(t-u)u^{-\frac{1}{2}}du\,.$$

Hence it becomes

$$\left.\begin{aligned} E_{ox} &= \frac{\sqrt{\rho_{xx}\mu_{yy}}}{2\pi}\left\{2\sqrt{\delta}\,H'_{oy}(t)+\int_{\delta}^{t} H'_{oy}(t-u)u^{-\frac{1}{2}}du\right\} = \frac{\sqrt{\rho_{xx}\mu_{yy}}}{2\pi}F_{ox}(t)\,. \\ \text{In a similar way, we have} & \\ E_{oy} &= -\frac{\sqrt{\rho_{yy}\mu_{xx}}}{2\pi}\left\{2\sqrt{\delta}\,H'_{ox}(t)+\int_{\delta}^{t} H'_{ox}(t-u)u^{-\frac{1}{2}}du\right\} = -\frac{\sqrt{\rho_{yy}\mu_{xx}}}{2\pi}F_{oy}(t)\,. \end{aligned}\right\} \quad (13)$$

Since the components which is parallel to the principal axes are obtained, we can calculate the components of any direction. For instance, the ξ- and η- components shown in Fig. 1 are calculated abbreviating the process of calculation. We have

$$\left.\begin{aligned} E_{o\xi} &= (P\cos 2\alpha+Q)F_{o\xi}-P\sin 2\alpha F_{o\eta}\,, \\ E_{o\eta} &= -P\sin 2\alpha F_{o\xi}+(P\cos 2\alpha-Q)F_{o\eta}, \\ \text{where}\quad P &= \frac{\sqrt{\rho_{xx}}+\sqrt{\rho_{yy}}}{4\pi}\,,\quad Q = \frac{\sqrt{\rho_{xx}}-\sqrt{\rho_{yy}}}{4\pi}\,. \end{aligned}\right\} \quad (14)$$

and μ is assumed to be unity in electromagnetic unit.

As the magnetic field at the surface produced by the electric current flowing in the earth crust are in general very small[5], $E_{o\xi}$ and $E_{o\eta}$

5) If we consider a current sheet in which the electric currents flow uniformly in one direction, the magnetic field produced by these currents are given by $H = 2\pi i$. Corresponding to to $H = 1\gamma$, i amounts to $1{\cdot}6\times10^{-3}$ amp. If the thikness of the sheet is assumed to be 10 km, the current-density becomes $1{\cdot}6\times10^{-9}$ amp. When we take 10 kilo-ohms as the value of the electrical resistivity, the electric field amounts to 1·6 v/km. Such a large variation is scarecely observed in earth potential. Thus we may say that the changes in the electric currents flowing in the earth crust are not parctically detected by the magnetic observation though it can be measured by the earth potential observation.

deduced from $H_{o\xi}$ and $H_{o\eta}$ can be regarded as the induced field by the changes in the external magnetic field. From this point of view, the differences between the observed earth potential and calculated

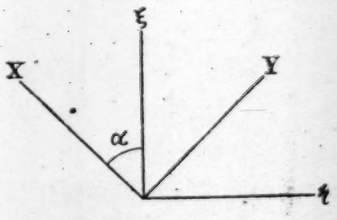

Fig. 1.

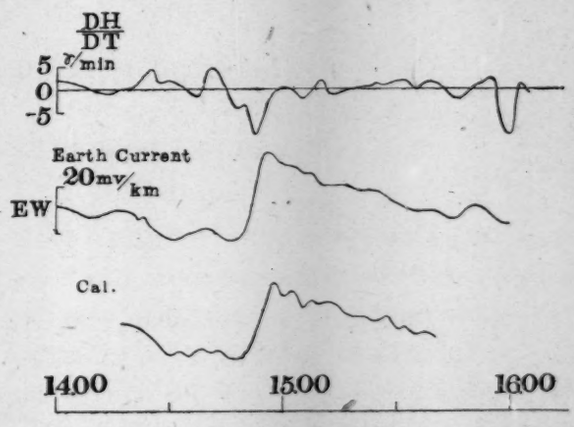

Fig. 2. An example of calculation. The calculated earth potential is shown in arbitrary scale.

one will give, if exist, anomalous changes due to electro-motive forces originated in the earth crust. Thus it is desirable to apply this method to changes which seem to relate to earthquakes

In order to show how well the observed and calculated earth potential coincide each other, for example, the change in earth current are calculated from the rate of changes in the earth's magnetic field measured at the time of solar eclipse Jun. 19, 1936 on the basis of the data obtained at Toyohara Magnetic Observatory where, according to H. Hatakeyama[6], anisotropy in the conductivity is comparatively small. Using the readings of every 2.5 min., the integrals are numerically calculated by means of Simpson's method. As shown in Fig. 2, the observed earth potential agrees well with the calculated one in their shapes.

The writer hopes that observations of earth potential and variability in the earth's magnetic field are both carried out in connection with earthquake occurrences. Applying, then, the method mentioned above, it may be expected to get some conclusions about occurrences of anomalous changes in earth current related to earthquakes.

---

6) H. Hatakeyama, *Jonrn. Meteorol. Soc. Japan*, **17** (1939), 209.

4. *On the Central Area of Seismic Sea Waves.*

By Syun'itiro OMOTE,

Earthquake Research Institute.

(Read Mar. 15, 1948.—Received June 20, 1948.)

To determine the central area of tsunami, or earthquake sea waves, on the basis of the data obtained from mareographic records, was the object of Dr. Miyabe's[1] interesting study, the first of its kind ever to be made, at the time of the Sanriku Earthquake of Mar. 3, 1933.

The great earthquake that took place on December 21, 1946, was also accompanied by violent tsunami waves, and the disturbance of the sea-water left good records at various mareograph stations in Japan. These records have been collected by the present writer and reproduced here in Fig. 1. From these records it was easy to find out the lengths of time that had elapsed between the commencement of the earthquake motions and the arrival of the tsunami waves at the respective stations. The lengths of time needed by tsunami waves to reach the stations are shown in Table 1. The average errors that might be involved in them will be about ± 5 minutes at the maximum. Five of these mareograms may be understood to contain also the records of the disturbance of sea-waters due to the earthquake motions. The probable errors of travel times measured at these stations do not exceed ± 2 minutes.

Table I.

	Station	I wave h m	II wave h m	II–I m		Station	I wave h m	II wave h m	II–I m
A	Hosozima	4 56	5 20	24	F	Matsusaka	5 30	5 56	26
B	Uwazima	5 02	5 31	29	G	Uchiura	5 00	5 20	20
C	Osaka	6 20	6 45	25	H	Ito	5 05	5 28	23
D	Sakai	5 53	6 15	22	I	Tokyo	6 20	—	—
E	Shimozu	4 50	5 15	21	J	Choshi	6 05	6 20	15

Now, taking each station as an imaginary wave source, and assuming that the tsunami waves started from this point into the offing with

the propagation velocity of a long wave, we can draw the curve of the imaginary wave front after the lapse of time that is equal to the observed travel time needed by the actual waves to reach each station. The curves drawn in this way, pertaining to the various stations, are shown with short lines in Fig. 2. The area bounded by them may be taken as the origin, or the central area, of the tsumani waves. The boundary curve of this area is referred to as C—I. The linear dimension of C—I is about 300 km.

Now, if we concentrate our attention to the initial part of the tsunami records, we notice that the tsunami begins with rather small up and down motions, which soon after are followed by large waves with a long period. We will call this latter wave the Second Wave (Wave II for short) and distinguish it from the wave that arrives at the station earliest, which will be called the First Wave (Wave I).

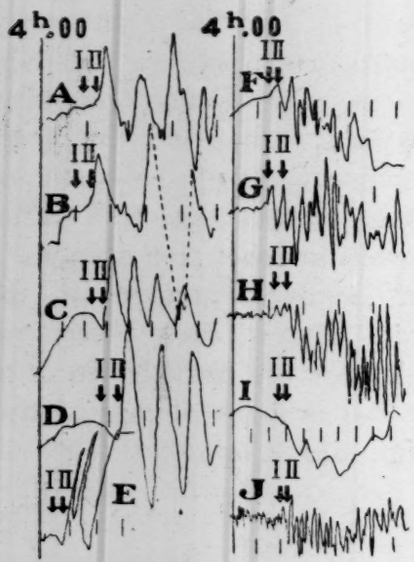

Fig. 1. Mareograms of the Nankai Earthquake of 1946.

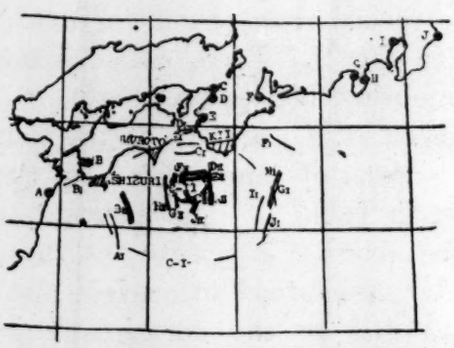

Fig. 2. Central area of the Nankai Tsunami. Letters attached to each curves are correspond to the respective station from which they were imagined to have started. Saffixes I and II represent respectively the I and II waves.

Glancing at Fig. 1, we notice that the two types of waves, I and II, are distinctly observed in most of the records. When, however, the commencement of Wave II was not clear, the following methods were taken. We first read out from the records the oscillation period of the large Second Waves and determined the time of the first maximum. Then we took a point at half the length of the period of Wave II backward from this first maximum, and decided this to be the time of the commencement of Wave II. The commencement of wave II in each

record is shown in Fig. 1, and its travel times tabulated in Table I. The imaginary fronts of Wave II pertaining to the respective stations are shown with heavy curves in Fig. 2. Though these wave fronts intersect each other, it is possible to think of the area that is enclosed by them. The outermost margins of this area are bounded by a heavy dotted line marked C—II.

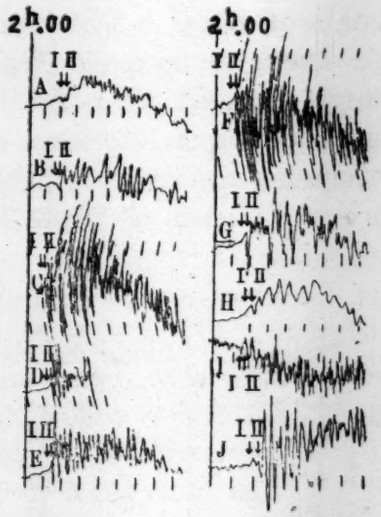

Fig. 3. The mareograms of the Sanriku Tsunami of 1933.

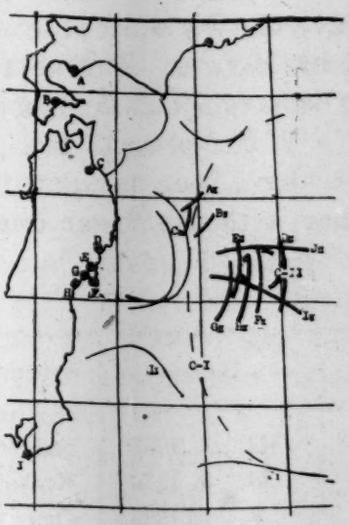

Fig. 4. The central area of the Sanriku Tsunami.

As the second example we will take up the Sanriku Tsunami[2] of 1933. The central area of this Tsunami with respect to Wave I was thoroughly studied by Dr. Miyabe, the result of which study is reproduced

Table II.

	Station	I wave h m	II wave h m	II–I m		Station	I wave h m	II wave h m	II–I m
A	Muroran	3 55	4 11	21	F	Ayukawa	3 05	3 15	10
B	Hakodate	3 48	4 04	16	G	Ishinomaki	3 40	3 45	5
C	Hachinohe	3 08	3 31	23	H	Shiogama	3 38	3 45	7
D	Kesenuma	3 39	3 50	11	I	Mera	3 21	3 34	13
D	Tsukihama	3 24	3 30	6	J	Chichizima	3 54	4 15	21

here in Figs. 3 and 4. In the mareographic records in Fig. 3, we were able to distinguish the two types of waves, I and II, in the same manner as we did in the case of the Nankai Earthquake.

On the other hand, as Dr. Miyabe had already pointed out in his paper, in some mareographic records one could observe a smaller movement of the sea water lasting for some time before the conspicuous rise or fall of the water began. Our Wave I seems to agree with Dr. Miyabe's smaller movement occurring first, and Wave II with the conspicuous rise or fall that follows. The travel times of these waves are shown in Table 2.

The heavy curves in Fig. 4 represent the wave fronts with respect to Wave II, worked out from the wave fronts of Wave I that had been given by Miyabe. The area enclosed by the heavy curves of Wave II fronts is very small compared with the central area of Wave I.

Up to the present time, the central areas of Wave I of five earthquakes[3] have been calculated. The five earthquakes are listed in Table III, together with the linear dimensions of the central areas of Wave I.

Table III.

No	Date	Epicentral region	R: Radius of felt area	Linear dimension of central area.
1	III, 3, 1933	Sanriku	920	600
2	XI, 3, 1936	Kinkazan	440	90
3	V, 1, 1939	Oga	410	50
4	VIII, 2, 1941	Kamuizaki	495	210
5	XII, 7, 1944	Tōnankai	570	130
6	XII, 21, 1946	Nankai	760	350

The relation between the linear dimensions of the central areas of tsunami waves and the radii of the felt areas of the respective earthquakes is given in Fig. 5. The magnitude of an earthquake will be represented by the linear function of the radius of its felt area, and so it may also be safely concluded that the greater the earthquake is, the greater is central area of tsunami waves too.

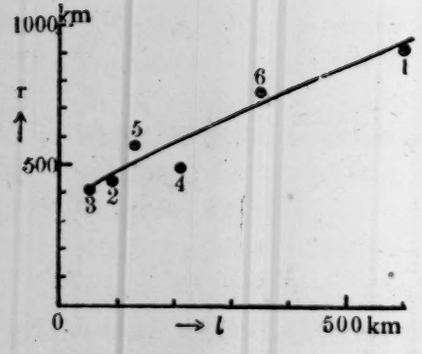

Fig. 5. l; length of the central area. r; radius of felt area.

The Nankai Earthquake was accompanied by a marked upheaval of land[4] at the southern parts of Muroto, Ashizuri and Kii Peninsulas shown as hatched areas in Fig. 1. We at once notice that the marginal lines

of this upheaved areas are located so near the C—I curve marking the boundary of the central areas of tsunami. In the case of the Tonanki earthquake of 1946, the crustal deformations were not so conspicuous, but still some evidence of such deformation was clearly discernible[5], and again the C—I curve was so near the shore lines. This seems to indicate that the central area determined from Wave I represents the area within which the crustal deformations have taken place.

Secondly, let us examine the area encircled by the curve C—II, which is the original area of Wave II. The data here collected are not numerous enough to enable one to draw any definite conclusion, but it can be surmised that this area represents the place where the discontinuities of the earth's surface happened at the ocean bed.

Conclusion.

In this paper we distinguished two types of waves, I and II, in the initial part of mareographic records, and concluded that they came from different origins. The central area responsible for Wave I has a linear dimension of several hundred kilometers, and is supposed to be the region within which the crustal deformations have taken place. Wave I of the tsunami records is supposed to have emanated from the marginal zones of the deformed area. On the other hand, the central area responsible for Wave II has a linear dimension of only 10 km or so, and it may be concluded that some actual discontinuity, such as a fault, which has taken place on the crustal surface of the sea-bottom, has sent out waves of large enery, which then are recognized as Wave II in mareographic records.

---

1) N. MIYABE, *Bull. Earthq. Res. Inst. Suppl.* Vol. I (1934), 112.
2) *Bull. Earthq. Res. Inst. Supple.* Vol. I, Part 2, 7.
3) N. MIYABE, *loc. cit.*, 1), 114.
N. MIYABE, *Bull. Earthq. Res. Inst.*, **15** (1930), 837.
F. KISHINOUYE and IIDA; *Bull. Earthq. Res. Inst.*, **17** (1939), 733.
N. MIYABE, *Bull. Earthq. Res. Inst.*, **19** (1941), 104.
S. OMOTE, *Bull. Earthq. Res. Inst.*, **24** (1946), 31.
4) T. NAGATA, *Bull. Earthq Res. Inst.*, **25** (1947).
5) OMOTE, *loc. cit.*, 3), 47.

5. *Tsunami in Tsubaki-tomari Bay.*

By Tsuneji RIKITAKE and Sadanori MURAUCHI,

Earthquake Research Institute.

(Read Jun. 17, 1947.—Received Jun. 20, 1948.)

The aspects of the tsunami acommpanied by the Nankai Earthquake of Dec. 21, 1946, were investigated in great detail by the members of the Institute. Among these investigations, the writers visited the eastern coast of Shikoku-Island with special interest to the mode of intrusion of sea-water in a bay. They measured the maximum heights attained by the tsunami in various parts of Tsubaki-tomari Bay, that is situated in the most eastern part of Tokushima prefecture, adjacent Cape Gamoda. As is shown in Fig. 1, the distance between the mouth and the head of bay amounts to about 4 km, while the depth increases almost linearly with distance from the head amounting to about 25 m at the mouth. The maximum heights from the sea level at the time of the tsunami were obtained with the aid of the tide-prediction at Muroto[1], the most southeastern part of Shikoku-Island. They are also indicated in Fig. 1.

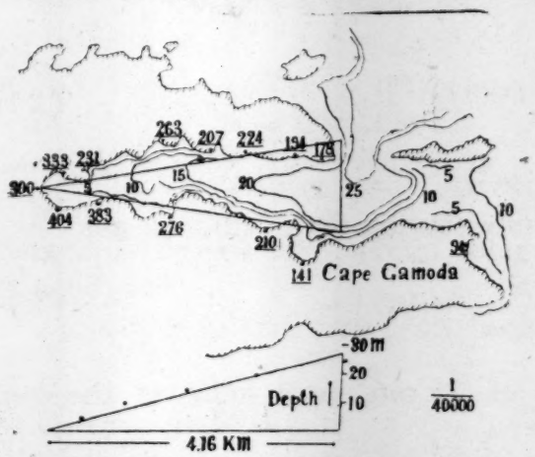

Fig. 1. Topography of Tsubaki-tomari Bay. (The maximum heights attained by the tsunami are shown by underlined numerals. Unit: cm.)

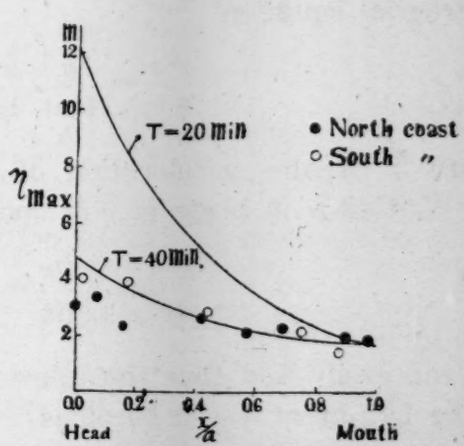

Fig. 2. The distribution of the maximum heights along the shores. The curves show the distribution expected from the theory mentioned later.

In Fig. 2, plotting these values against the distance measured along the shores, they could obviously see that the heights increase with

1) The prediction was made by Prof. H. Kawasumi.

distance from the mouth as was observed in some bays in the cases of the Sanriku Tsunami, 1933[2], and also in the present one[3].

When the tsunami-waves arrive at the mouth of a bay, the free oscillations with certain periods will be set up in the bay. The closer the period of the tsunami-waves to that of the free oscillation of the bay, the larger become the amplitude of it. Thus it is of interest to study to what extent the free oscillation may be excited in a bay.

G. Nishimura, K. Kanai and T. Takayama[4,5], discussed the motion of sea-water in a rectangular bay with uniform depth by means of Stokes' method. In this paper, the writers estimate, by means of opertional method, the oscillation of water in a bay whose breadth and depth vary linearly from its mouth to head with application to the tsunami in Tsubaki-tomari Bay just mentioned.

As is shown in Fig. 1, assuming that this bay can be replaced by an idealized bay whose breadth b and depth h vary respectively

$$b = b_0 x/a \quad \text{and} \quad h = h_0 x/a\,, \tag{1}$$

where x, b_0, h_0 and a denoted respectively the distance measured along the central line of the bay, breadth and depth at the mouth and the length of the bay. As is well known in the theory of wave-motion in a canal of variable section, the elevation of surface η satisfies the next differential equation

$$\frac{\partial^2\eta}{\partial t^2} = \frac{g}{b(x)}\frac{\partial}{\partial x}\left\{b(x)h(x)\frac{\partial\eta}{\partial x}\right\}, \tag{2}$$

where g denotes acceleration of gravity.

Writing p in place of $\partial/\partial t$ and substituting (1) in (2), we get

$$\frac{d^2\eta}{dx^2}+\frac{2}{x}\frac{d\eta}{dx}-\frac{ap^2}{gh_0}\frac{\eta}{x^2}=0\,. \tag{3}$$

We can easily find that the solution of (2) remaining finite at the head of the bay or at $x = 0$ becomes

$$\eta = \frac{A}{p\sqrt{\dfrac{ax}{gh_0}}}I_1\left(2p\sqrt{\frac{ax}{gh_0}}\right), \tag{4}$$

---

2) *Bull. Earthq. Res. Inst. Suppl. Vol.*, **1**, Part 2 (1934), 9.
3) *Special Bull. Earthq. Res. Inst.*, No. **5** (1947), 98.
4) G. Nishimura and K. Kanai, *Bull. Earthq. Res. Inst. Suppl. Vol.*, **1**, Part 1 (1934), 182.
5) G. Nishimura, K. Kanai and T. Takayama, *Bull. Earthq. Res. Inst.*, **13** (1935), 64.

where I_1 denotes modified Bessel function of the first order. A is determined by the boundary condition at the mouth of the bay or at $x = a$ as follows.

If we assume that $\eta = 0$ for $t < 0$

$$\eta = C \sin \omega t \quad \text{for} \quad t < 0 \tag{5}$$

at $x = a$, it becomes

$$A = \frac{p\sqrt{\frac{a^2}{gh_0}}}{I_1\left(2p\sqrt{\frac{a^2}{gh_0}}\right)} \frac{C\omega p}{\omega^2 + p^2}, \tag{6}$$

considering that the operational form of (5) is expressed by $\frac{C\omega p}{\omega^2 + p^2}$.

From (4) and (6), we get

$$\eta = \sqrt{\frac{a}{x}} \frac{I_1\left(2p\sqrt{\frac{ax}{gh_0}}\right)}{I_1\left(2p\sqrt{\frac{a^2}{gh_0}}\right)} \frac{C\omega p}{\omega^2 + p^2}. \tag{7}$$

Solving this operational equation, η becomes

$$\eta = \frac{\omega C}{2\pi i} \int_L e^{\lambda t} \frac{I_1\left(2\lambda\sqrt{\frac{ax}{gh_0}}\right)}{I_1\left(2\lambda\sqrt{\frac{a^2}{gh_0}}\right)} \frac{d\lambda}{\lambda^2 + \omega^2}, \tag{8}$$

where L is Bromwich's path of integration having all singularities to its left-hand side.

According to the theory of contour integration, (8) becomes

$$\eta = C\sqrt{\frac{a}{x}} \left\{ \frac{J_1\left(2\omega\sqrt{\frac{ax}{gh_0}}\right)}{J_1\left(2\omega\sqrt{\frac{a^2}{gh_0}}\right)} \sin \omega t + \sum_{s=1}^{\infty} \frac{J_1\left(\alpha_s\sqrt{\frac{x}{a}}\right)}{J_0(\alpha_s)} \frac{\omega\sqrt{\frac{gh_0}{a^2}}}{\frac{gh_0}{4a^2}\alpha_s - \omega^2} \sin \frac{\sqrt{gh_0}}{2a}\alpha_s t \right\} \tag{9}$$

where α_s denotes the s-th root of $J_1(x) = 0$. The we can estimate the elevation at any time from (9).

When t is very small, we can easily get more convenient expression by use of asymptotic expansion. As is well known, it becomes that

$$I_1(z) = \sqrt{\frac{1}{2\pi z}} e^z \left\{1 - \frac{3}{8}\frac{1}{z} - \frac{15}{128}\frac{1}{z^2} \cdots\cdots\right\} \tag{10}$$

for large values of $|z|$. Then taking the first term, (8) becomes

$$\eta = \frac{\omega C}{2\pi i}\left(\frac{a}{x}\right)^{3/4} \int_L e^{\lambda\left\{t - 2\sqrt{\frac{a}{gh_0}}(\sqrt{a} - \sqrt{x})\right\}} \frac{d\lambda}{\omega^2 + \lambda^2}$$

or

$$\eta = C\left(\frac{a}{x}\right)^{3/4} \sin\omega\left\{t - 2\sqrt{\frac{a}{gh_0}}(\sqrt{a} - \sqrt{x})\right\}. \tag{11}$$

This expresses the wave proceeding into the bay with velocity $\frac{\sqrt{gh_0}}{2}$ while the amplitude increases proportionally to $x^{-3/4}$.

Taking $a = 4.2$ km and $h_0 = 28$ m, the writers estimate the elevation of the surface in the bay both in the cases of the tsunami having the periods 20 and 40 minutes. The results are shown in Fig. 3a and Fig. 3b where it is clearly seen that the increasing rate in amplitude with distance from the mouth is remarkably larger in the case of 20 min. than that of 40 min. On the other hand, the period of the seiche

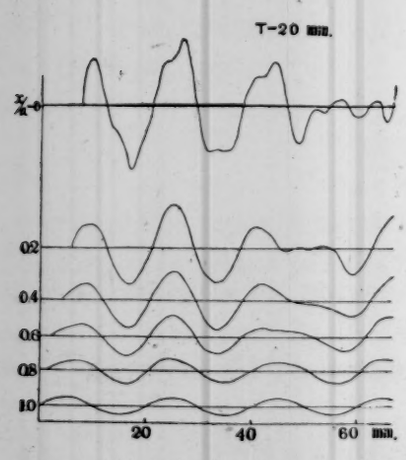

Fig. 3a. The elevation of sea-water at various parts of the bay. The period of the tsunami-wave is assumed to be 20 minutes.

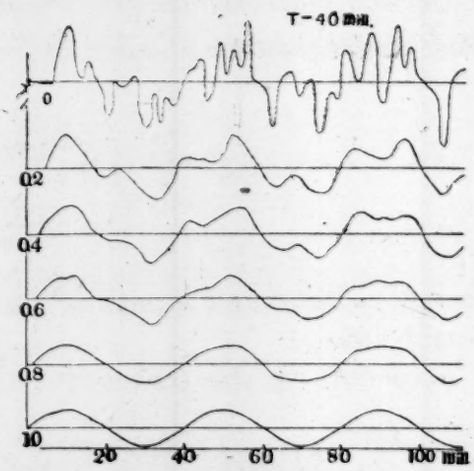

Fig. 3b. The elevation of sea-water at various parts of the bay. The period of the tsunami-wave is assumed to be 40 minutes.

of this bay T_0 is given by putting $\eta = 0$ at the mouth, that is, they get from (4)

$$J_1\left(\frac{4\pi}{T_0}\sqrt{\frac{a^2}{gh_0}}\right) = 0. \tag{12}$$

Then the longest period becomes 14.2 min.. The actual observations executed by the writers at the head of the bay gave about 11 min. as shown in Fig. 4. Then, with resonance phenomena in mind, it seems reasonable that the amplitude becomes larger in the case of 20 min. than that of 40 min..

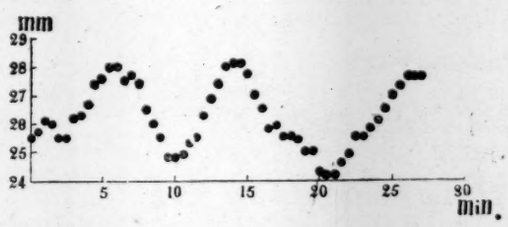

Fig. 4. The seiches measured at the head of the bay.

Assuming that the amplitude of the tsunami-waves amounts to 1.8 m at the mouth, in the next place, it is found that the maximum heights of sea water during a few oscillations vary along the shore as is also shown in Fig. 2. As the agreement between the theory and the observation seems good in the case of 40 min., we may consider that the tsunami-waves have a period which does not differ materially from 40 min.. At the head of the bay, however, the observation gives smaller values than the calculated ones. This may be explained if we take into account the difference between the actual condition and the boundary condition that there does not occur horizontal flow at the head of the bay.

In conclusion, the writers wish to express their sincere thanks to Professors R. Takahashi and T. Hagiwara for their kind advices and helpful suggestions.

6. *Observation of Changes in the Inclination of the Earth's Surface at Mt. Tsukuba (Third Report).*

By Takahiro HAGIWARA,

Earthquake Research Institute.

(Read April 15, 1943; Jan. 20, 1948.—Received June 20, 1948.)

The writer, in his previous papers, described the changes in inclination of the earth's surface that were observed at Mt. Tsukuba with the silica tiltmeters during the period from 1935 to 1940[1]. Those observations were made in two rooms ("A" and "B" in Fig. 1) lying

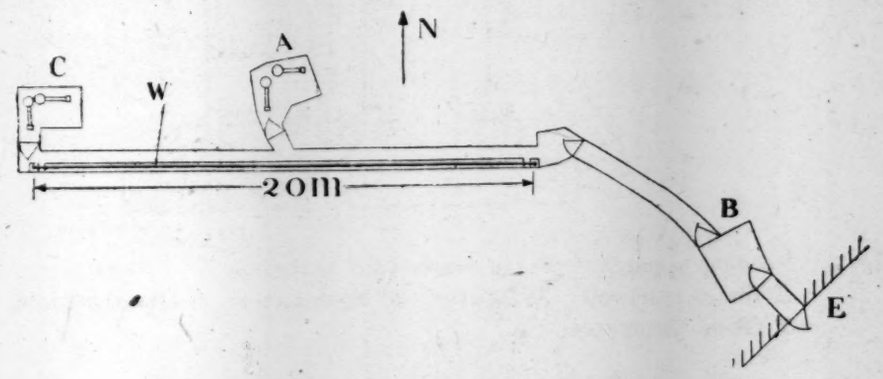

Fig. 1. Plan of the gallery. A, C Silica tiltmeter. W Water-tube tiltmeter. E Entrance.

in the gallery that was bored horizontally through the mountain side. The observations, however, showed that the changes in inclination of room "A" and "B" differ entirely. The main object of the observation was to ascertain the changes in inclination related to the earthquake occurrence, but the foregoing result showed that the measurements of such kind is a very difficult matter.

On the other hand, it is well known that the crustal deformations were found successfully by the revision of the precise leveling. This success must be due to the sufficient length of the distance between bench marks. If, as shown in Fig. 2, we suppose that there

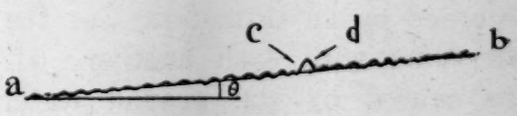

Fig. 2.

1) T. HAGIWARA, *Bull. Earthq. Res. Inst.*, **16** (1938), 366; **19** (1941), 218.

exist small disturbances superposing on the main inclination between "*a*" and "*b*" the inclination at points "*c*" or "*d*" will show a very large amount of inclination. The precise leveling measures the mean inclination angle between "*a*" and "*b*", while the silca tiltmeter registers such local disturbance as "*c*" or "*d*".

For this reason, a water-tube tiltmeter with a length of 20 m was installed along the gallery in EW direction and the comparisonal observation was commenced since 1943. Fig. 3 shows the water reservoir of the water-tube tiltmeter.

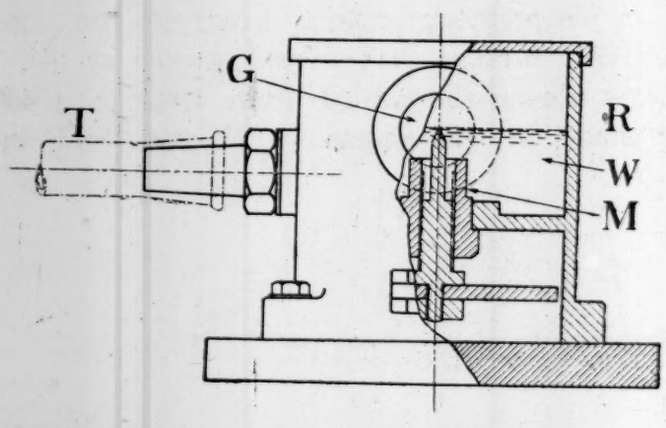

Fig. 3. Reading apparatus of the water-tube tiltmeter.
R Water reservoir. W Water. M Micrometer. G Glass window.
T Glass water-tube.

Two water reservoirs with such construction were installed separetely at a distance of 20 m, and the water contained in them was connected by a glass tube with diamater of 2.5 cm. The change in inclination of the ground is obtained from the difference of reading in two micrometers, 0.0103″ corresponding to 0.001 mm. The measurement was made twice a day. For the comparison, a pair of silica tiltmeters was installed in room "*C*" that was bored newly at a greater distance from the entrance of the gallery. The observation with the silica tiltmeters in room "A" was also continued.

Fig. 4 shows the observational results during the period from 1943 to 1948. In the case of large precipitation, the remarkable changes are recorded by all tiltmeters, but the amount and direction of them are not same with each another. If it is assumed that such disturbances are caused by the ground water near the very point, at which the instrument is installed, irregularity just mentioned may be explained. Although the water-tube tiltmeter is not free from disturbances due to the precipitation, the secular variation measured by this instrument

during a long period of time is far smaller compared to that of the silica tiltmeters in room "A" and "C". Its total variation is less than 1″ since the beginning to the present. We may be able to say that the water-tube tiltmeter is more reliable than the silica tiltmeter for observing the secular changes in inclinaion.

The relation to the earthquake occurrence will be discussed after making further observations.

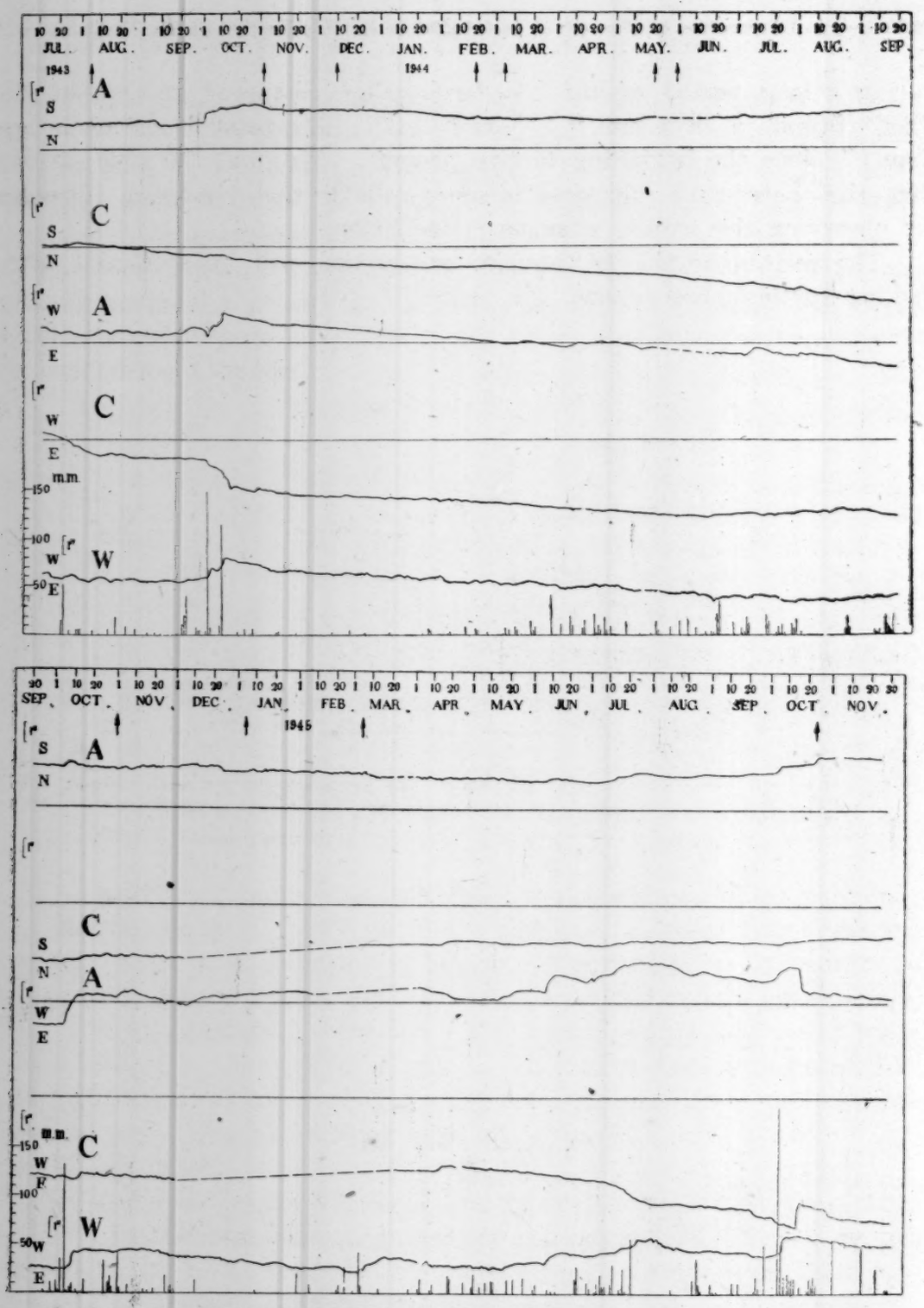

Fig. 4, a. A Changes in inclination in room "A".
C Changes in inclination in room "C".
W Changes in inclination measured by the water-tube tiltmeter.
↑ Fairly severe earthquake occurred in the neighbourhood of Mt. Tsukuba.
Vertical lines drawn below show the precipitation in mm observed at 10h on that day.

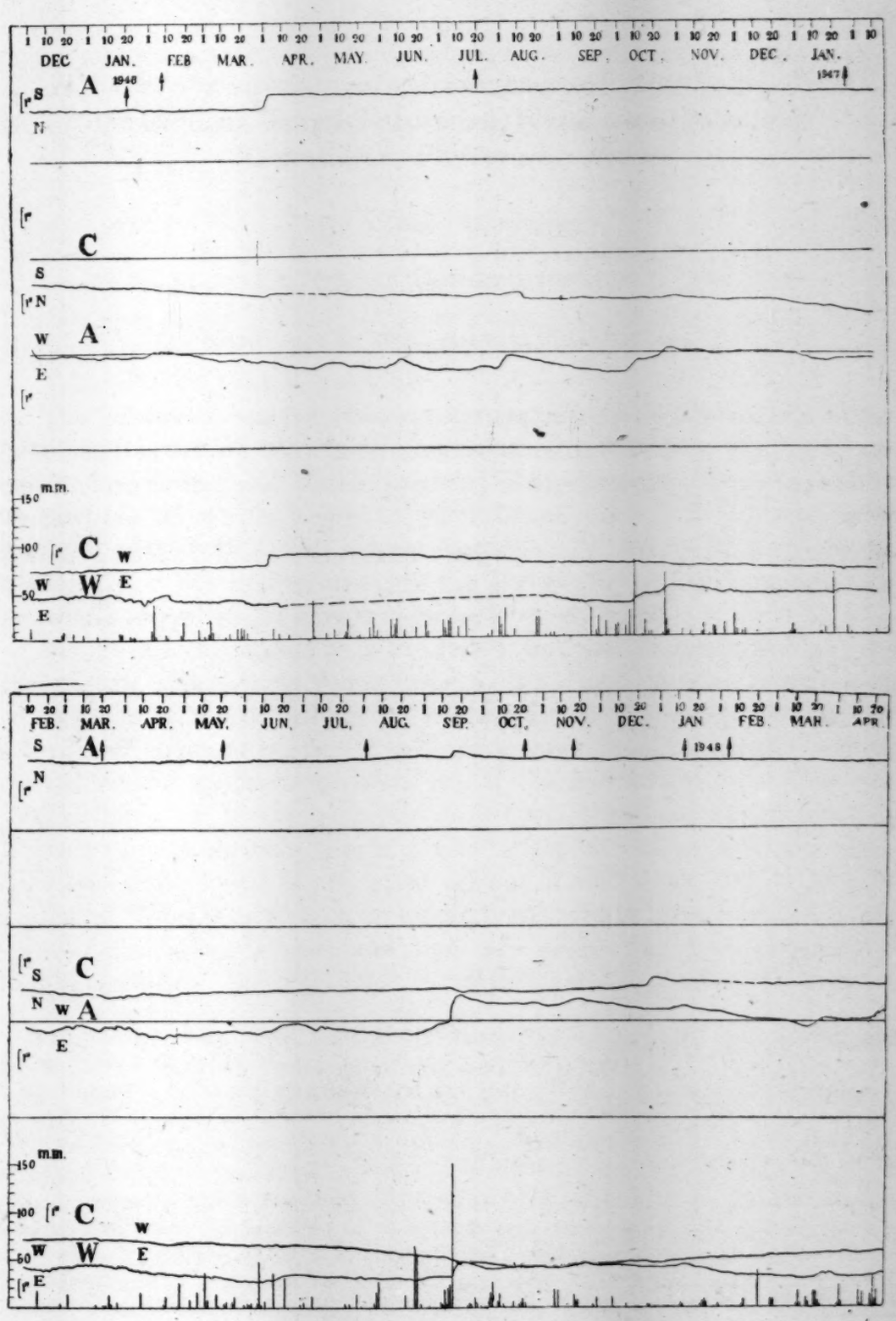
DEC JAN. FEB MAR. APR. MAY JUN. JUL. AUG. SEP. OCT. NOV. DEC. JAN.
1946
1947
S
A
N
C
S
N
W
A
E
m.m.
150
100
50
C
W
W
E
E
FEB. MAR. APR. MAY. JUN. JUL. AUG. SEP. OCT. NOV. DEC. JAN FEB. MAR. APR.
1948
S
A
N
S
C
N
W
A
E
m.m.
150
100
50
C
W
W
E
E

Fig. 4, b.

7. *On the Modes of Occurrence of Cordierite from Sakkabira, Town Taru-mizu, Kimo-tsuki Province, Kagoshima Prefecture, Japan.*

By Ryōhei MORIMOTO,

Earthquake Research Institute.

(Read Apr. 21, 1946.—Received June 20, 1948.)

The cordierite-bearing lava is petrographically biotite-bearing hypersthene-plagioliparite[1], containing plagioclase (An 35–48%), quartz, hypersthene[2], magnetite, and biotite as phenocysts scattered in the groundmass, the texture of which varies in parts, being microfelsitic in the brittle porous liparitic rock facies, cryptocrystalline in the hard and compact obsidian. Locality of the lava and the geology of the surrounding area are briefly shown in an annexed geologic route map[3].

Distribution of cordierite in the rock is quite heterogeneous: Crystals of cordierite concentrate remarkably to the drusy cavities in the brittle porous parts of the country rock[4] and almost have never been recognized in hard and compact parts. There are usually no crystals of cordierite even where the cavities preponderate, if the flow-structure of the rock is remarkable or if the country rock around the cavities is hard and compact. In the brittle porous rock facies, the comparatively higher crystalline groundmass is composed mainly of tridymite, irregular grains of alkaline feldspar, and a little quantity of quartz, accessorily of a few flakes of fox-brown biotite and iron ore dust. In those parts of the groundmass where the considerable tridymite are concentrated, irregular

1) K. YAMAGUCHI, "Petrological study of Ash stone around the Bay of Kagosima (Part 4)" *Jour. Geol. Soc. Japan* **45** (1938), 33, (in Japanese).

2) (−) $2V = 62°$ $\rho > v$ about X, ($En_{60}Fs_{40}$ after KUNO's Figure, *Proc. Imp. Acad. Tokyo* **17** (1941), 205. (−) $2V = 58$–$59°$, $n_1 = 1.717$, $n_2 = 1.727$ (YAMAGUCHI *loc. cit.* 335). It is *note-worthy* that in the present hypersthene, there are some ones which have more ferruginous composition, near to En_{50} Es_{50}

3) Prepared in March 1944, with Hideo MINATO of the Mineralogical Institute. Some geological data were supplemented by H. MINATO and Masatsune TANI in Dec. 1944.

4) Nov. 11, 1942, a specimen of porous liparitic rock in the druse of which are contained short prismatic crystals of cordierite with dark bluish lustre, attaining to 1–2mm in length, associated with tridymite, was given by Mr. Junosuke MASUTOMI who found it at first, quite accidentally from the block laid at the roadside near Sakurajima-guchi on his Journey to Osumi.

formed crystals of fayalite[5] or cordierite are ofen found. Euhedral prismatic or tabular crystals of cordierite associated with scaly crystals of tridymite and a little quartz, which are seriate to those minerals in the groundmass, are recognized in the drusy cavities predominating in

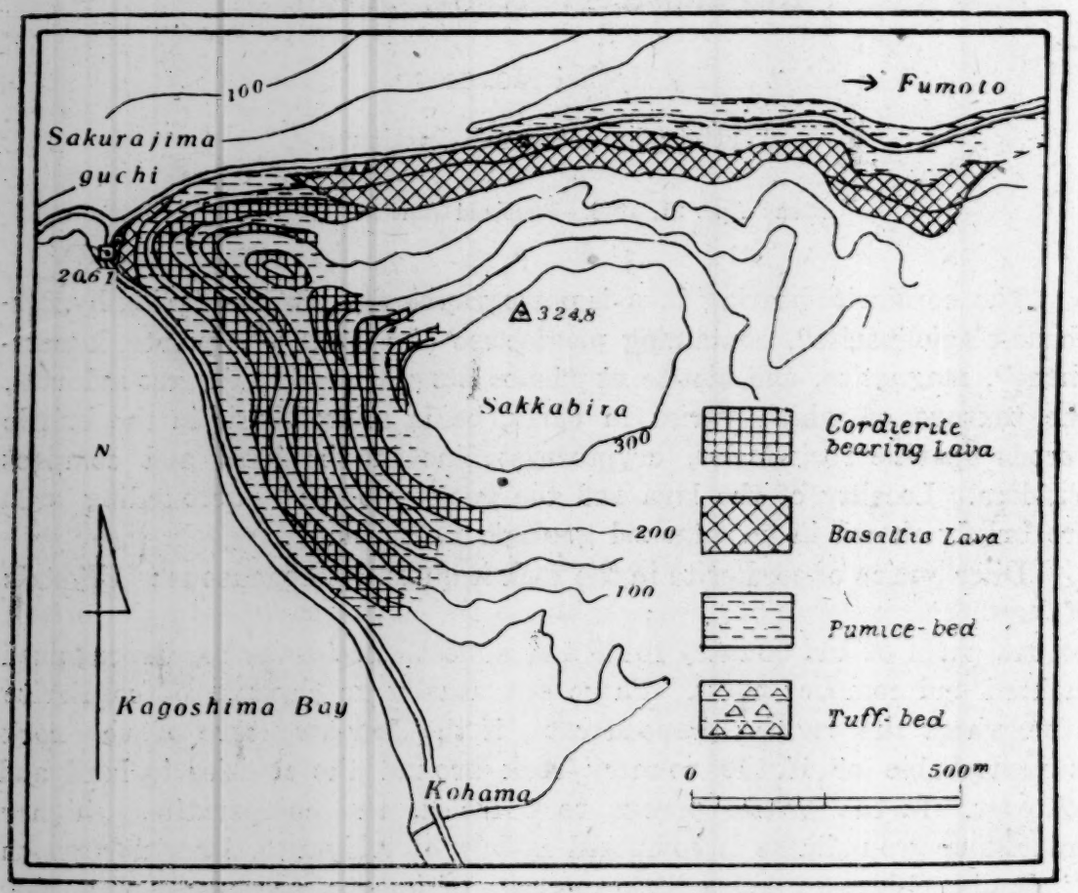

such parts of the groundmass. Parallel growth of the tabular crystals are common, but the pseudohexagonal twinning characteristic to cordierite has not been observed. In thin slices, these cordierite indicate low retardation, remarkable pleochroism (Light Glaucous Blue[6] to colourless), and distinct dispersion ($\rho > v$ about Z). Optically positive crystals with small optic angle or uniaxial positive crystals are not rare. Among the principal refractive indices, the intermediate β_D varies even in a single crystal,

5) Occurrence of this mineral will be reported separately.

6) WADA's Colour Chart No. 131.

7) Range of the principal refractive indices measured on several individuals: $\alpha_D = 1.545$-1.548, $\beta_D = 1.546$-1.549, $\gamma_D = 1.549$-1.551 (± 0.001). Mean chemical composition of the prismatic crystals: SiO_2 50.78, TiO_2 0.01, Al_2O_3 24.85, Fe_2O_3 1.95, FeO 9.97. CaO 0.61, MnO 0.40, MgO 6.68, Na_2O 1.00, K_2O 1.42, $H_2O(-)$0.27, $H_2O(+)$1.73, Total 99.67 wt%. Anal. Hideo MINATO.

1
1 mm

2
1 mm

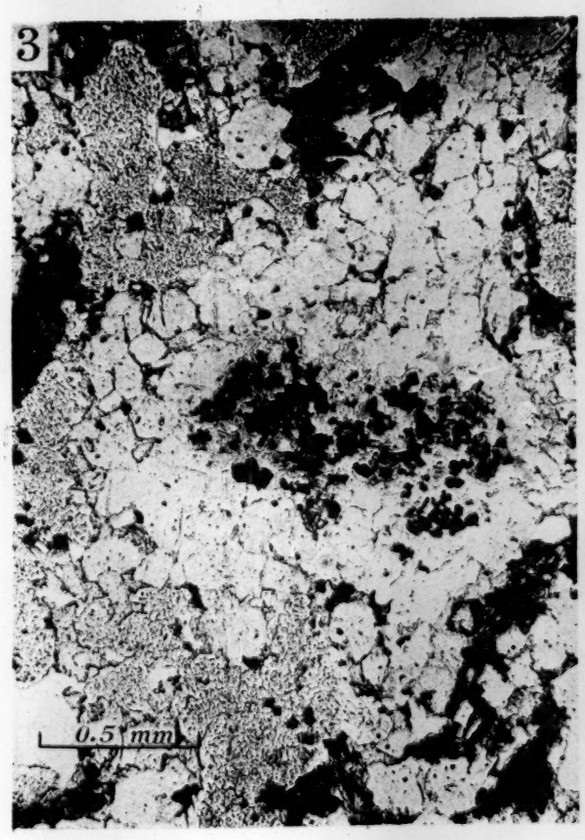
3
0.5 mm

4
0.5 mm

so the optic angle is quite variable from almost uniaxial positive to biaxial negative. In the crystals microphotographed in Fig. 1–2, an optic elasticity axis Z, being an acute bisectrix in the central part of the crystals, is an obtuse one in the peripheral zone[8]. In the hard and compact parts of the rock in which no crystals of cordierite being observed, the groundmass consists of light-brownish glass of low refractive index ($n_D \fallingdotseq 1.48$) with scattered minute grains of iron ore dust, microlites or crystallites. Considerable existence of angular fragments of the phenocrysts in those parts of the rock where the flow structure remarkably predominates, indicates that these earlier formed crystals were broken down mechanically into smaller angular flakes by the flowing magma. According from the above-description, it will be afforded for the writer to think that the present cordierite must have crystallized out *in situ*, in other words, where we observe them now, without mechanical disturbance, from the residium at the later stage of consolidation of the magma, irrespectively of their occurrence as euhedral crystals in the drusy cavities, or as anhedral irregular formed crystals in the comparatively coarse grained groundmass. They are not found in the glassy parts of the groundmass which are the quenched product of the residual magma, or in the parts of the rock where the flow structure indicating the mechanical disturbance during its crystallization is remarkable: But they are found in the drusy cavities or in the comparatively higher crystalline parts of the groundmass, in which the considerable tridymite representing those parts of the groundmass where the volatiles were concentrated during the final stage of crystallization are observed.

Quite differently in its mode of occurrence from the above-mentioned cordierite, the mosaic aggregate of cordierite was found in the xenolith[9] included in the cordierite-bearing lava (Fig. 3–4). Occurrence of cordierite like this are common in pyrometamorphosed xenolith. There is no direct relation between these two modes of occurrence represented respectively by the cordierite in the lava and in the xenolith, though foreign assimilation in the magma might have lead to crystallization of cordierite from residual magma.

In conclusion, the writer's sincere thanks are due to Prof. Seitarô TSUBOI of this Institute for his kind guidance and help throughout this study. Special thanks are due to Mr. Hideo MINATO for his co-operation and also to Mr. Junosuke MASUTOMI for gifts of specimen.

8) Crystals of corierite in the druse, wall of which is covered by scaly crystals of tridymite, shagreen appearance in Fig. 1. Inclusions in cordierite are quartz.

9) Spinel-bearing cordierite-hypersthene-biotite-plagioclase-xenolith. The dark mineral grains in the central part of Fig. 3–4 are green spinel.

8. *Possibility of Optical Explanation of Visible Wave-motion of Ground.*

By Yasuo SATÔ,

Earthquake Research Institute.

(Read Oct. 15, 1947.—Received June 29, 1948.)

1. Introduction. We have heard a number of reports from epicentral regions of great earthquakes that the wave-motions of ground or some structures such as roofs of buildings were noticed by the naked eyes[1]. Of course these reports are not necessarily trustworthy, and some of them are concerned with the objects on the ground such as trees, grass and so on[2]. But even if we exclude these cases, it is rather hasty to abandon all the other reports, considering them as illusion, for we have now few data and it is difficult to intorduce a decisive opinion. Therefore, while on one hand we should endeavor to collect correct and sufficient data, it is desirable to try to explain the fact reasonably. Now, as an attempt of this we will investigate the possibility of optical explanation of the fact; that is to say, if the compressional waves in the air, caused by the vertical movement of ground surface, may make the air density change and consequently the optical path of this region may have some curvature.

In the following discussion, we will assume the wave front horizontal and the problem to be two dimensional; and x-axis as horizontal and y-axis as vertical.

2. Relation between air-density and refractive index. According to Pernter-Exner[3], the relation between refractive index n and air density δ is expressed as $n = 1+c'\delta$ where c' is a small constant, somewhat dependent to the wave-length of light, for which we may adopt an average value ·000293 for white light.

Next, using the notations $\rho = \rho_0+\rho'$, $p = p_0+p'$, where p, ρ are pressure and density respectively and the suffix "o" means the average

(1) C. E. DUTTON, "Earthquakes" (1904) P. 13. W. H. HOBBS, "Earthquakes" (1907) P. 85. "MONTESSUS DE BALLORE, La Science Séismologique," P. 436. N. G. HECK, "Earthquakes" (1936) P. 21.

(2) N. H. HECK, loc. cit. T. MATUZAWA, "Disin." 9 (1937), P. 469.

(3) PERNTER-EXNER, "Meteorologische Optik." 2nd ed. P. 58 See also FUJIWHARA, KITAOKA; "Kisyô-kôgaku" (Iwanai, Buturigaku) P. 5.

value, and assuming the frequency (in one second) as ω, and the wave legth λ, substitute the expressions $V = V_0 \sin 2\pi(y/\lambda - \omega t)$, $\rho' = \rho_0' \sin 2\pi(y/\lambda - \omega t)$, in the fundamental equation of sound waves; then we have $\rho_0'/\rho_0 = v_0/(\lambda\omega) = v_0/V$, where, V is the velocity of sound wave. Therefore the rate of variation of density is equal to the ratio of maximum particle velocity to the propagation velocity of sound. For the present purpose we may take $\delta = \rho/\rho_0$, therefore we have

$$\delta = 1 + \varepsilon \sin 2\pi(y/\lambda - \omega t),\ \varepsilon = v_0/V \ldots\ldots\ldots\ldots\ldots \quad (A)$$

On the other hand, v_0 is determined by the vertical displacement of ground surface, so that ε is a small quantity in the case of real earthquakes. Substituting (A) into the expression of n, we have

$$n = (1+c')\{1 + K \sin 2\omega(y/\lambda - \omega t)\},\ K = c'\varepsilon/(1+c') \ldots\ldots\ldots \quad (B)$$

3. Optical path. From Fermat's principle, equation of optical path is $\delta T = \delta \int_{Qo} \frac{ds}{c} = 0 \cdots (C)$, where c is the light velocity and Q, O represents the position of the object and the eye respectively. (See Fig. 1). Using refraction index, we may write $c = c_0/n$, where c_0 is the light velocity in vacuum. Now, we adopt as the unit of length $\lambda/2\pi$, and unit of time $1/2\pi\omega$, and use ξ, η and τ instead of x, y and t; then we have the equation

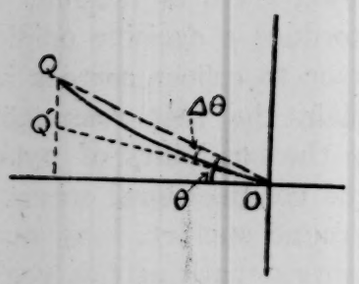

Fig. 1.

$$\delta T = \delta \frac{1}{c_0}(1-c') \int_{-a}^{0} \{1 + K \sin(\eta - \tau)\} \{1 + (d\eta/d\xi)^2\}^{\frac{1}{2}} d\xi = 0 \ldots\ldots\ldots \quad (D)$$

This is solved rigorously by the aid of elliptic integral. But the main object of the present paper exists in getting the apparent change of position of objects, so we will at first treat the case in which the light velocity varies according to the formula $c \propto 1 - K'\eta \ldots\ldots\ldots$ (E)

3.1. Relation between two velocity distributions. Now we will assume the form of integrand in (C) as $f(\xi, \eta, \eta')$. At first we take $\eta = \phi_0(\xi)$ as the equation of optical path, and $\eta = \phi_0(\xi) + \epsilon\,\psi(\xi)$ as another path that lies near $\eta = \phi_0(\xi)$. Here ϵ is a small constant and $\psi(\xi)$ vanishes at the points Q and O. Denoting the reciprocal of velocity as $\sigma(\eta)$, we have the following expression; $f(\xi, \eta, \eta') = \sigma(\eta)(1+\eta'^2)^{\frac{1}{2}}$. Introduce this into (C), and we have

$$\delta T = -\int_{QO} \psi(\xi)(1+\phi'^2)^{-\frac{3}{2}} F(\xi, \eta)d\xi, \quad F(\xi, \eta) \equiv \sigma(\eta)\phi''(\xi) - \sigma'(\eta)\{1+\phi'(\xi)^2\}^2 \quad \cdots\cdots\cdots\cdots\cdots\cdots \text{(D)}'$$

If the velocity is given by the formula $\sigma(\eta) = \sigma_0(\eta) \equiv 1 + c\sin(\eta-\tau)$, and the corresponding path is determined by the equation $\eta = \phi_0(\xi)$, then from (*D*) ;

$$\phi_0'' = [K\cos(\eta-\tau)/\{1+K\sin(\eta-\tau)\}](1-\phi_0'^2) \quad \cdots\cdots\cdots\cdots \text{(F)}$$

Next, we will consider another kind of medium in which $\sigma(\eta)$ is given by

$$\sigma(\eta) = \sigma_1(\eta) \equiv 1/(1-K'\eta), \quad K' \ll 1,$$

and express the path of this case by the equation $\eta = \phi_1(\xi)$. Our present purpose is to detect what difference may exist between two functions $\phi_0(\xi)$ and $\phi_1(\xi)$. Substituting (F) into (D)'

$$F(\xi, \eta) = (1-K'\eta)^{-2}\{1+K\sin(\eta-\tau)\}^{-1}[(1-K'\eta)K\cos(\eta-\tau) - K'\{1+K\sin(\eta-\tau)\}](1+\phi_0'^2)$$

$$< \quad ,, \quad ,, \quad [(1+K'\cdot 2\pi)K - K'\{1-K'\}](1+\phi_0'^2)$$

Now if we assume $K' = K(1+8K)$, then $[(1+K'\cdot 2\pi)K - K'\{1-K'\}] < 0$, therefore $F(\xi, \eta)$ is negative without regard to ξ. To make δT as small as possible we ought to take $\psi(\xi)$ always negative. This means that the optical path in a medium $\sigma(\eta) = \sigma_1(\eta) = 1/\{1-K(1+8K)\eta\}$, lies always in the lower side of $\eta = \phi_0(\xi)$ which represents a path in a medium $\sigma(\eta) = \sigma_0(\eta)$. On the other hand, when $-\frac{\pi}{2} \leq \eta-\tau \leq \frac{\pi}{2}$, the curve $\eta = \phi_0(\xi)$ lies in the lower side of a straight line that passes Q and O. Therefore the deflection angle, in the former case, is larger than in the latter.

By the above theory we may see the possibility of using a medium, in which $\sigma(\eta) = \sigma_1(\eta) \equiv 1/(1-K'\eta)$, to get an upper bound of deflection angle ; we shall see later that this gives also a good approximation of the largest value of it.

3. 2. Estimation of deflection angle. Brachistchronic line in a medium $\sigma(\eta) = \sigma_1(\eta)$ is obtained by equating the expression $F(\xi, \eta)$ of $(D)'$ to zero.

$$(1-K'\eta)^{-1}\eta'' - K'(1-K'\eta')^{-2}(1+\eta'^2)^2 = 0$$

Integrating the expression we have the following solution easily, where L and M are integration constants. $K'(\xi^2+\eta^2) - 2\eta + 2L\xi - M = 0$. From a boundary condition $\xi = 0, \eta = 0$, we have at once $M = 0$, and

$$\{\xi+L/K'\}^2+\{\eta-1/K'\}^2=\{1+L^2\}/K'^2$$

This is an equation of circle whose radius is $(1+L^2)^{\frac{1}{2}}/K'$. Arbitrary constant L, in this expression is obtained by putting another boundary condition $\xi=-\alpha$, $\eta=\beta$. Thus $L=\{K'(\alpha^2+\beta^2)+2\beta\}/2\alpha$. This quantity is, as compared with unity, very small. Hence the radius of circle is approximately $1/K'$, which depends neither on α nor on β.

Deflection angle of optical path, denoted by $\Delta\theta$ in Fig. 1, is obtained by the following process.

$$\tan\theta=\beta/\alpha,\ \tan(\theta+\Delta\theta)=[-d\eta/d\xi]_{\xi=-\alpha,\eta=0}=\{K'(\alpha^2+\beta^2)+2\beta\}$$

$$\therefore\quad \Delta\theta=\frac{1}{2}K'\alpha$$

Thus the deflection angle depends only on distance.

As time goes on, distrbution of air density becomes reversed and $\Delta\theta$ changes its sign to become $-\frac{1}{2}K'\alpha$. Therefore, the total deflection angle amounts to $K'\alpha$. When the object point Q lies on the same horizon with O, β becomes zero and L becomes as $L=K'\alpha/2$. Maximum value of η, in this case, is $\eta_{\max}=\frac{3}{8}K'\alpha^2$, which is fairly small compared with unity; therefore we may legitimately adopt the following approximation when $|\eta-\tau|$ is small.

$$\sigma_0(\eta)\equiv 1+K\sin(\eta-\tau)\fallingdotseq 1/\{1-K(\eta-\tau)\}\propto 1/\{1-K'\eta\}\equiv\alpha_1(\eta)$$

Thus the above obtained amount $K'\alpha$ gives not only an upper bound of deflection angle, but also a good approximation.

4. Numerical values in a practical case. Now, we will examine the possibility of the explanation by introducing numerical values adequate in the case of real earthquakes.

At first, we adopt the value $c'=\cdot 000293$. Next, since ε is equal to v_0/V, taking a greatest value thinkable for v_0, we put $v_0=100\text{cm/sec}$. Then we have $\varepsilon=100/33{,}000\fallingdotseq\cdot 003$, therefore

$$K=c'\varepsilon/(1+c')\fallingdotseq 1\cdot 0\times 10^{-6},\quad K\fallingdotseq K'$$

As the unit length we have used $\lambda/2\pi$, which nearly becomes, taking a frequency a little larger than 3 sec^{-1}, 15 metres.

On the other hand, the maximum total deflection angle is about $K'\alpha$. Therefore, for a distance 150 metres ($\alpha=10$), we have $|\Delta\theta|_{\max}=$

10^{-5}. But this is too small to be detected by the naked eyes. Besides, the apparent displacement of the object point (QQ′ in Fig. 1) is only about 1 mm., which is by far smaller than the real displacement of ground. So we may conclude that the visible wave motion of ground surface is no more easily explained by assuming optical effect. Even if we assume shorter sound waves, the deflection angle by no means increases. We have hitherto adopted a most favorable case for the optical explanation, but now we are to give up this intention.

The above idea is due to Prof. H. Kawasumi who encouraged the author throughout this work. Also Mr. K. Yosida, of Gepophysical Institute of Tokyo University, kindly gave useful suggestions.

9. A *Study of Microseisms after A. W. Lee's Method.*

By Fuyuhiko KISHINOUYE and Ryôhei IKEGAMI,

Earthquake Research Institute.

(Read Feb. 17, 1948.—Received June 20, 1948.)

INTRODUCTION.

The direction of the propagation of microseisms have been brought to focus of discussions. In countries except Japan there are many researches concerning the travelling directions of microseisms[1]. The conclusions were that the microseisms are propagated in the earth's crust from origin, which is caused by a storm depression, to the observatories. In those studies, microseisms were assumed that they are Rayleigh waves, and under this assumption their travelling directions had been discussed.

Turning to the studies of microseisms in Japan, these are also many researches concerning the characters of the microseisms[2]. The results of the studies in Tokyo do not always agree with those obtained in the other countries. Although there is nearly no objection to the point that the microseisms are caused by a storm depression, we could not obtain the clear results that the direction to their origin, or to the centre of the storm.

As a conclusion to this question, one of the writers mentioned that "microseisms are combinations of two stationary waves excited by oceanic waves in some manner yet unknown[3]".

In this paper, we again deal with the direction of microseismic motion and inspect the microseisms obserbed at Hongo. In Tokyo, by the same method as that of A. W. Lee[4] who discussed the microseisms observed at the Kew Observatory.

---

1) S. K. Banerji: *Phils. Trans. Roy. Soc. London*, **229** (1930), 287-328. A. W. Lee: *Proc. Roy. Soc, London*, **149** (1935), 183-199. J. E. Ramirez: *Bull. Seism. Soc. America*, **30** (1940), 35-84, 139-178. M. H. Gilmore: ditto, **36** (1946), 89-120. ect.

2) F. Omori: *Bull. Imp. Earthq. Investig. Comm.* **3** (1909), 1-35; 4 (1913), 109-147. n. Matuzawa: *Journ. Fac. Sci. Imp. Univ. Tokyo* **2** (1926-1930). 205-263. F. Kishi-Touye: *Bull. Earthq. Res. Inst.* **13** (1935). **18** (1940), ect.

3) F. Kishinouye: Ditto, **18** (1940), 402-418.

4) A. W. Lee: loc. cit.

If the periods or the phases of every component are remarkably different each other in Tokyo, it will be absurd to attempt the present investigation. But we applied the method, because the periods and phases, in comparison with Lee's records, are in good agreements.

AN OUTLINE OF LEE'S METHOD.

For the convenience of describing our results, we mention the outline of Lee's method.

First, for the purpose of this investigation the phases at the beginning of the minute marks, on the seismogram are allotted numbers according to a scale, Fig. 1. from 0 to 15. The entries 0 and 8 indicate that the beginning of the break coincides with the crest and trough respectively.

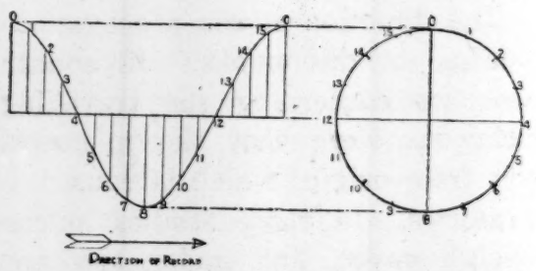

Fig. 1. Scale of tabulation for phase angles.

Next, on the tabulation of the phases of the microseisms, we see each phase difference between the different components, and tabulate the number of occurrences of these specified phase differences. By these results we examine statistically the most probable phase differences. On the basis of these results and the asumption that microseisms are Rayleigh waves, we can deduce the arrival direction of this microseiems.

APPLICATION OF THE METHOD TO THE MICROSEISMS AT TOKYO, AND COMPARISON BETWEEN LEE'S RESULTS AND OURS.

(1) Lee's Method.

We again used the data which one of the writers previously used. Those data had been obtained from the records of the large microseisms on Oct. 21, 1938 and Aug. 31, 1938 observed at the Tokyo University. Those seismograms were recorded by Omori's seismographs which have two horizontal and one vertical components. The constants of these seismographs were shown in Table I of the previous paper[5].

On the record on Oct. 21, we picked up the data in every 50 minutes at about 11h, 16h, and 20h on that day to examine how the arrival direction of the oscillations changed according to transfer of the centre of

5) F. Kishinouye: loc. cit., p. 403.

depression, if the microseisms were propagated truely from its origin.

In every one of these four occasions, the measurements of the phases are made at every minute marks in fifty minutes on the basis of the scale, Fig. 1. Next, the phase differences between the components are calculated. On that occasion, it is not necessary to consider the phase lag between the components, because the phase lag of these seismographs between the components were nearly equal to each other. Finally, the numbers of occurences of specified phase differences are counted. The distributions of the number of these differences are shown in Table 1.

Table I.

(a)	0	1	2	4	3	5	6	7	8	9	10	11	12	13	14	15	—	1—7	9—15
NS—UD	4	3	2	2	4	3	2	2	5	4	1	3	6	3	2	2	3	18	21
EW—UD	2	2	1	4	4	1	3	6	2	5	6	4	1	1	3	3	3	21	23
EW—NS	3	9	4	1	3	2	2	4	4	1	3	4	2	4	1	4	0	25	19
(b)																			
NS—UD	3	1	2	3	2	3	3	3	2	4	5	3	2	1	4	6	4	17	25
EW—UD	0	0	2	3	3	4	2	6	6	1	5	3	3	4	2	4	3	20	22
EW—NS	5	4	2	1	5	5	0	3	2	4	3	1	3	3	4	3	3	20	21
(c)																			
NS—UD	4	3	2	3	2	2	2	4	3	3	0	2	3	4	1	4	9	18	17
EW—UD	3	1	0	2	3	1	2	6	3	2	5	2	2	4	1	3	11	15	19
EW—NS	3	3	2	0	4	4	3	4	1	5	4	3	5	2	4	2	2	20	25
(d)																			
NS—UD	4	4	5	1	3	4	6	4	1	5	2	3	2	3	4	0	0	27	19
EW—UD	3	3	2	0	2	5	5	6	3	2	2	4	1	2	5	5	1	23	21
EW—NS	4	4	4	2	1	2	5	2	3	3	2	3	4	2	4	5	1	20	23

The values of these distributions are smoothed by overlapping groups of five values, giving double weight to the second and fourth, and treble weight to the third; thus, if F_n denotes the number of observation of any phase differece (n), the smoothed frequency expressed as the percentage of the total number of values is

$$F'_n = \frac{F_{n-2}+2F_{n-1}+3F_n+2F_{n+1}+F_{n+2}}{9} \times \frac{100}{50}.$$

These smoothed frequencies for the four above mentioned cases and one of Lee's cases are shown in Fig 2. In Fig. 2(e), which is Lee's results, there are clear maximum values at 270° and 90°, on NS-UD and EW-UD components respectively. This fact will be a strong evidence to

deduce that the waves arrived from north-west, if the microseismic oscillations may be considered as Rayleigh waves.

On the other hand, in Fig. 2 (a), (b), (c) and (d), or in the results at Tokyo, the phase difference curves are smooth in comparison with (e)-curve, and maximum value are not clear, therefore we could not deduce the arrival directions from these results.

Incidentally, the situations and tracks of the depressions (typhoon) at these cases were shown in the previous report.

(2) Comparison of microseisms at two places according to their orbits.

Assuming that the microseismic oscillations are a kind of Rayleigh waves, the arrival direction of the waves may be deduced on the basis of the rotating direction of the orbits of an earth particle.

The portions of the records, obtained at Kew on Jan. 11, 1930, are conveniently shown in the Lee's paper. We took a copy and enlarged that record, and described the orbits of microseisms in the prime vertical plane and the meridional one, pairing the UD-component with NS- and EW-component respectively. These orbits are shown in Fig. 3(a).

Judging from those orbits,

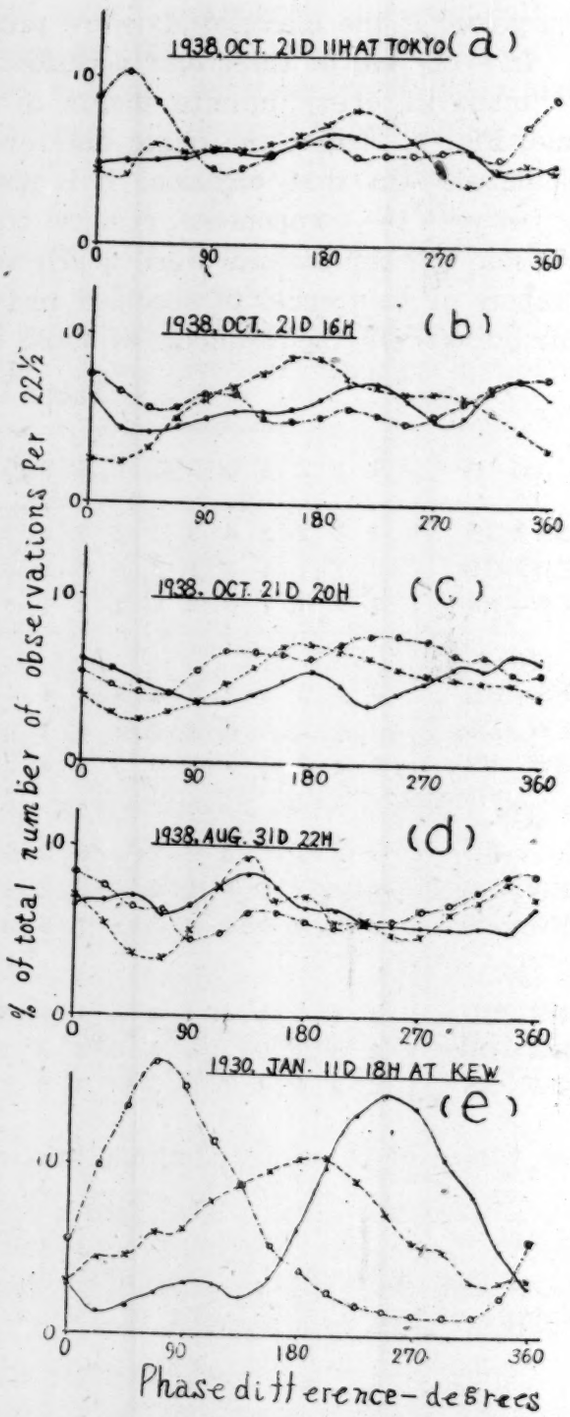

Fig. 2. Smoothed frequencies of specified phase differences between the components of the microseisms.

—●—●— NS~UD
---○---○--- EW~UD
---×---×--- EW~NS

a regular rotation of the constant direction of an earth particle will be distinctly seen. It suggests Rayleigh waves came from north-west or south-east.

On the other hand, describing the orbits on the basis of the records at Tokyo, these orbits were formed as shown in Fig. 3(b). The latter does not show the arrival direction so clearly as the former.

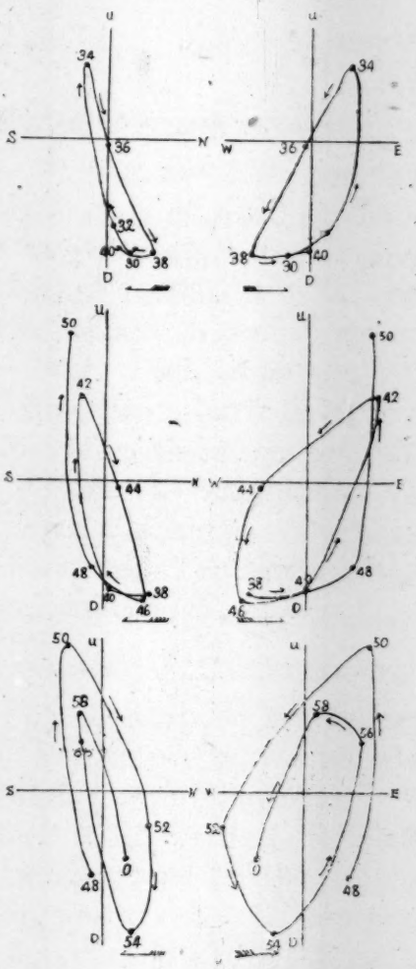

Fig. 3 (a) The orbits of an earth particle at Kew Observatory.

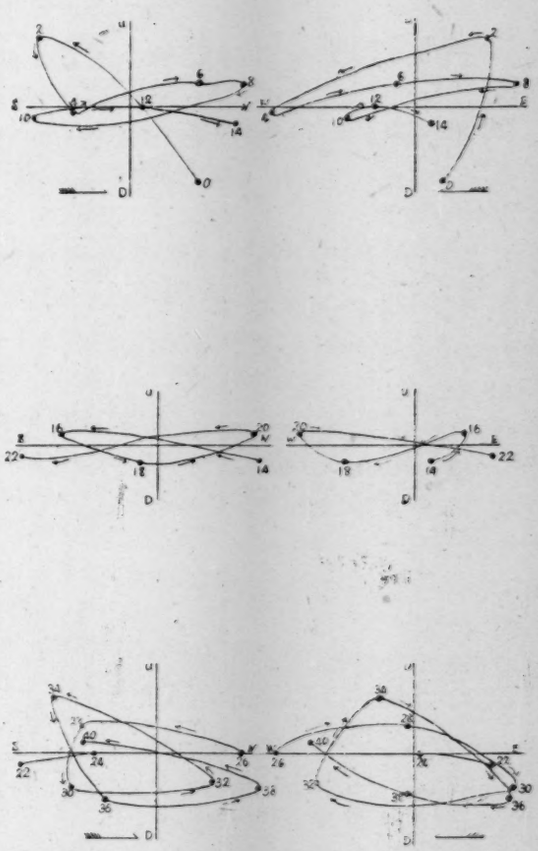

Fig. 3 (b). The orbits of an earth particle at Tokyo Observatory.

Additional remark: J. E. Ramirez[6] also determined the arrival direction of the microseismic waves by the same method in his paper. In the diagrams of the orbits, the constant rotations of particle were clearly shown.

6) J. E. Ramirez: loc. cit., p. 145.

CONCLUSION.

From the above mentioned results, it may be considered that the microseisms are Rayleigh waves which travel from an origin to a station on the earth's surface, in England or America, but in Tokyo, the microseisms do not clearly show their arrival direction. The cause of this results be considered in many ways, and now we do not discuss about this problem, because this queation contains still many unknown problems.

10. A Study on the Overturning of Rectangular Columns in the case of the Nankai Earthquake on December 21, 1946.

By Ryôhei IKEGAMI and Fuyuhiko KISHINOUYE,

Earthquake Research Institute.

(Read June 17, 1947.—Received June 20, 1948.)

INTRODUCTION.

It is a well-known expedience in Japan that the magnitude of the acceleration of great earthquakes were commonly deduced from the ratio of *height* to *width* of overturned grave-stone which are rectangular column in shape[1]. But it is at times found that the grave-stone which has great height in comparison to the width, which in appearance is apt to be overturned, does not. On the contary one which has great width, in appearance hard to be overturned, is overturned. In this paper, we will study these phenomena theoretically and will exploit these results to deduce the magnitudes of the Nankai Earthquake of 1946 at two places; Kainan-Shi in Wakayama Prefecture and Kinomoto-Shi in Miye Prefecture. The latter data were kindly offered to us by Dr. H. Kawasumi and Mr. Y. Sato.

THEORETICAL CONSIDERATIONS.

(1) CONDITIONS OF OVERTURNING.

For simplicity, we consider the rocking or overturning of rectangular column in two dimensions. When a column, ABCD, is moved to AB′C′D′ which is the critical declination for overturning caused by the ground motion, the center of gravity, G, moves to G′ where it is vertically above the point A in Fig. 1. The work of the center of gravity, G, to be done during the displacement GG′ is given by

$$W_G = Mga - Mga\cos\alpha = Mga(1-\cos\alpha), \qquad (1)$$

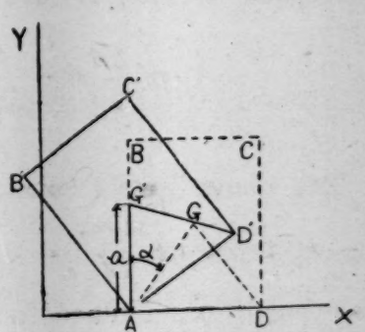

Fig. 1.

1) F. Omori, *Rep. Imp. Earthq. Comm.* **32** (1900), 19–33. H. Kimura and K. Iida, *Jishin* **6** (1934), 125. R. Ikegami and F. Kishinouye, *Bull. Earthq. Res. Inst.* **24** (1946), 11–18.

in which M is the mass of the column, g is the acceleration of gravity, a is the length of AG and α is the angle of $\angle$ GAB.

Next, when a column is moved by a ground motion, $\epsilon \sin p(t+\delta t)$, the equation of motion is given by

$$(a^2+k^2)\frac{d^2\theta}{dt^2} = -ag\sin(\alpha-\theta)+a\varepsilon p^2 \sin p(t+\delta t)\cos(\alpha-\theta), \qquad (2)$$

in which k is the moment of inertia at G and δt is the time-lag.

In this paper, vertical motions were neglected, for the Nankai Earthquake occurred off the coast of Kii and the vertical component of the earthquake motions were very small as compared with the horizontal motions.

It is difficult to obtain the general solution of the equation (2), so we attempt to obtain an approximate solution of equation (2).

We took approximately,

$$\sin(\alpha-\theta) \fallingdotseq \alpha-\theta, \quad \cos(\alpha-\theta) \fallingdotseq 1.$$

Then the solution of the equation is obtain as follows;

$$\alpha-\theta = A_1 e^{nt}+A_2 e^{-nt}+\frac{m}{n^2+p^2}\sin p(t+\delta t), \qquad (3)$$

where $n^2 = \dfrac{ag}{a^2+k^2}$, $m = \dfrac{a\varepsilon p^2}{a^2+k^2}$, and A_1 and A_2 are arbitrary constants.

Suppose at $t=0$; $\theta=0$, $\dfrac{d\theta}{dt}=0$,

so constants A_1 and A_2 are determined as follows,

$$A_1 = \frac{1}{2}\left\{\alpha-\frac{mp}{n(n^2+p^2)}\right\}, \quad A_2 = \frac{1}{2}\left\{\alpha+\frac{mp}{n(n^2+p^2)}\right\}.$$

The above initial conditions may be not reasonable for $\dfrac{d\theta}{dt}$ must be finite at $t=0$ or $\left(\dfrac{d\theta}{dt}\right)_0 \neq 0$. But we cannot solve the equation from the given conditions. Therefore we assumed $\left(\dfrac{d\theta}{dt}\right)_0 = 0$ and then consider the effects as the velocity increases gradually from zero.

From equation (3), the work of the ground motion done by the rocking motion of the column, dW_D is given by

$$dW_D = -(a^2+k^2)M\frac{d^2\theta}{dt^2}d\theta.$$

Therefore, the work in a quarter period of the ground motion is given by

$$W_D = -(a^2+k^2)M\int_0^{\frac{\pi}{2p}}\frac{d^2\theta}{dt^2}\frac{d\theta}{dt}dt\,, \tag{4}$$

When we substitute the solution (3) in equation (4), we obtain

$$W_D = \frac{a^2M}{6}\left[\frac{m^2p^2}{(n^2+p^2)^2}\left(10+\cosh\frac{n\pi}{p}\right)-\alpha^2n^2\left(2-\cosh\frac{n\pi}{p}\right)-\frac{2mn\alpha p}{n^2+p^2}\sinh\frac{n\pi}{p}\right], \tag{5}$$

in which δt is neglected as $\delta t \fallingdotseq 0$.

One condition of the overturning of the column due to any given motion is obtained from equation (1) and (5).

Namely, when $W_G > W_D$ (6), the column will be not overturned and when $W_G < W_D$ (7), the column will be overturned.

(2) Condition of Beginning of the Rocking Motion.

At equation (2), if we assume initial conditions $t = 0\,;\ \theta = 0,\ \frac{d^2\theta}{dt^2} = 0$, we obtain a condition at the begining of the rocking motion, then

$$\delta t = \frac{1}{p}\sin^{-1}\frac{g\tan\alpha}{\epsilon p^2}, \tag{8}$$

In equation (8), in order that δt is significant, the following condition is necessary ;

$$\frac{g\tan\alpha}{\epsilon p^2} < 1\,, \tag{9}$$

Namely, the column will begin to rock if acted on by a ground motion that satisfies the condition (9).

Application to the Practical Data.

The recent Nankai Earthquake occurred just before the newvyear, so the overturned grave-stones were unexpectedly restored in their places quickly for the new year festival, and data obtained were less than our expectations.

In this paper, we will apply the above results to the data obtained at Kainan-Shi and Kinomoto-Shi. (Table I).

TABLE I.

Place		Width	Height	α	a
Kainan-shi	Overturned	13 cm	43 cm	0.293	22.3 cm
	Non-overturned	24	115	0.218	55.3
Kinomoto-shi	Overturned	17	44	0.449	23.4
	Non-overturned	31	168	0.189	85.5

We applied equation (7) to the data of the overturned grave-stone and equation (8) to the non-overturned one in TABLE I and calculated the values of ε giving the values $p = 5, 6, 7, 8, 9, 10, 11, 12, 13$.

These results are shown in Fig. 2 and 4 respectively by curve I and II. The values of ε to be satisfied by equation (9), for these values of p, namely, the conditions to begin the motion, are shown by broken lines.

Furthermore, in order to indicate an acceleration, we calulated the values of p and ε from the following equation (10), in this case acceleration A was treated as parameter.

$$\varepsilon p^2 = A \tag{10}$$

The values of ε for various values of p are plotted in Fig. 2 and 4 by dotted lines.

(1) OVERTURING AT KAINAN-SHI.

In Fig. 2, when a ground motion that consisted of p and ε which are above the broken line, and furthermore exists between the hatched part, surrounded by curve I and II, is given, the high grave-stone is not overturned and the low one is overturned. Namely, at Fig. 2, assuming that a frequency of the ground motion, p, were nine (period $T = 0.70$ sec), we will deduce that the amplitude ε must be about from 5.2 to 5.5 cm in order that the above mentioned phenomena will occur.

At this time, we see from Fig. 2 that the acceleration is a little greater than 400 gal. Of course we can not uniquely determine the magnitude of the earthquake motion, but if we assume any one of p or ε or acceleration, we can deduce the motion at that place.

It is an interesting fact that if the frequency exceeds a certain limit, (period becomes larger), the above mentioned phenomena can not occur independent of amplitude. Namely, in this case, unless $p > 5.5$ or $\varepsilon < 12$ cm, the above mentioned phenomena does not occur. From the above mentioned facts, we can deduce that on firm ground where

the vibration period of the ground are short these phenomena may offen occur, and on the contrary, on soft ground, any and every grave-stone may overturn.

The Sennen-ji where we got these data, stand at the foot of a mountain in Kainan city and we believe that this place is located on firm ground. Namely, we are willing to deduce that at this place, the damages had been caused by an earthquake which had a period of about 0.7 sec and an amplitude of from 5.2 to 5.5 cm, in other words by the earth motion which had an acceleration of about 430 gal.

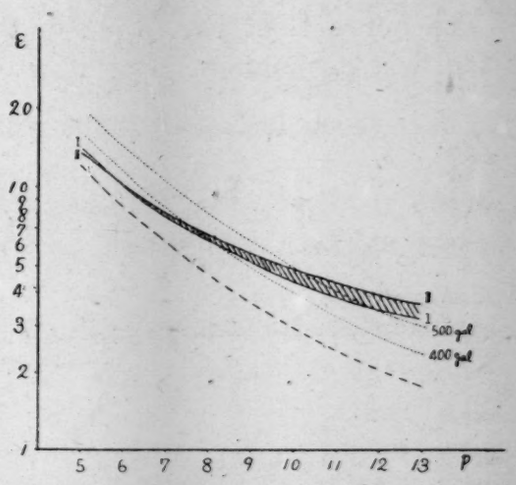

Fig. 2. Curve I and II show the limits of overturning and non-overturning of the grave-stone at Kainan-shi.
- - - - - - - - shows the acceleration
— — — — — shows the beginning of the rocking motion.

Tentatively, we will study how these grave-stones of two kinds move, when the ground motion which has $p = 9$ and $\varepsilon = 5.2$ cm is given.

For the purpose of mechanical integration, we transfer the equation (2) to the equation (11).

$$\left.\begin{aligned}
\frac{d\theta}{dt} &= -\frac{ag}{a^2+k^2}\sin(\alpha-\theta)(t-t_0)+\frac{a\varepsilon p}{a^2+k^2}\cos(\alpha-\theta) \\
&\qquad \times[\cos p(t_0+\delta t)-\cos p(t+\delta t)]+\left(\frac{d\theta}{dt}\right)_0 \\
\theta &= -\frac{ag}{a^2+k^2}\sin(\alpha-\theta)\frac{(t-t_0)^2}{2}+\frac{a\varepsilon}{a^2+k^2}\cos(\alpha-\theta) \\
&\qquad \times[p(t-t_0)\cos p(t_0+\delta t) \\
&\quad -\{\sin p(t+\delta t)-\sin p(t_0+\delta t)\}]+\left(\frac{d\theta}{dt}\right)_0(t-t_0)+\theta_0
\end{aligned}\right\} \quad (11)$$

By the equation (11), the relations of the angle θ of rotation of the grave-stones to the time t are calculated. These relations among θ and t are shown by Fig. 3. Namely, in Fig. 3, curve I shows the relations to the non-overturned grave-stone and curve II shows that to overturned one. When the ground motion which has $p = 9$ and $\varepsilon = 5.2$ cm is given,

we can deduce that the grave-stone of great width, which is in appearance hard to overturn, will be susceptable to rocking more than one of great height.

The curve II of Fig. 3 shows that the grave-stone does not overturn by the first declination. But if we took into considerration, the side-slip of the grave-stone when it declines, we can deduce that the earthquake motiohs at Kainan-shi from the data correspond to the hatched part in Fig. 2. Moreover, in Fig. 3, the given ground motion is shown by the dotted line.

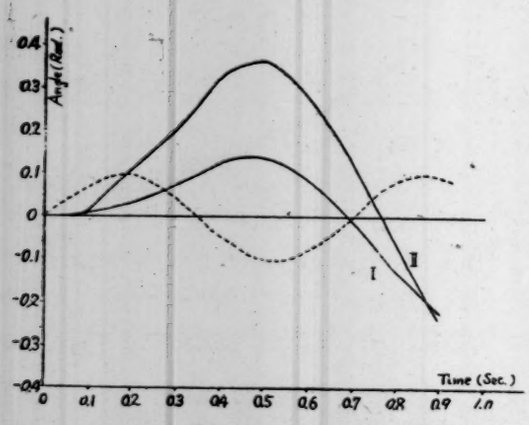

Fig. 3. Curve I shows the motion of the non-overturned grave-stone.
Curve II shows that of the overturned one.
.....shows the given ground motion.

(2) OVERTURNING AT KINOMOTO-SHI.

From the data at Kinomoto we calculate in a similar manner by equations (6), (7), (9) and (10), and obtained Fig. 4 by plotting these values.

In this case, we can deduce the amplitude of the ground motion from the hatched part in Fig. 4. If we assume the period of the ground motion to be about 0.7 sec (p = 9), its amplitude would be between 5.80 to 5.87 cm (maximum acceleration is about 474 gal), and if the period were about 0.62 sec $p = 10$), the amplitude should be between 5.3 to 5.4 cm (maximum acceleration is about 535 gal).

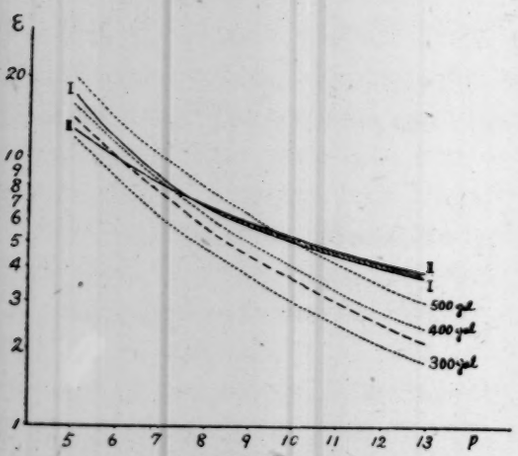

Fig. 4. Curve I and II show the limits of overturning and non-overturning of the grave-stone at Kinonoto-shi.

CONCLUSION.

To determine the magnitude of a great earthquake, it is necessary that proper seismographs are distributed in many places near the epicentre. But in the present circumstances we cannot expect such an ideal condition. Therefore, observations made of the rocking or overturning of comparatively

regularly formed bodies, for instance, grave-stones or stone-lanterns, have been utilized to determine the magnitude. At the same time this was usually deduced simply from the ratio of height and width of the body. But we believed that the estimation of magnitude deduced solely from the ratio of height to width was not complete, for we found at times that the grave-stone which had great height in comparison with width did not overturn, and on the contrary one which had great width did overturn.

We investigated the method which deduced the magnitude of earthquake taking advantage of these special phenomena and obtained the above mentioned results.

In the future, we hope that this method will be applied to investigate the magnitude of earthquakes.

11. *Strong Motion Vibrograph.*

By Nobuji NASU,

Earthquake Research Institute.

(Read Oct. 15, 1947.- Received June 20, 1948).

For the purpose of measuring strong vibrations, such as those of the railway bridges, or railway banks, due to the passage of trains, a new instrument has been constructed and tested. The size of the instrument is so minute that it can be installed in small places, for example, the top of the pier and the upper side of the main structural member of a bridge. Three component motions are recorded mechanically on a common recording drum, Figs. 1, 2 and 3.

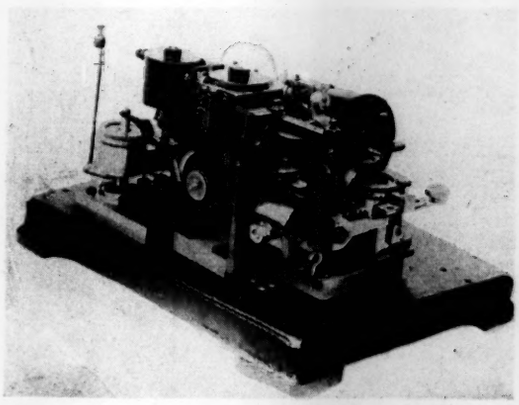

Fig. 1. Strong motion vibrograph.

Fig. 2. Vibrograph installed on a plate girder bridge.

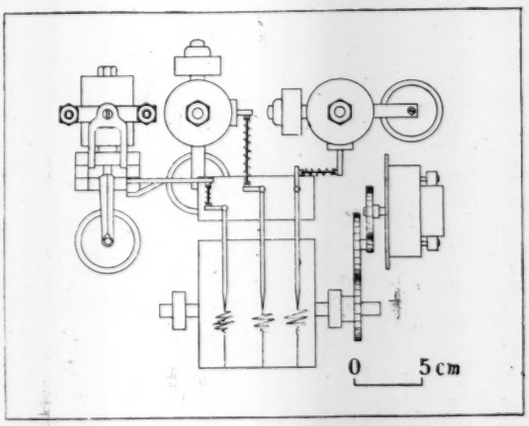

Fig. 3. Arrangement of pendulums and record-receiver.

The horizontal component pendulum has the type of an inverted pendulum as shown in Fig. 4. The axis of rotation is kept constant by the use of the crossed-strip coupling: the strips of each pair lie in a plane, and two planes are arranged at right angles. The movable part of

the pendulum is held in place by these strips with such stiffness as to give a period of 0.4 second. This type of axis of rotation is preferable for the instrument used in the measurement of strong vibration. The bob of the pendulum weighs 1.5 kg., which would be the minimum to overcome friction. To obtain damping, an air-damper is used. But, if desired, it can be secured by means of a liquid-damper. In this case, another piston is used, which moves in either oil or water filled in the

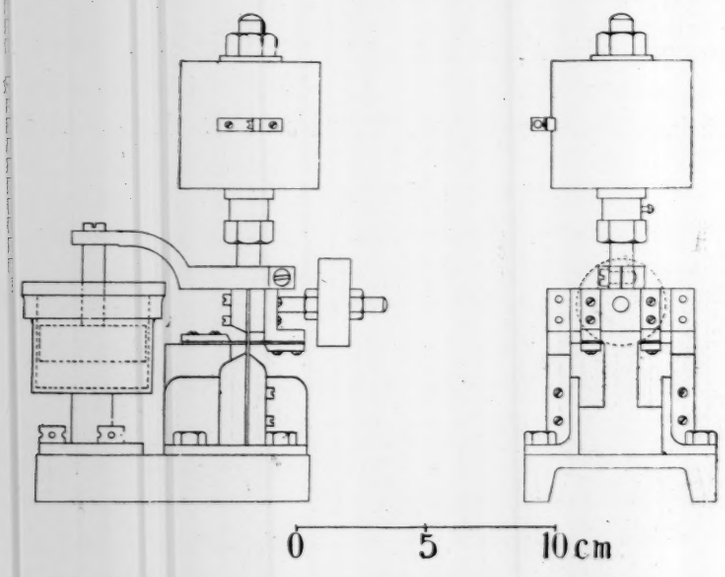

Fig. 4. Horizontal component pendulum.

same receptacle as that of the air-damper. Of course, the clearance between piston and cylinder must be properly chosen according to the fluid employed. Although, the liquid-damper is more or less inconvenient in transportation, it may be sometimes more practicable than the air-damper which necessitates fine adjustment.

In the vertical component pendulum, Fig. 5, the movable part is suspended by a pair of herical springs, the lower ends of which are hooked to the bob of the pendulum weighing 1.45 kg. The damping device is the same as that of the horizontal component pendulum. The period of the vertical pendulum is also 0.4 second.

The motion of each component pendulum is multiplied by means of a lever having a magnification of seven which is suitable for the instrument used in the strong motion-work. In the multiplying lever, a contrivance is made to the index-end so as to be more elastic. Thus, it presses lightly the surface of the smooth paper which is lamp-blacked in petroleum flame. Although, solid friction is increased to a certain

degree, the index-end otherwise is hardly in condition for recording the strong vibration. The index-end which is not made to press the paper is liable to skip when it subjects to the repetition of the strong and rapid vibrations. As the result, the tracing left by the index is not clear, because it is interrupted at places. The pressure at the end of

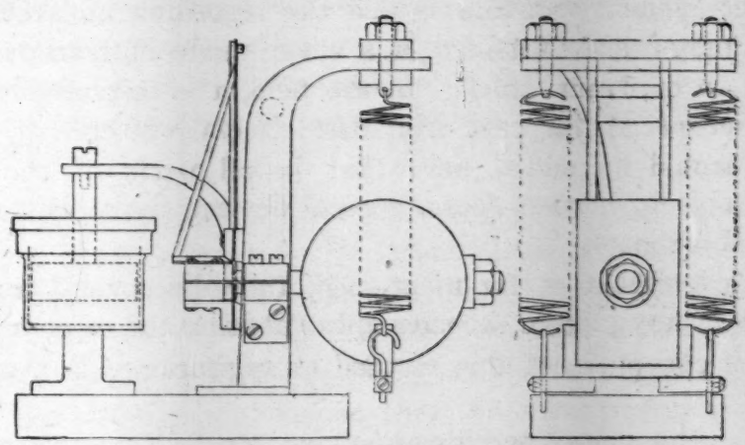

Fig. 5. Vertical component pendulum.

the index, however, should not be so large as the motion of the pendulum is visibly obstructed. To avoid the risk of demolition, the index-end must be held up so that it does not touch the smoked paper when the recording drum is put in or removed from its holder. The contrivance for this purpose is shown schematically in Fig. 6, where P is the index-end; F the small framework supporting the index at the pivotted ends, EE', of the axle. With certain limitations, this framework can turn upward about axis A without injuring the junctions of the short arm of the writing index and the pendulum-bob.

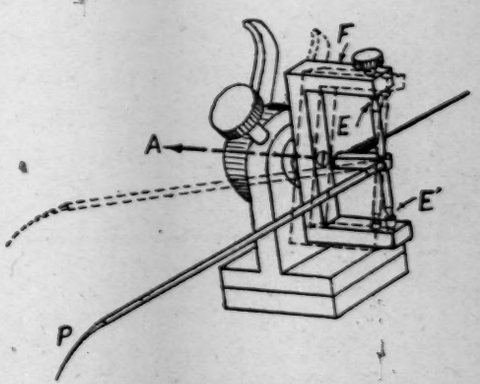

Fig. 6. Framework supporting index.

The recording drum, 10.4 cm. in diameter and 9.4 cm. in length, is driven by a Warren motor, operating on 100-volt, 50-cycle alternating current drawing 6 watts power. But, to secure independence from this current, another source of power has to be used, such that the direct current from an ordinary 6-volt automobil storage battery is transformed to 100-volt alternating current by means of a transformer equipped with a vibrator operated at a fre-

quency of 63 per second. In the former case, the speed of registration is 19.5 mm./sec., while in the latter it is 24.5 mm./sec. By means of a deep helix cut in the spindle the drum is made to translate sideways as it revolves by 7 mm. per revolution so that the registration continues for about 30 seconds.

Three component pendulums and the recording apparatus including the driving motor are contained in a cover made of transparent organic glass plates 10 or 6 mm. thick. In the field, the instrument is fastened to the structure at its cast iron base, 30 cm. × 39 cm., by sea-clamps, Fig. 2. It should be added here that in all parts of the instrument which are liable to become loose, special devices have been made to get rid of this objection.

In the instrument so far mentioned, there lie several troubles which are common in any kind of seismographs adopting the mechanical registration, yet the cheapness of this method of registration is a great recommendation.

Recently, the writer and his assistants, Mr. S. Kawashima and others, made the measurements with this instrument on a plategirder bridge and a bank of the railway. By these measurements, we could successfully determine the natural period and the decay constant of the free vibration of the bridge and further, the attenuation of the ground motion with increasing distance from the center of the track.

12. *On the Damages to Buildings due to Earthquakes.*

By Kiyoshi KANAI,

Earthquake Research Institute.

(Read Oct. 15; Nov. 17, 1946, Jan. 21; May 20; Oct. 21; Nov. 18; Dec. 16, 1947.—Received June 30, 1948.)

1. The problem of destruction of a building due to great earthquakes were investigated experimentally by Omori, Imamura and others[1]. The mathematical treatment of it was made by many authors: Sano, Suyehiro, Majima, Mononobe, Muto, Taniguchi, Sezawa, the author and others[2]. From our past investigations[3], owing to the dissipation of vibrational energy into the ground, we showed that the resonance amplitudes may be smaller by increasing the effective stiffness of a structure relative to that of the ground. The same problem was dealt with experimentally by Ishimoto[4] and Saita taking into account of the vibratory motion of the ground. They concluded that the damages to the buildings due to earthquakes will be mostly depended on the proper predominant period of seismic vibrations on each ground.

But the standpoints, on which these authors are based, are mainly to apply the principle of pure vibration problem. As a matter of fact, the dynamical actions causing damages of the buildings subjected to earthquake are not steady pure vibrational force.

The first section of the present paper discusses theoretically and model experimentally the transeint vibration problem of a structures, and the second section shows that there were large number of damages to buildings caused by the unequal settling of foundation with the data of the past great earthquakes of 1891-1947. whereas for the third section, we investigated theoretically the special cases of earthquake-damages to Japanese-style buildings.

2. *The transient vibration problem of a structures.*

In order to clear the vibrational mode of a structures subjected to the earthquakes, we investigated theoretically the shearing motion of

1) See the *Rep. Earthq. Inv. Comm.*
2) See the footnote of the *Bull. Earthq. Res. Inst.*, **10** (1932), 767.
3) K. Sezawa and K. Kanai; *Bull. Earthq. Res. Inst.*, **13** (1935), **14** (1936).
4) M. Ishimoto; *Bull. Earthq. Res. Inst.*, **10** (1932)—**14** (1936).

the structure from the transient point of view. We used Heaviside's operational calculus in solving the problem. These results were ascertained model experimentally by means of the vibration table. The model is the singled-storied, one-span framed structure which has construction of two thin steel plates and one thick wooden plate. The results of the experiments are shown in Fig. 1.

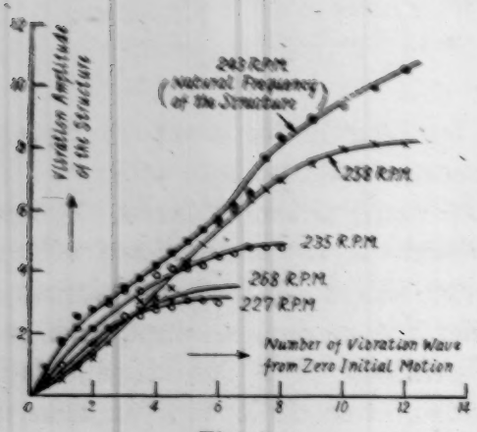

Fig. 1.

These investigations showed that the motion of a structure reaches to the maximum amplitude by repeating several times the displacement of the ground with zero initial displacement, when the period of displacement of the ground differes from the natural period of the structure, while the motion of a structure does not approach to the asymptote even by repeating more than one hundred times the displacement of the ground with zero initial displacement when both periods are equal, that is, in a resonance-like condition.

The observed fact in connection with the vibrational mode of some structures caused by the Nankai earthquake of Dec. 21, 1946, which were made by a few attentive people of Kochi city in the seriously damaged region, are seems to fairly agreed with the results of this section.

3. *Dynamical actions causing damages of the structures due to earthquakes.*

Investigations in the area devastated by past three great earthquakes[1] were carried out by us from the point of view of finding the relation between damage to buildings caused by the earthquakes and the motion of the ground. From these investigations, we found out that the serious damage to Japanese frame houses situated on the soft ground at the time of the great earthquakes were originated not only from the coincidence of the natural periods of the houses and the soft ground or from the large vibrational amplitudes of the soft ground, but also in that the soft ground beneath the buildings are liable to yield unequally.

In order to make more clearly the dynamical actions causing damages

1) Nagano Earthq. of July 15, 1941, Tōnankai Earthq. of Dec. 7, 1944, Nankai Earthq. of Dec. 21, 1946.

of the structures by the earthquakes, we studied the relation between the totally-destructed and semi-destructed buildings and the ground conditions with the data of the past great earthquakes of 1891-1947. The relation of them are shown in Fig. 2.

In this figure, the notation of TOTALLY, SEMI and NUMBER represented the number of the totally-destructed, of the semi-destucted houses at each village or town, and the number of villages and towns respectively. From the above investigation, we found that the damages to buildings subjected to pure vibrational forces had occurred mainly on the rigid ground with safe or else totally-destructed buildings, whereas the damages to buildings caused by the unequal settling of foundation arose mostly on the soft ground with large number of semi-destructed buildings.

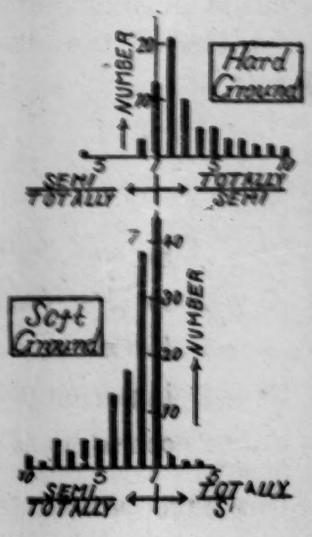

Fig. 2.

4. *Theoretical investigation to the special cases of earthquake-damages to Japanese-style buildings.*

We have calculated the maximum bending moment of the column and the acceleration of the top of a single-storied framed structure with endless extent of the series of successive spans. The notations used are as follows...y; transverse deflection of the columns, m; concentrated mass at floor, E, I, ρ, a; Youngs modulus, sum of moment of inertia of crossection, density, and sum of crossectional areas of the columns respectively. The equation of motion of the bar is expressed by

$$EI\frac{\partial^4 y}{\partial x^4}+\rho a\frac{\partial^2 y}{\partial t^2}=0. \qquad (1)$$

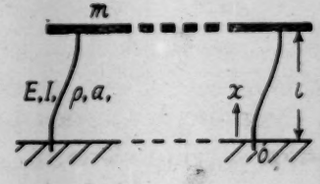

Fig. 3.

When the bottom of each column is oscillating horizontally with amplitude ξ and with period $2\pi/p$, the boundary clamped conditions at the bottom, are written by

$$x=0; \qquad y=\xi\cos pt, \quad \frac{\partial y}{\partial x}=0. \qquad (2),(3)$$

If the roof construction is extremely rigid, the clamped boundary conditions at the top may be written as follows;

$$x = l\,; \qquad m\frac{\partial^2 y}{\partial t^2} - EI\frac{\partial^3 y}{\partial x^3} = 0, \quad \frac{\partial y}{\partial x} = 0. \qquad (4), (5)$$

Substituting the solution of (1) in the conditions (2)–(5), and writing $n^4 = \rho a p^2/EI$, $\nu = m/\rho a l$, we get finally the equation of the ratio of the maximum bending moment of the column (B. M.) and the acceleration of the top of the cloumn (Accel.). The above equation becomes as follows:

$$\rho a l^2 \frac{Accel.}{B.\,M.} = \frac{(nl)^2 Q}{P\max.} \qquad (6)$$

where

$$\left.\begin{aligned} P &= A\cos nx + B(\sin nx + \sinh nx) - C\cosh nx, \\ Q &= A\cos nl + B(\sin nl - \sinh nl) + C\cosh nl, \\ A &= 2\sinh nl\cos nl + nl\nu(\cosh nl\cos nl - \sinh nl\sin nl - 1), \\ B &= 2\sinh nl\sin nl + nl\nu(\cosh nl\sin nl + \sinh nl\cos nl), \\ C &= 2\cosh nl\sin nl + nl\nu(\cosh nl\cos nl + \sinh nl\sin nl - 1). \end{aligned}\right\} \qquad (7)$$

We have plotted the results of the numerical calculations in Fig 4. In this figure, the vertical strips indicate the natural frequency of each cases.

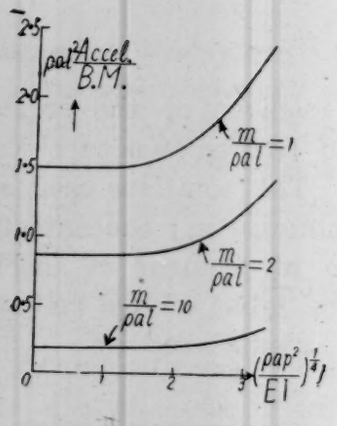

Fig. 4.

From this mathematical investigation, it may be seen that the heavy house-top will be liable to fail the vertical members of a building, and roof tiles will be liable to fall at higher frequency of seismic disturbances such that seismic vibration on the rigid ground. We do not doult that these results will be useful to explain various conditions of earthquake-damages to Japanese-style buildings.

5. *Concluding remarks.*

It will be seen from these studies that the dynamical reasons of the damages to Japanese-style buildings at the time of earthquakes are of two kinds, one being of the condition subjected to pure vibrational forces and the other of the secondary condition caused by seismic vibrations, namely, of the unequal settling of foundation of the building.

In conclusion, I wish to express my thanks to Messrs. T. Tanaka, T. Suzuki and S. Kaneko, who assisted me much in the course of the present investigation.

13. *Recent Activities of Volcano Usu (I).*

By Takeshi MINAKAMI,

Earthquake Research Institute.

(Read September 19, 1944.—Received June 30, 1948.)

According to the ancient chronicle, Volcano Usu erupted four times up to the year 1853, namely, July 1662, December 1768, November 18, 1822, and March 1853. All these eruptions occurred on the upper part of the southern somma about 300–400 m above sea-level. While active in November 1822, a large amount of mud and detritus outflowed from the explosion-craters and buried villages situated on the southern foot of the volcano.

A complete and comprehensive report[1] of the eruption of July—August, 1910, was submitted by the late Prof. F. Omori. According to his report, severe earthquakes lasting four days were followed by violent explosions from many a number of newly opened craters at the northern foot of the volcano. On the other hand, the ground surrounded by these craters rose rapidly during August—November 1910, attained the height of 160 m above the surrounded area. In this eruption, as in the previous one, ejecta were only detritus, mud and muddy ash, and neither new lava nor incandescent bombs were found. Since that eruption, no information was available for the subsequent 34 years.

The present activity started on December 27, 1943, with numerous series of severe earthquakes which were most strongly percepted during the period December 1943 and January 1944, by the people at Dôya Hot Spring located at the north-western foot of the volcano. But, as soon as the seismic activity on the north-western foot of the volcano gradually came to an end in February 1944, a great number of extremely shallow earthquakes occurred at the eastern foot of the volcano, in vicinity of Yanagiwara and Hukaba, villages shown on the map (Fig 1), and simultaneously the ground near the epicentres where had been 50–70 m above sea-level, began to rise rapidly as seen in Fig. 3 and Fig. 4. As the result of this rise, numerous cracks and fissures appeared on the earth's surface. Road, canals, the Osaru River and its tributaries, run from north to south through the rising area. Due to remarkable

1) F. Omori; *Bull. Earthq. Inv. Comm.*, **5** (1911).

upheaval and huge cracks of the earth, canals, rivers and railroads were cut at several points rendering the area in question impassible.

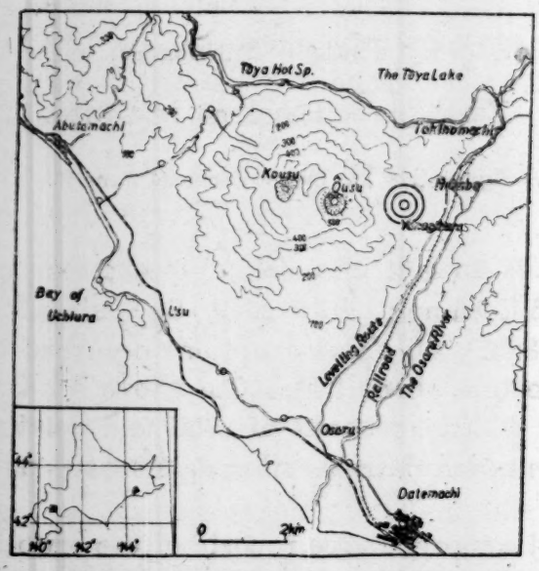

Fig. 1. Geographical map near Volcano Usu.

To study the topographical deformation, over 40 levellings along the eastern foot of the volcano were carried out during the period between March, 1944 and August, 1945. The summarized results of these levellings are illustrated in Fig. 2 and Fig. 3; in which the former shows the daily rising rate of the ground along the levelling route in 24 periodic intervals; and the latter the total rise in five periodic intervals. In addition to these levellings, triangulation and extensometric surveys at various spots on and around the area were carried out for accurate study of the topographical deformation prior to and in the course of the present outburst.

After the seismic activities and the remarkable upheaval lasting six months, the upheaval at the center of the rising area reached about 50 m on June 23, 1944, when at last the first explosion took place near the center of the rising area. The explosions lasted till the end of November, 1944. Of these explosions, the ones of June 23 and 28, July 1, 3 and, 11 and August 1, and 5 were remarkable in their volume of ejecta, as shown in the following (Table I).

These ejecta thrown out by the eruptions during the period June ~November were only detritus, mud and muddy ash, but no incandescent lava-fragments were found.

Although in these explosions, several craters were newly opened near the first crater on June 23, 1944, some of them combined one another and became a large crater.

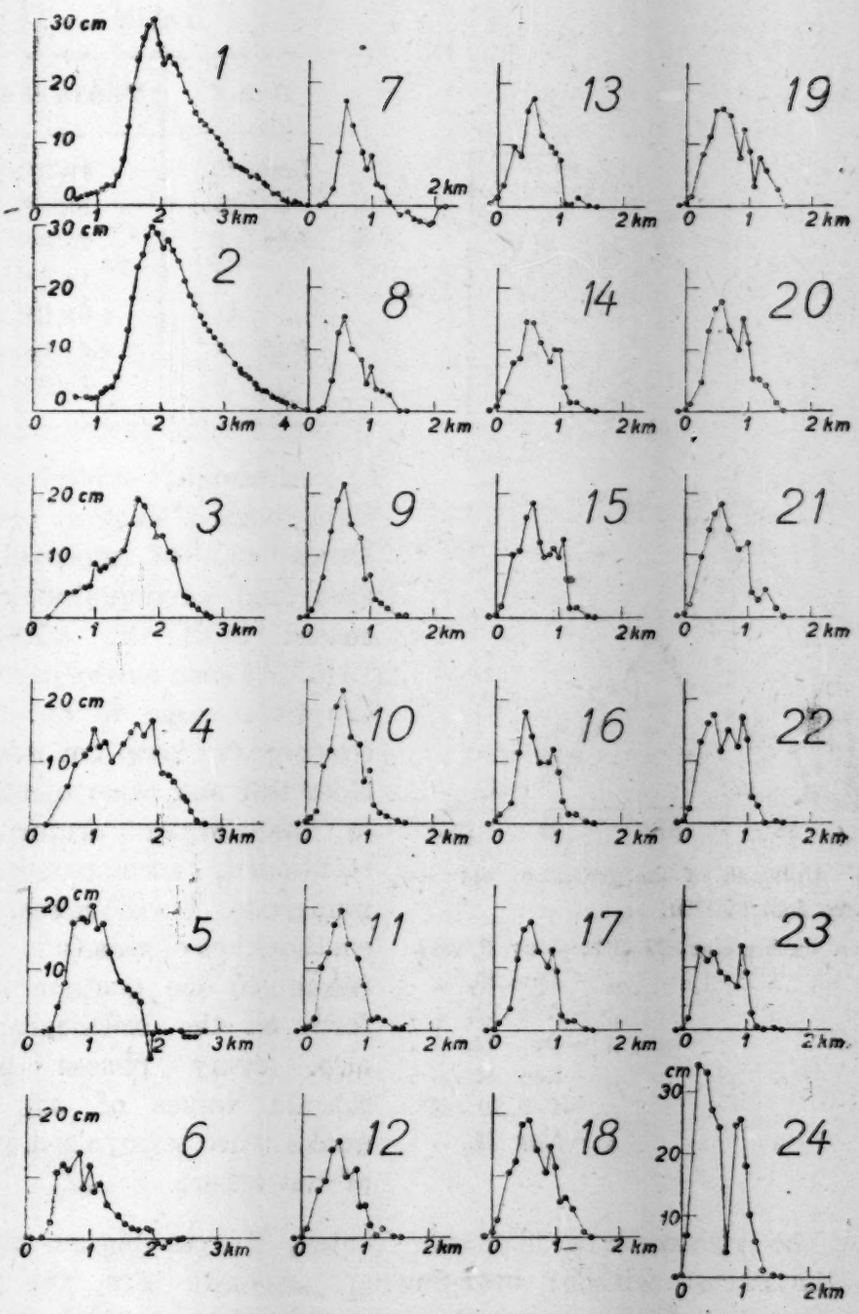

Fig. 2. Daily velocities of upheaval at the eastern foot of Usu.

(1)	Mar. 18, 1944	(9)	Aug. 29, 1944	(17)	Jan. 9, 1945
(2)	Apr. 4, ,,	(10)	Sept. 16, ,,	(18)	Jan. 21, ,,
(3)	Apr. 27, ,,	(11)	Oct. 4, ,,	(19)	Feb. 3, ,,
(4)	May 12, ,,	(12)	Oct. 27, ,,	(20)	Feb. 17, ,,
(5)	May 30, ,,	(13)	Nov. 10, ,,	(21)	Mar. 4, ,,
(6)	June 16, ,,	(14)	Nov. 23, ,,	(22)	Mar. 19, ,,
(7)	June 24, ,,	(15)	Dec. 4, ,,	(23)	Apr. 29, ,,
(8)	July 13, ,,	(16)	Dec. 31, ,,	(24)	May 16, ,,

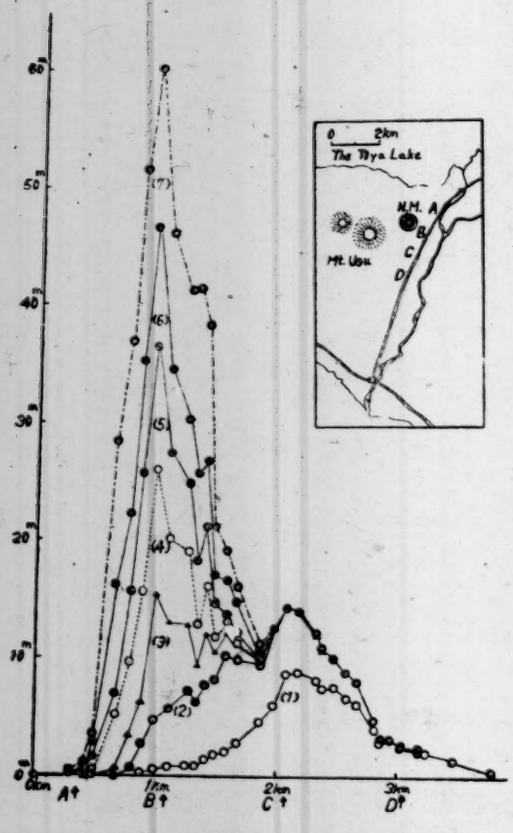

Fig. 3. Upheaval of the ground at the eastern foot of Usu.

(1) Upheaval during Mar. 29, 1944~May 2, 1944.
(2) ,, ,, ~June 20, ,, .
(3) ,, ,, ~Aug. 21, ,, .
(4) ,, ,, ~Oct. 11, ,, .
(5) ,, ,, ~Dec. 14, ,, .
(6) ,, ,, ~Feb. 10, 1945.
(7) ,, ,, ~May 19, ,, .

Table I.

Date	Volume of ejecta.
June 28	4×10^5 tons
,, 28	1×10^5 ,,
July 1	2×10^6 ,,
,, 3	1×10^6 ,,
,, 11	8×10^5 ,,
Aug. 1	1.6×10^5 ,,
,, 5	3×10^5 ,,

Although, explosive eruptions ceased entirely early in December 1944, upheaval of the area and earthquakes did not ceased until the autumn of 1945. As soon as the paroxysmal eruptions came to an end, incandescent lava covered with older tuff and other ejecta came in the former crater above mentioned, accompanying with numerous earthquakes. The earthquakes of this type not only resembled one another in their form on the seismograms but also every phases of the seismic waves of any earthquake were recognized in those of the others.

After the viscous lava filled the crater, it rose higher than the brim of the crater without over-flowing. At any rate, the present lava-dome hardly took seven months to the height of 80 m above the crater. On July 20, 1945, the center of the rising area reached about 200 m in upheaval and top of the lava dome was about 80 m higher than the former. The photographs in Fig. 5 show four stages of growth of the new mountain seen from the same spot at the north-eastern foot.

On the basis of its colour, the temperature of incandescent lava in the new dome was estimated at 900°–1000°C on July 20, 1945.

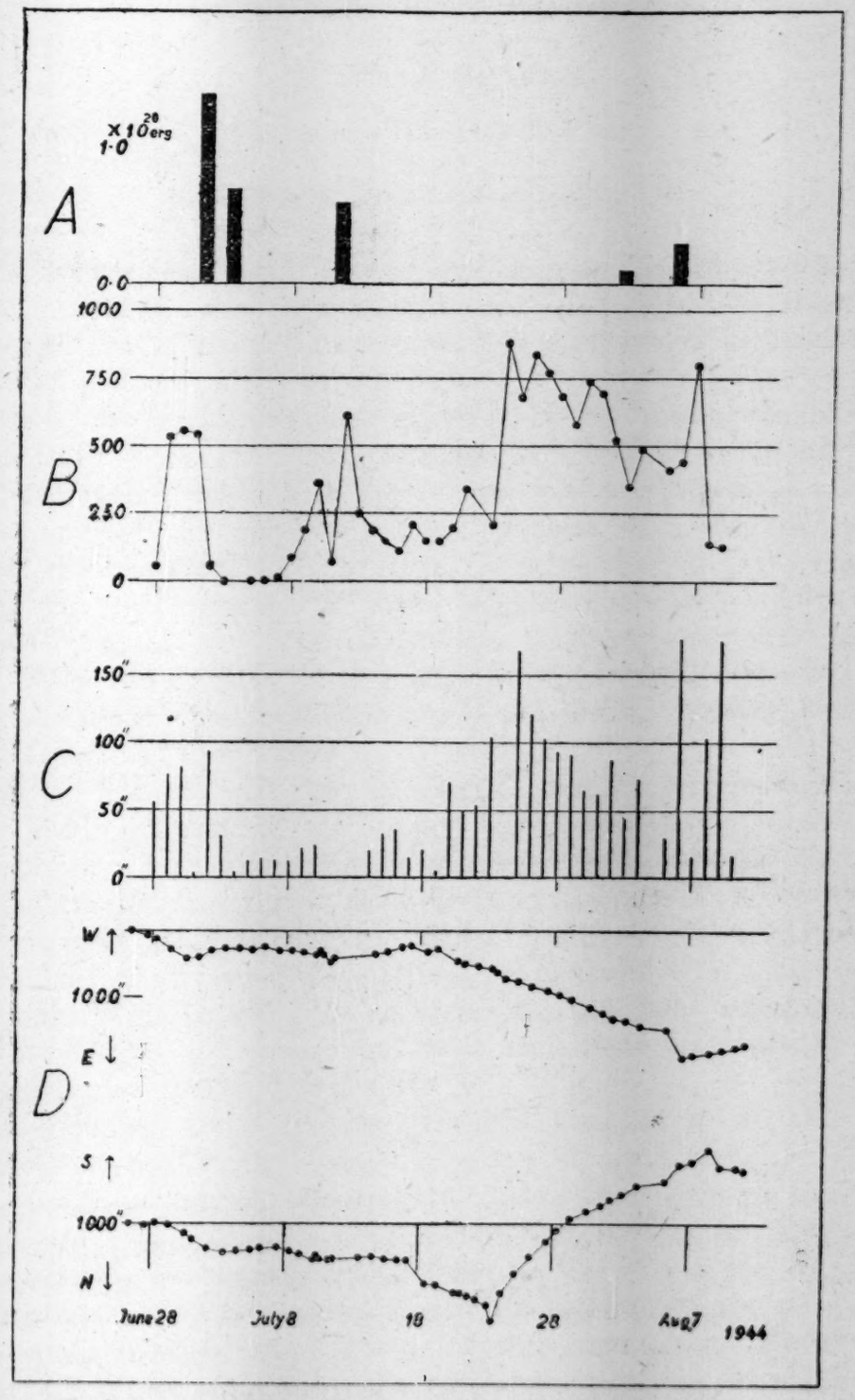

Fig. 4. Explosive eruptions, seismic activities and tilting of the earth's surface during July~August, 1944.

A; Energy of explosion.
B; Daily frequency of volcanic earthquake observed at Hukaba.
C; Daily rate of tilt at Hukaba.
D; Tilting at Hukaba.

14. *Recent Activities of Volcano Usu (II).*

By Takeshi MINAKAMI,

Earthquake Research Institute.

(Read May 18, 1948.—Received June 30, 1948.)

The writer carried out seismometric observations and tilt-observations on and around the new volcano at the eastern foot of Usu, during July —October, 1944. The outline of observations conducted during the above mentioned period is given in this paper.

Beside the continuous observations of tilt by means of spirit-levels set at Hukaba and Takinoue, and levellings covered the rising area, a set of four bench marks in a square form was established at 18 places on and around the upheaving area. Length of a side of these 18 squares is taken from 15 m to 40 m in proportion to the topography. Setting the Zeiss' level at the centre of the square where is the equal distance from the four bench marks, the heights of them were precisely observed by use of Zeiss' invar staff. During July 21, 1944—August 10, the observations were repeated 7 times and during October 3-12, they were carried out three times.

On the basis of variations of relative heights on the top of four bench marks, tiltings of the ground were made clear. As the result, it is remarked that two triangles separated by a diagonal line of the square show different tilts in their direction and magnitude, though their areas are very small as described above. On the other hand, the result of levellings on the same place shows the upheaval with almost constant rate in the same period. As an example, the daily velocities of tilt of two triangles of a square and those along four sides of the square are represented in Fig. 1 and Table I.

In order to know the topographical distribution of tilt at the eastern side of Volcano Usu, variations of inclinations at 18 spots in the period of July 21—October 10, 1944, are shown on the map in Fig. 2. In this map, tilts of a rectangular rombus at 18 places are represented by two vectors respectively, in which the one is tilt of a triangle formed by a diagonal line of the square and the other is that of the other triangle. At a glance of the geographical distribution of tilt, it will be seen that the marked deformation of the ground is limited in the narrow region and no remarkable crustal deformation took place at the north side of Usu. Consequently, the northern side of the new mountain has very steep, and the northern side of the new mountain

Table I. Daily velocities of tilt along four sides of the square at the spot No. 12.

	Date	N−E	W−S	S−E	W−N
1	July 23	+ 51″	+24″	− 8″	−32″
2	,, 25	+ 34	+15	− 4	−25
3	,, 27	+ 27	+17	−11	−21
4	,, 29	+ 28	+12	− 8	−24
5	Aug. 1	+ 21	+13	−20	−27
6	,, 4	− 3	+ 4	−23	−17
7	,, 8	− 46	−20	−41	−14
8	Sept. 7	−126	−43	−81	0.0
9	Oct. 4	−100	−65	−40	− 7
10	,, 8	− 97	−85	−37	−15

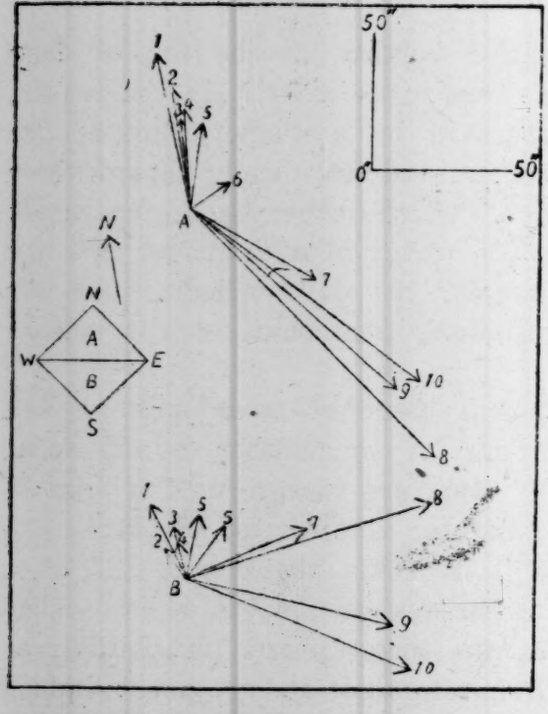

Fig. 1. Daily velocities of tilt of two triangular parts (A, B) at the station No. 12.

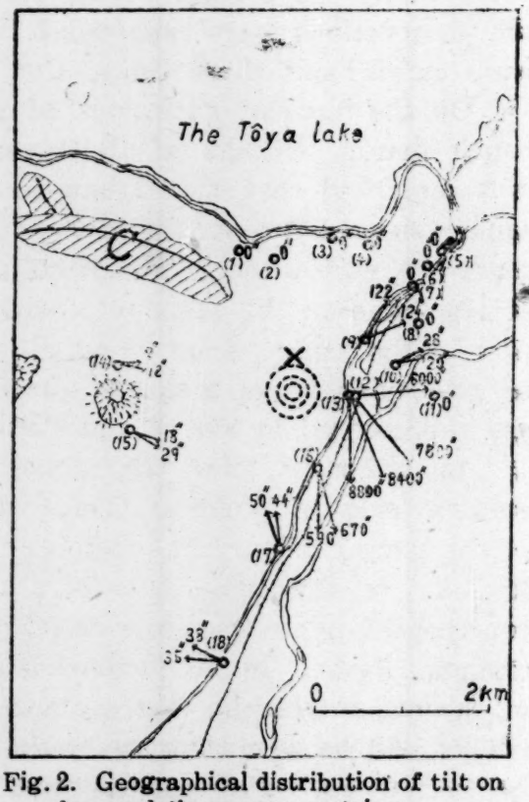

Fig. 2. Geographical distribution of tilt on and around the new mountain.
X; new mountain.
C; explosion craters in 1910.

where is only one km from the centre of the rising area, does not show tiltings of the earth's surface in the period. These characteristics of the topographical deformation harmonizes with the geological structures of the region in which the northern part of the new mountain is not the formation of the Usu ejecta, but is the older and more stable formation (Takinoue lava) than that of the southern part. As seen on the map of Fig. 2, the southern part of the new mountain which is located in greater distance than 4 km from the center of rise, is markedly disturbed by the present volcanic activities.

Table II. Tilts of two triangles (A, B) at 18 places on and around the new mountain during July 21,—October 10, 1944.

Places	A		B	
No. 1	0″		0″	
,, 2	0		0	
,, 3	0		0	
,, 4	0		0	
,, 5	0		0	
,, 6	0		0	
,, 7	0		0	
,, 8	0		0	
,, 9	122″	N 23° E	124″	N 66° E
,, 10	28″	N 59° E	20″	N 75° E
,, 11	0		0	
,, 12	6000″	N 84° E	7800″	N 141° E
,, 13	8400″	N 157° E	8800″	S
,, 14	9″	N 88° E	12″	N 99° E
,, 15	18″	N 120° E	29″	N 110° E
,, 16	670″	N 166° E	590″	N 179° E
,, 17	50″	N 20° W	44″	N 8° W
,, 18	38″	N 85° W	36″	N 60° W

During July to September 1944, a component of micro-seismographs was set at five temporary stations around the volcano, one of which was set at the station on the north-western foot, was operated during March, 1944 to July, 1945. On the basis of these seismograms at the five stations, positions of hypocentres of these earthquakes were studied in detail. The geographical distribution of hypocentres of the earth-

quakes occurred during July, 1944, is illustrated on the map in Fig. 3. In addition, in order to show the depth distribution of these hypocentres, they are projected on the vertical plane (ab in Fig. 3) as seen on the map (Fig. 3).

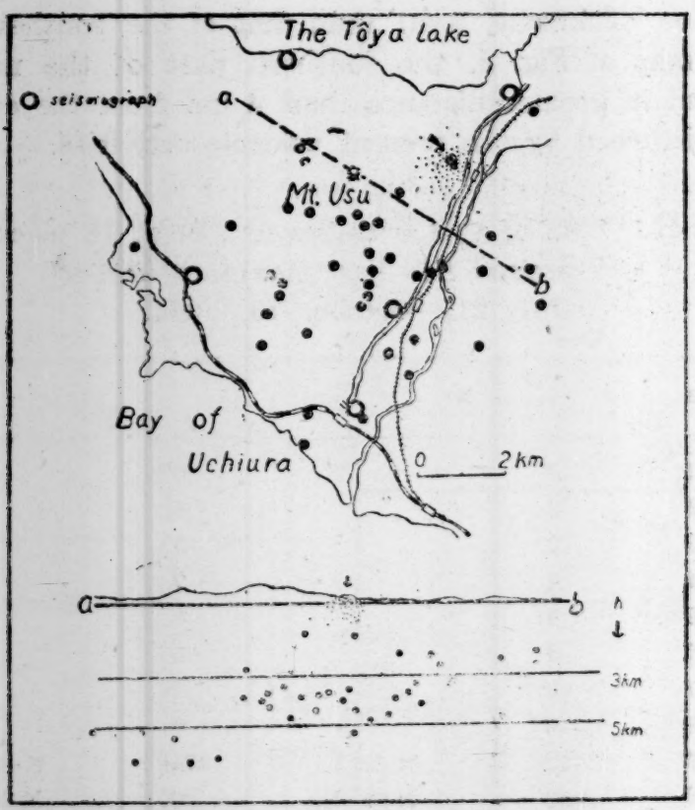

Fig. 3. Geographical distribution of hypocentres of the volcanic earthquakes during July, 1944.

As the map indicates clearly, no earthquake occurred at the northern foot of the volcano, where in 1910, many a number of craters newly opened. Moreover, it is remarked in Fig. 3, that these hypocentres in the western side of volcano Usu are deeper on the average than those in the eastern. As already described, severe earthquakes took place almost under the western side of the volcano at the beginning of the present activities. Though, it is impossible to show precisely on the map, a great number of the extremely shallow earthquakes less than 1.0 km in depth concentrated near the crater which is the center of the rising area.

On the basis of these seismometric and geodetic studies, and from various observations conducted on the present activity, it may be con-

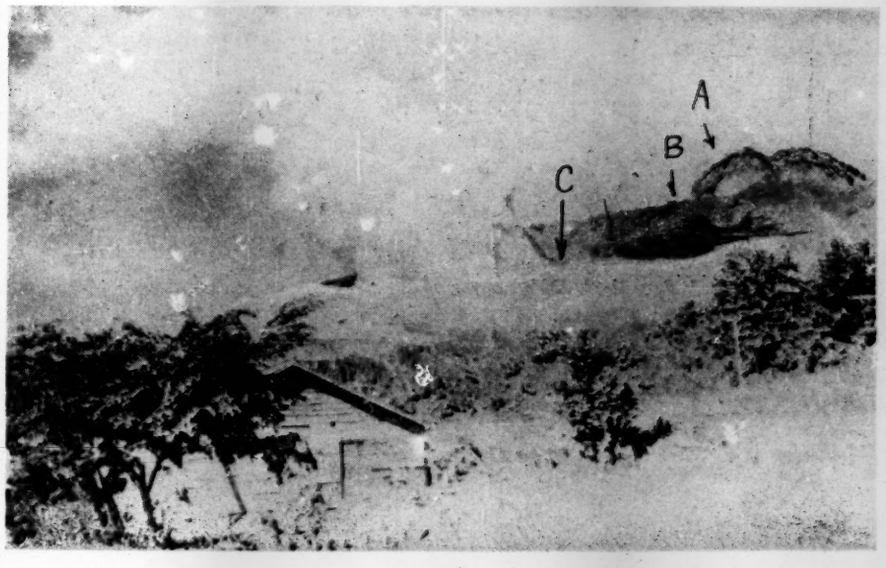

(a)

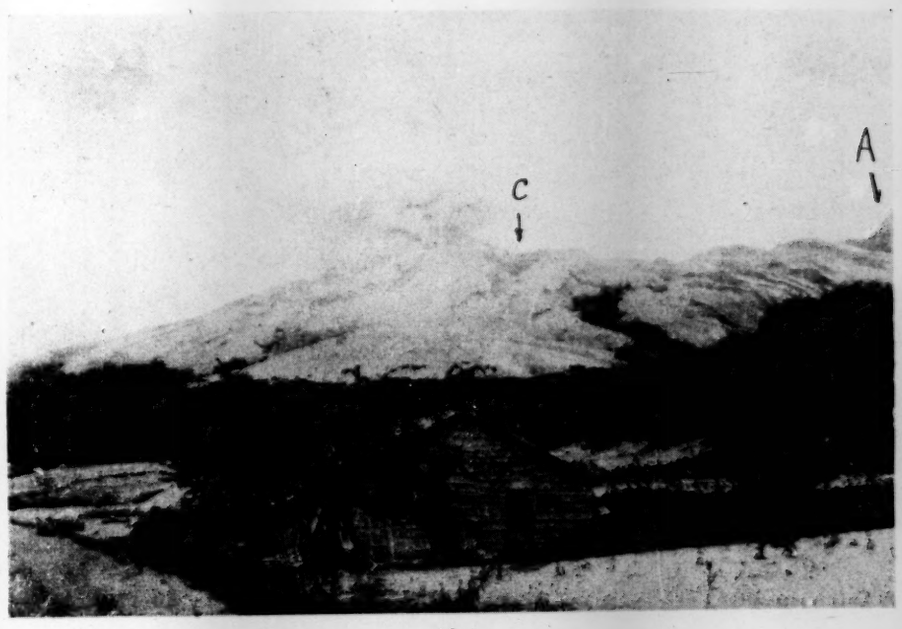

(b)

Fig. 5. Four stages of growth of the new mountain.

A, Ôusu (top of Volcano Usu). B; Somma.
C; New mountain. D; New lava-dome.
E; Hukaba (village).
(a) June 30, 1944, (b) August 10, 1944.

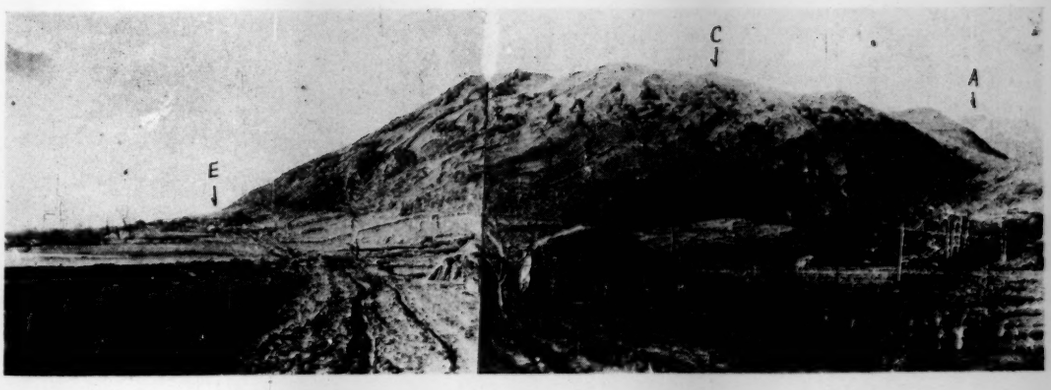

(c)

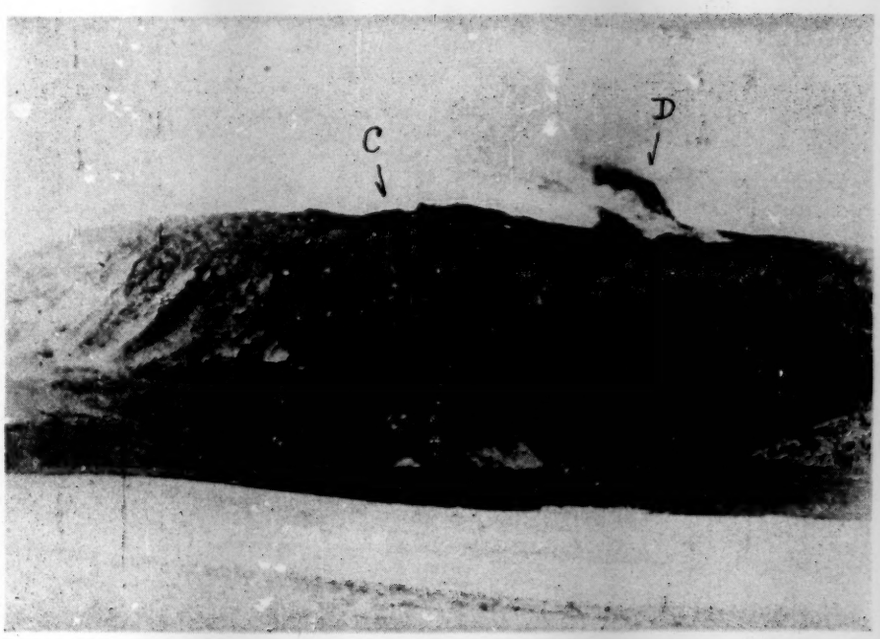

(d)

Fig. 5. (c) October 5, 1944. (d) July 10, 1945.

cluded that the present activity was caused by the intrusion and extrusion of the viscous lava: in other words, juvenile lava at the depth 1–3 km under the volcano, was intruded in the upper crust near the eastern foot of Usu and at last extruded on the earth's surface. Whereas, intrusion and extrusion of the lava which is such highly viscous as the one of the present Usu are possible only by the great pressure. Owing to such high pressure acting to the earth's ground on and around the volcano in the course of growth of the new lava-dome, numerous earthquakes and the large scale topographical deformations took place during this period. From the view-point above mentioned, it will be remarked that the rising area where is remarkable also in tilting of the earth's surface, harmonizes perfectly with the epicentral area.

Most of the expense necessitated for this study was defrayed from the funds for Scientific Research of the Department of Education.

15. *Land-slides at Nōdani and Nechi in 1947.*

By Shūzō SAKUMA,

Earthquake Research Institute.

(Read June 17, 1947.—Received June 20, 1948.)

Introduction.

Nōdani and Nechi are both situated in the Kubiki district, Niigata Pref., known for frequent land-slides from ancient times[1]. The localities of these two are shown in Fig. 1. In May 19, a fairly rapid land-slide attacked the Village Maseguchi in Nōdani, destroying more than 50 houses. Fortunately, it having occurred in the daytime, no human life was lost. At Nechi, another very slow land-slide was then progressing.

1. Nōdani land-slide.

Topography and geology. The topographies of Maseguchi and its vicinities can be seen in Fig. 1. The village is situated on the slope (20°–10°) between Mt. Gongen and the river Nō. Profile of the slope is somewhat stepwise and contour-lines around the slope show a horse-shoe-form. Thinking of geographical features of land-slide-region studied by Terada and Miyabe[2], they should be traces of past land-slides. In fact, about forty years ago, occurred a land-slide at the same place as today.

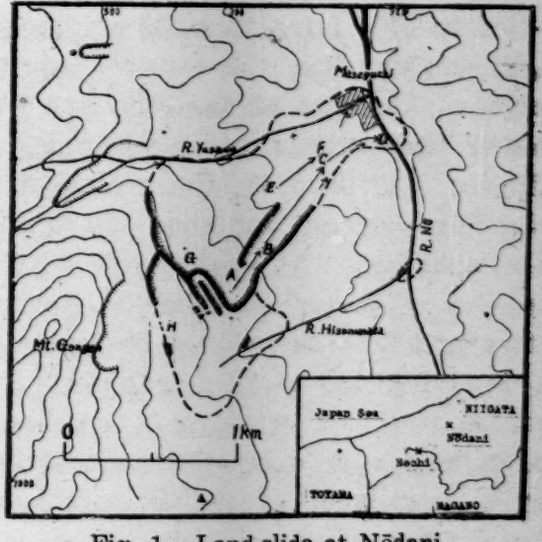

Fig. 1. Land-slide at Nōdani.

The Kubiki district is known for much snow, and at Nōdani the snow fell unusually in January and February in 1947 and still remained

1) T. Terada & N. Miyabe, *Bull. Earthq. Res. Inst.*, **10** (1932) 192, (In Japanese) K. Nakamura, "Yama-Kudure" (In Japanese).

2) T. Terada & N. Miyabe, loc. cit.

as deep as 4 m in March yet.

According to a geological map, Mt. Gongen is a huge block of hornblende-basalt, surrounded by sandy shales of tertiary formation which cover almost all of the Kubiki district. The boundary between them is about 500 m above sea-level, where the slope also changes abruptly. The upper end of the present land-slide coincides fairly well with this line.

Progress of the land-slide. Since two years ago, in spring, after the snow had melted away, it was noticed that the surface of rice-fields on the slope had tilted mainly towards the Yusawa. On April 14 of this year, an earthquake occurred, the epicentre of which was 4 km east of Maseguchi, where the seismic intensity was 4–5 of the C. M. O. scale. Due to the earthquake many cracks appeared on the snow, and springs and wells in the village became unusual and showed fluctuations in quantity and transparency since then. They say that mineral spring Shimamichi stopped and the temperature of hotspring Sasakura rose. These phenomena suggest that paths of underground-water changed at the time of the earthquake. After the snow had melted away, many cracks were found on the rice-fields. Especially to the south of line A-B-C in Fig. 1, north sides of cracks were found subsided. From the night of May 18, the water of springs in Maseguchi became unusually muddy. At dawn of the following day (19th), villagers were alarmed at finding that cracks had appeared during the night at the foot of Mt. Gongen. At 9h a. m. the ground near A and B crept down trees on it with a velocity of about 30 cm/min, but near the village no sign of slide was seen. At noon, surface-soil of land-slide broke into pieces at the end of a terrace near C (made by a past land-slide), mixed with water and flew down over the southern part of the village and arrived at the riverside in 30–60 minutes. Northern part of the mud-flow also arrived at the riverside in a few hours and dammed up the Nō. Houses on its way were destroyed and carried away to the river. In the evening a new layer of rather soft shale thicker than 6m appeared from beneath the soil which accumlated on the riverside. On the following day (20th), northern part of the village continued to slide down with a velocity of 1.0–1.5 m/hour, and new cracks were reported near Tamugidaira. On 23rd, one part of a cliff at the upper-reaches of the Hisonomata fell to pieces, ran down to Tamugidaira and dammed up the Nō again. Landslide wholly ceased on 24th.

Outline of deformation. The total area where cracks and slide were seen amounts to 1.2 km^2 (surrounded by broken lines in Fig. 1). Main

cracks are indicated by heavy lines. Main part of the present land-slide was the southern half, especially the area about 200m wide along A-B-C, where the surface soil was broken to pieces and no small crack remained. Beneath the new cliff, a new basin "A" in Fig. 1 was produced after the soil moved away. In the northern region, a number of cracks were seen, most of which showed that the lower part subsided and dragged the higher. Displacement of surface soil varies from place to place. From distances which trees and houses travelled, directions and absolute values of displacements were determined by simple triangulations with the aid of a handcompass. Results are shown with arrows in Fig. 1. Displacement amounts to 600m in maximum.

In the middle of Mt. Gongen, a band-shaped trace of slide of weathered soil could be seen on andesite (about 10m in width), which occurred after the basin "A" was produced. To the northwest of "A" another small basin (G) was noticed. Though no villager could tell when it was made, inferring from severe stone-rollings from cliffs above the place which happened in the afternoon of 19th, another land-slide might have occurred there at that time.

Possible causes of the land-slide & Conclusion. On the mechanism of the land-slide, the explanation presented by Miyabe[3] seems most suitable. That is, a land-slide occurs at the time when the pull of gravity of soil exceeds its friction and cohesion. It is found through many experiments[4] that coefficients of cohesion and friction of soil change greatly as water-content varies.

At the upper end of the land-slide there remained fragments of shale and at the lower end a layer of shale was seen beneath the broken soil. These facts suggest that shales contributed to the land-slide. Taking this into account, the course of this land-slide may be explained as follows. The shales became weathered and water-rich chiefly by slush-water, so the ground at the foot of Mt. Gongen slid little by little in every spring (at least for these three years). In addition to much snow of this year, the severe earthquake loosened the soil (consisted of weathered andesite) and changed paths of undergroundwater. Consequently, water permeated easily into the surface soil and a part of shale. And a slow land-slide occurred resulting fluctuations in the watersupplies. Meteorological phenomena which might acceralate the slide, for instance rise of air-temperature or rainfall, could not be pointed out. Land-slide of the northern region were caused by changes in paths of water and dragging

3) N. Miyabe, *Bull. Earthq. Res. Inst.*, **13** (1935), 85.
4) *Report of Soil Investigation Committee*, Vol. 2 (In Japanese).

due to the southern land-slide.

Generally speaking, the land-slide belongs to Type 3 associated with Type 2 in the classification of Miyabe[5].

2. Nechi Land-slide.

Topography. Ōkubo in Nechi has been threatened by land-slides for many years. At the foot of a fairly steep mountain Togura runs a low-pitched slope (10°–20°) down to a branch of a river Hime. The tertiary shale covers the slope and it inclined about 20° to the riverlet.

The land-slide. For these three years, the ground of the village continued to slide, so slowly that people became aware of it merely by cracks, deformations of their houses, changes of watersources and tilting of rice-fields. However, houses deformed more largely than before and long cracks were found on the slope in spring of this year. According to the result of a survey, sliding-region is 100–200m wide and 1.5km long. General features of deformations are subsidence of the higher side and lifting of the lower side. Maximum vertical dislocation amounts to 6m at southeastern side of the region. Horizontal movements were comparatively small and various in direction. One interesting proof of slide was traces of slippers of iron rails which passed through the sliding region and remained unremoved. As their traces on the soil went more or less out of shape by melting snow, ratio of displacement before and after spring could be roughly determined. According to that, velocity of slide increased to twice of the last year in this spring.

The mechanism of this land-slide seems to be the same as that of Nōdani.

In conclusion, the writer wishes to express thanks to Dr. Minakami for his encouragement.

5) N. Miyabe, loc. cit.

16. *Local Phenomena of Tsunami (Part 1).*

By Nobuji NASU and Toshiaki SHIRAI,

Earthquake Research Institute.

(Read Oct. 15, 1947.—Received June 29, 1948.)

The tsunami, that followed the big earthquake of December 21, 1946, attacked the western coast of the Kii-Peninsula and the southern coast of the Island of Shikoku, both being well known regions of frequent destructive tsunamis facing the Pacific Ocean. On this occasion, however, the waves were much smaller than those of the historical tsunamis of 1707, and 1854, in magnitude as well as in destruction wrought. Yet, 1496 houses were washed away by the present tsunami. As detailed descriptions of this tsunamis and the accompanied earthquake have been already published[1], it is not our intention to repeat them in this paper. But, as an addendum, this paper has been written based on the results of our leveling survey carried out in the districts which were of special interest in the study of tsunami.

As well known, the height and the velocity of tsunami wave are the important factors which determine the intensity of tsunami. Especially, the height is a large factor in the extent of the damage caused by the water. It, however, varies considerably with the geographical feature of the innundated area. Through the precise leveling, the fact has been well recognised in the last destructive tsunami of the northeast Japan of 1933. In a paper written by one of the writers[2] refering to this tsunami, he has pointed out that the water did not increase its height as it advanced inland, even though it rushed in the narrow part of the V-shaped harbor. Good example which was found in the present tsunami is the Bay of Kure in the Kochi Prefecture, Fig. 1. The bay is of the V-shape with its mouth facing the direction of seismic origin and the depth in the bay grows larger with increasing distance from the shore. However, our survey has revealed that the height of the water did not increase at the head of this bay where the town of Kure was situated, but it rather decreased as the water proceeded inwards. At Kamata, 2 km. to the east of Kure and situated halfway between

1) *Spec. Bull. Earthq. Res. Inst.*, No. 5, April, 1947.

2) N. Nasu, *Bull. Earthq. Res., Inst., Suppl.* Vol. 1, March 1934.

the mouth of the bay and its head, the height of the tsunami was 3.0 m., Fig. 2, whereas on the coast of Kure it was 2.3 m., Fig. 3.

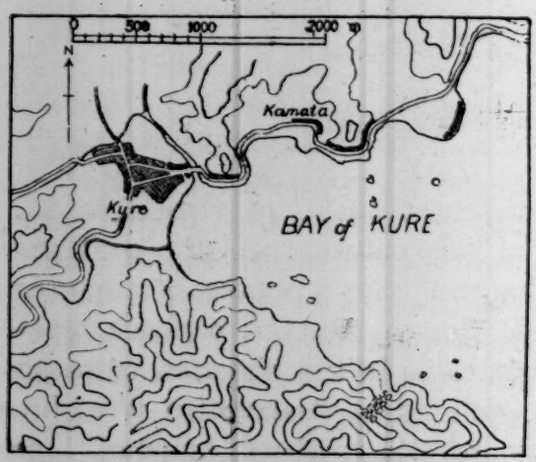

Fig. 1. Bay of Kure, Kochi Prefecture.

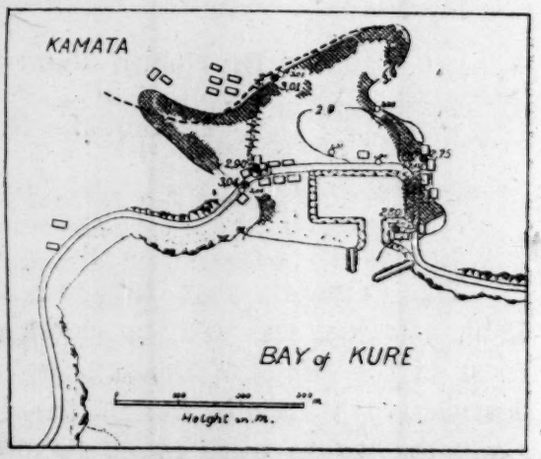

Fig. 2. Heights of tsunami at Kamata. (Dot indicates the point where the height of tsunami was measured. Boundary of invaded area is shown by lattice-shading.)

The waves invaded the town of Kure from the opposite side of the sea shore where a sand dune about 4 m. high existed. The water could not cross over it, but rushed up the river and flowed the low ground lying

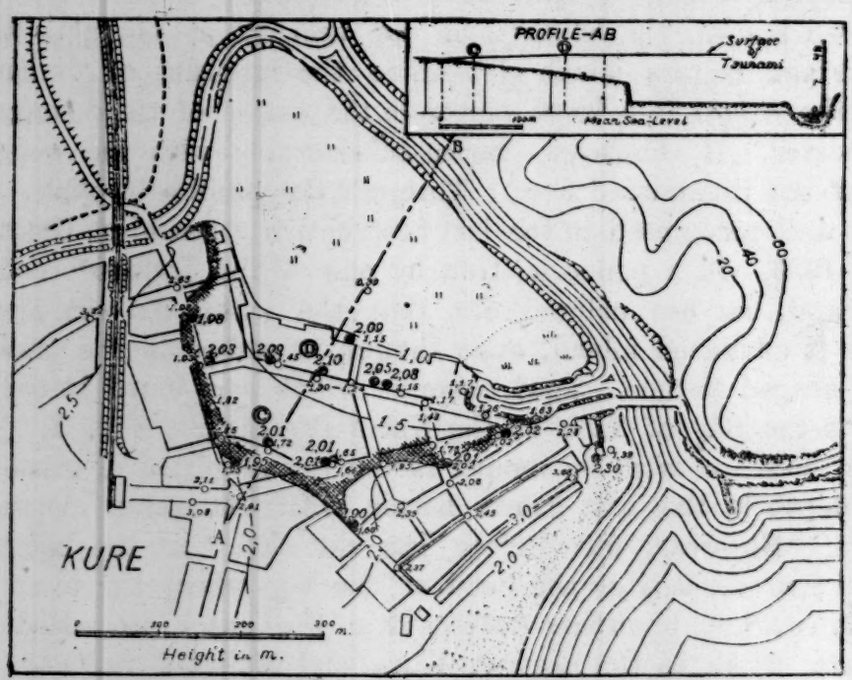

Fig. 3. Heights of tsunami at Kure, Kochi Prefecture. (Dot indicates the point at which the height of tsunami was measured. Boundary of invaded area is shown by lattice-shading.)

behined the dune. On entering the town, the waterfront, however was opposed until it was stopped approximately along the contour-line of the ground indicating 2 m. In profile AB, shown in Fig. 3, a head-loss of about 10 cm. can be seen between two points C and D, mutual distance being 110 m. A rough estimation of the velocity of the tsunami can be made as follows:

Let i be the mean inclination of the land and 3.81×10^{-3}; dH/dl be the rate of change in water-depth, H, with distance l and 4.64×10^{-3}; R be the hydraulic radius and 0.5 m.; C be Chézy's constant and 40 in this case. Putting in these values in expression, $dH/dl = i+v^2/(C^2R)$, we have $v = 0.82$ m/sec. Actually, the waves did not advance with such a large velocity as several meters per second which had been experienced in other regions suffered serious damage. This fact has been endorsed by an eye-witness who could escape from tsunami by walking fast just in front of the waves without being overtaken by them.

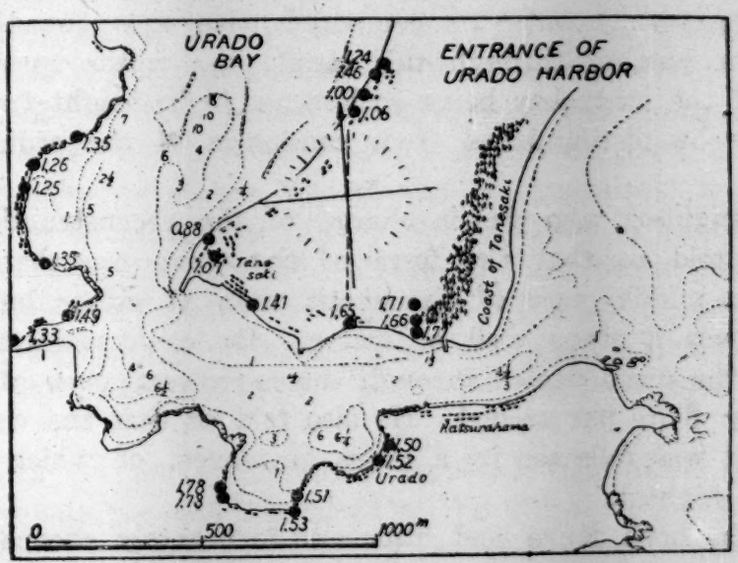

Fig 4. Heights of tsunami at the Entrance of Ura'o Harbor.
(Dot indicates the point where the height of tsunami was measured. Height of tsunami in m., depth of sea in fathom.)

Another example of the tsunami of which motion has been thought to be fairly influenced by the feature of bay or strait was that at Tanesaki, south of Kochi City. The mouth of the Urado Bay opens towards the east. Hydrographic map, Fig. 4, shows that in the bay near this mouth, the depths of the sea are less than 10 fathoms and those at the narrowest part are 4 fathoms in the maximum. The tsunami was not so energetic as it could cause serious damage, because its height had

already been diminished before it reached the mouth of this bay. Perhaps, it was lower than 3 m. The wave, however, has been reported[3] to be highest and 4.2 m. at Usa, 10 km. west of this bay, causing the severest damage on the coast of the Kochi Prefecture.

By the leveling survey of the heights of tsunami which was carried out along both coasts of the Urado strait, it has been found that there was a considerable change in height of water and further the height was rather increased on the shore which was attacked in front by the wave. The southern and western bay shores had several indentations and the water was heaped up to higher level than other places when it rushed in them. It is natural that the wave advances along a line of least resistance, that is, along the line joining the deepest points of the cross-sections of the strait. In this strait, however, the depth of the sea was larger at points near the southern and western shores than near the northern shore. Thus, the bulk of the water might advance along the former shores. Consequently the heights of tsunami on these shores were generally large as compared with those on the northern shore. After passing through this strait, the water spreaded over a wide area of the inner bay being so lessened in its height that its inrush could hardly be distinguished from coming-in of the ordinary tide or wind wave.

A civil-engineer who was in charge of the reconstruction work of this harbor told us that the form of the wave was that of a dome, higher at the middle part of the strait than at either bank and the wave-front was a steep wall of water. He could estimate the speed with which the wave passed through the narrowest part of this strait to be nearly 3 m. per second. He also told us that the wave was not single, but it was followed by a series of waves, of which the second one was the highest.

Although, both Kure and Tanesaki fortunately escaped from the havoc of the presest tsunami, it should be mentioned that in 1707, these places were totally destroyed by the attack of the seismic sea waves. At the latter place, the water attained to a height of 28 m. This history must not be overlooked when we try to mitigate the damage which will be wrought by the next tsunami.

---

3) S. Omote, *Spec. Bull. Earthq, Res. Inst.*, No. 5, April, 1947.

17. *Land Deformation of the Muroto Point before and after the Nankaido Great Earthquake on Dec. 21, 1946.*

By Takesi NAGATA, Earthquake Research Institute, and

Atsushi OKADA, Geophysical Institute.

(Read Dec. 17, 1946.—Received June 30, 1948.)

(I) The remarkably regular change in height of the Muroto Point of South-Eastern Shikoku and of the Shio-no-misaki point of Kii Peninsula before 1942 was noted with special attention by some investigators[1]; that is to say, both points had been sinking with almost constant rate, about 7 *mm/year* at the Muroto point and about 4 *mm/year* at the Shiono-misaki, at least during the period after 1895 when the first precise levelling surveys in their neighbourhood were carried out.

On the contrary, both points abruptly upheaved accompanying the Great Earthquake in the South-Western Japan on Dec. 21, 1946, the magnitude of upheaval at the Muroto and Shio-no-misaki amounting to about 95 *cm* and 60 *cm* respectively. The re-survey of precise levelling in the areas covering Shikoku and Kii Peninsula has begun just after the occurrence of the earthquake by Geographical Suruey Bureau of Japan, the results of this survey obtained until the present showing a striking regularity of the behaviour of land deformation accompanying the Great Earthquake.

The writers, on the other hand, repeated four times the precise levelling survey in the neighbourhood of the Muroto Point for the purpose of studying the progress of tilt in the said place after the Great Earthquake.

(II) The levelling route about 14 *km* long, from Bench Mark No. 5137 to No. 5144 in Fig. 1 in the neighourhood of Muroto Point was surveyed during Jan. 6–14 in 1947, about 20 days after the Great Earthquake, and again during Mar. 4–6 in the same year, while the route from No. 5136 to No. 5147, which is about 22 *km* in length and includes the above-mentioned route, was surveyed during Jan. 30-Feb. 4 and again during July 5–9 in the same year. Thus, the route from

1) A. IMAMURA, *Zisin* (*Earthquake*), **6** (1934), **9** (1937), 200.

No. 5137 to No. 5144 was surveyed four time after the earthquake. The instrument and method of each levelling survey followed the regulations for the first order levelling survey defined by Geographical Survey Bureau of Japan; that is, the closing error for the route $s\,km$ long should be less than $1.5 \times \sqrt{s}\,mm$.

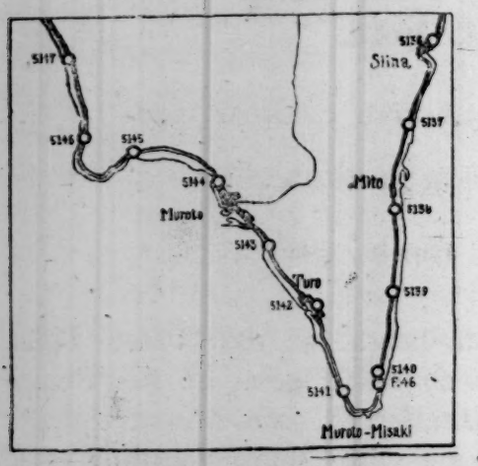

Fig. 1. Levelling route in the neighbourhood of Muroto Point. (1/200,000)

This levelling route was first surveyed in 1895, and again in 1929, and further the route along west coast of the peninsula alone was surveyed in 1935. For the purpose of showing the tilting motion in the neighbourhood of Muroto point, the results of those all surveys are given in Tables I and II and in Figs. 2 and 3, where Bench Marks No. 5137 and No. 5136 are respectively taken as the base-points, to which change in height of the other bench marks are referred.

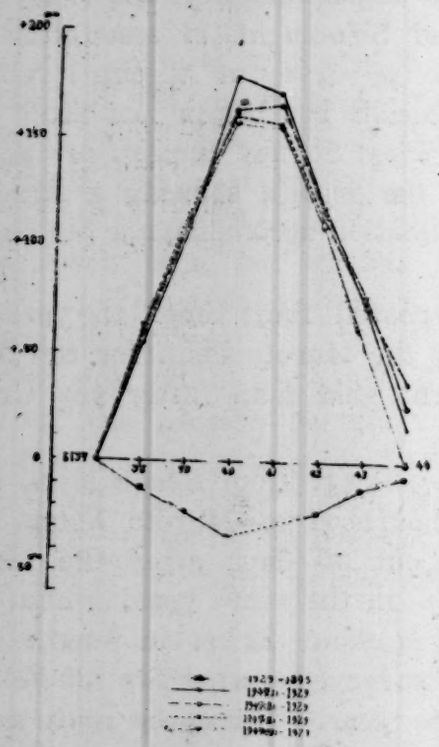

Fig. 2. Change in height of bench marks.

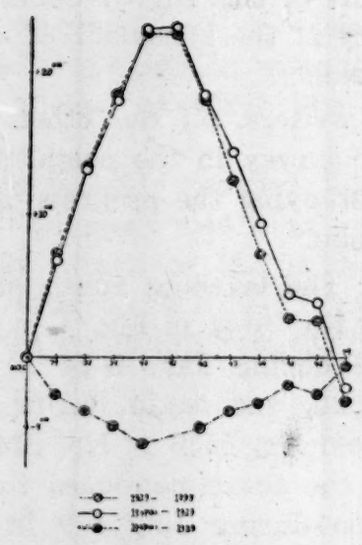

Fig. 3. Change in height of hench marks.

(III) The results given in Tables I and II being compared with the distribution of bench marks shown in Fig. 1, it will be seen that, generally speaking, the land in the neighbourhood of the Muroto point had continued to incline southward before the earthquake, while it abruptly inclined northward at the time of occurrence of the earthquake. The precise direction of tilting motion during 1895–1929 and that during 1929–1947, (practically almost all parts of the latter movement being a sudden tilt accompanying the earthquake), was determined by Miyabe's method[2], the result showing that the former tilt was in the direction of N10°W, while the latter was in the direction of S10°E, just opposite

Table I.

B.M.	1929—1895	1935—1895	1947 Jan. —1929	1947 Feb. —1929	1947 Mar. —1929	1947 July —1929
	mm		mm	mm	mm	mm
5137	0.0	— —	0.0	0.0	0.0	0.0
5138	−11.9	——	+ 54.7	+ 63.9	+ 63.7	+ 60.9
5139	−22.5	——	+108.6	+112.5	+113.7	+111.9
	mm					
5140	−34.1	0.0	+178.5	+163.5	+160.6	+157.0
5141	——	——	+171.0	+165.6	+156.8	+156.7
5142	−23.5	——	+118.8	+117.0	+113.0	+108.9
5143	−11.9	——	+ 71.9	+ 76.2	+ 74.3	+ 52.6
5144	− 6.4	+27.7	+ 16.2	+ 26.0	+ 37.0	− 0.3

Table II.

B.M.	1929 1895	1935—1895	1947 Feb. —1929	1947 July —1929	1947 July—Feb.
	mm	mm	mm	mm	mm
5136	0.0		0.0	0.0	0.0
5137	− 26.6		+ 67.8	+ 72.2	+ 4.4
5138	−38.5		+131.7	+133.1	+ 1.4
5139	−49.1		+180.3	+184.1	+ 3.8
5140	− 60.7	0.0	+231.3	+229.2	− 2.1
5141	——	——	+233.4	+228.9	− 4.5
5142	−50.1	——	+184.8	+181.1	− 3.7
5143	−38.5	— —	+144.0	+124.8	−19.2
5144	−33.0	+27.7	+ 93.8	+ 71.9	−21.9
5145	−19.9	+43.9	+ 43.5	+ 26.6	−16.9
5146	−26.1	+40.4	+ 37.5	+ 24.9	−12.6
5147	− 6.3	——	− 21.6	− 31.0	− 9.4

2) N. MIYABE, *Bull. Earthq. Res. Inst.*, **9** (1931), 256.

to the former case. Hence, the change in height of each bench mark along the route from No. 5137 to No. 5144 during 1895–1929; 1929–Jan., 1947; Jan., 1947–Feb., 1947; Feb., 1947–Mar., 1947; and Mar., 1947–July, 1947 are projected on a plane of N10°W-S10°E in direction, the results being shown in Fig. 4. As will be seen in this figure, the land around Muroto point is, generally speaking, again inclining southward after the earthquake, though it seems that undulations of short wave length superpose on the said general inclination, and further that the land is inclining also in westward direction especially during the period of March, 1947–July, 1947.

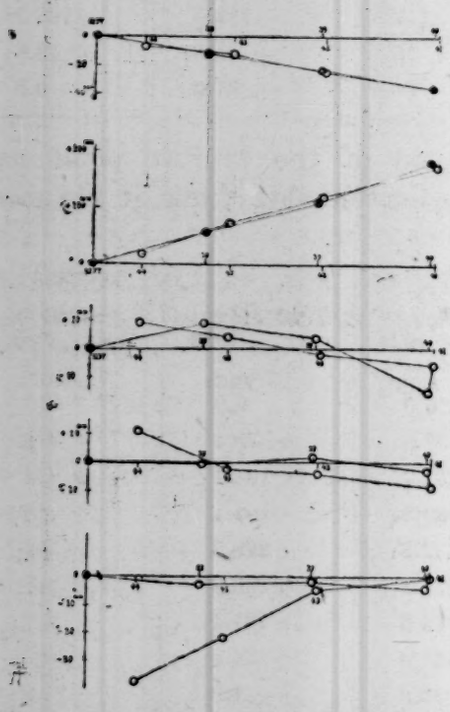

Fig. 4. Change in height of bench marks No. 5137~No. 5144, projected on a vertical plane in direction of N 10°W-S 10°E.

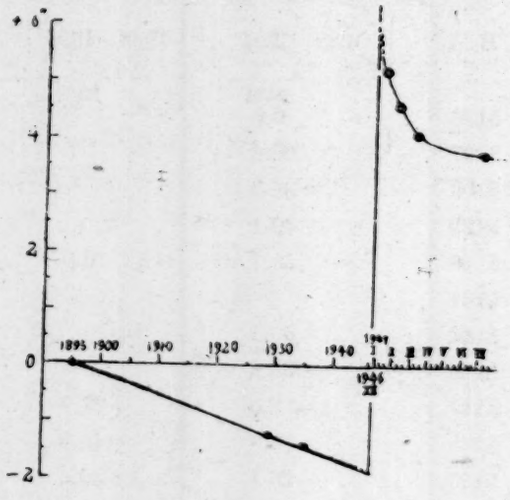

Fig. 5.

In Table III and in Fig. 5, the amount of tilt in the direction of N10°E at each epoch is summarized, where the corresponding value at 1935 was derived with reduction from the observed values along the west-side sea coast alone. It will be concluded here that the neighbourhood of the Muroto point had been inclining toward S10°E direction with nearly constant velocity of 0.0001″/day until, at least, 1935 and probably until the time little before the occnrrence of the great earthquake, and the abrupt tilting motion toward the reverse direction ac-

companying the earthquake exceeds 7″; while the land is now rather rapidly tilting again toward the direction of S10°E, the velocity of

Table III.

Date	Tilt in the direction of N 10° W-S 10° E	Change in Tilt	Mean Velocity
1895	0 (Assumption)		
1929	−1.2″	−1.2″	-1.0×10^{-4}″/day
1935	−1.4″	−0.2″	-0.9×10^{-4}
1947, I	+5.2″	+6.6″	——
1947, II	+4.6″	−0.6″	-3×10^{-2}
1947, III	+4.1″	0.5″	-1.7×10^{-2}
1947, VII	+3.8″	−0.3″	-2×10^{-3}

tilting motion is gradually decreasing with time, though it is much larger than that before the earthquake.

(VI) It must be mentioned that the mode of deformation of the land after the earthquake has been much complex compared with those before and accompanying the earthquake. This fact may be interpreted as that the upper parts of the earth's crust, which were much disturbed by the occurrence of earthquake, are recovering their new equilibrium individually, probably in the manner of movement of crustal blocks.

As to the westward tilt during March to July, 1947, the result of repeated surveys from No. 5136 to No. 5147, which is shown in Fig. 3, will give a clear picture. This result shows that west-side sea coast from No. 5142 to No. 5147 subsided remarkably during a few months before July, 1947. For the purpose of detecting the areal distribution of such land deformation as mentioned above, a new levelling route connecting Bench Marks No. 5137 and No. 5144 was set and surveyed in December, 1947. The triangular levelling route of No. 5137-No. 5140-No.5144-No.5137 will hereafter be surveyed intermittently, much more clear picture of the land deformation in the neighbourhood of the Muroto being expected from the results of this triangular-route surveys.

The most important problem here will be the dynamical cause of the said tilt, especially relating to the great earthquake and its after shocks. This point will be examined in future by careful and continuous surveys and studies.

In conclusion, the writers wish to express their sincere thanks to Ministry of Education for the grant received and to Mr. Y. Harada of Geographical Survey Bureau for his valuable help in the course of our surveys.

——所　　報——

○談話會記事

第230回談話會（昭和22年1月21日）

1. 南海地震に關する餘震、傾斜變動、地電流等の計測結果速報　永田　武
2. 南海地震の震害、概報　金井清、田中貞二、金子重彦
3. 南海地震による鐵道の被害概報　高橋龍太郎
4. 棒を傳はる撓曲波について　高橋龍太郎
5. 高橋伏見の方法による地震動の尾部の解析訂正　表俊一郎
6. 日本沿岸の大平洋深溝の構成とイソスタシー　長岡半太郎

追加

1. 油壺に於ける海水面の永年變化に就いて　山口生知
2. 岡山、香川、高知、德島、兵庫、大阪、奈良、和歌山、三重諸府縣踏査報告　河角廣、佐藤泰夫

第231回談話會（昭和22年2月18日）

1. 南海地震に伴ふ道後温泉の變化　武者力、今村常次
2. 兵庫縣（特に淡路島）における南海地震の被害　宮村攝三、増田秀夫、佐久間修三
3. 和歌山縣御坊町附近及び切目村における南海地震の震害　宮村攝三、秋間哲夫
4. 大阪府、岐阜縣における南海地震の被害　秋間哲夫
5. 昭和21年南海地震について和歌山縣下數個所における調査　岸上冬彦、池上良平
6. 南海地震に就て（第二報）　河角廣、佐藤泰夫
7. 南海地震災害調査報告補遺　金井清、田中貞二郎、鈴木富三、金子重彦
8. 和歌山縣由良灣附近における津浪狀況　宮村攝三、秋間哲夫、宮崎務
9. 南海大地震報告（1）　那須信治、白井俊明、大島正治、内田秋三
10. 南海地震に伴つた津浪の調査報告（其の一、和歌山縣の部）　高橋龍太郎
11. 津浪の流速について　同
12. 南海地震と日本島の列綽　長岡半太郎

13. 日本沿岸の深溝とイソツタシー（第二）　長岡半太郎
14. 昭和21年南海地震の本郷における觀測結果　岸上冬彦
15. 南海地震の餘震（德島縣及び高知縣に於ける出張觀測）其の一　村山必典／田重平／萩原尊禮
16. 微動計による南海地震の餘震觀測（概報）　水上武／宮村攝三／佐久間修
17. 南海地震後德島縣富岡町に於いて行つた地電流の觀測　力武常次／山田重平
18. 室戸岬に於ける水管傾斜計觀測　萩原尊禮／山田重平
19. 震度に及ぼす表面層の影響　高橋龍太郎
20. 鐵筋コンクリート實在建物の振動實驗結果　金井清／田中貞二／鈴木富三郎／金子重彦

第232回談話會（昭和22年3月18日）

1. 波江野地震計の特性（其の一）　早川正巳／森喜夫
（萩原所員紹介）
2. 地震探鑛に於ける三次元問題（其の一）　立石哲夫／早川正巳
（萩原所員紹介）
3. 日立鑛山に於ける電氣探鑛（第三報）　岸上冬彦／增田秀夫
4. 地球内部の電氣的性質（其の二）磁氣嵐の急始に依る考察　力武常次
5. 月の地球より分離により生したる東半球に於る大陸の偏在　長岡半太郎
6. 地震波速度の時間的變化（南海道地震の場合）　早川正巳
（萩原所員紹介）
7. 南海地震に伴ふ道後温泉の變化（補遺）　力武常次
8. 南海地震に關する四國沿岸の調査　表俊一郎
9. 津波の局部的現象について　那須信治
10. 海底の變動に因る津波の生成（第三報）　高橋龍太郎

第233回談話會（昭和22年4月15日）

1. 東滿の臺地玄武岩（Plateau basalt）について　久野久
2. 地球内部の電氣的性質（其の四）再び磁氣嵐の急始に依る考察に就て　力武常次
3. 地形變動の時間的經過に關する一考察　表俊一郎
4. ゴンドワナ大陸の崩壞と其周邊の變化　長岡半太郎
5. 高知縣における震害と地盤（其の一）主として濱堤上の街村について　宮村攝三／西條八束／貝塚爽平

6. 四國及び紀伊半島水準檢測結果　　內務省地理調査所

7. 南海地震前後に於ける室戸岬の傾斜變動　　永田武・岡田恒

8. 室戸岬における土地傾斜變化（水管傾斜計とシリカ傾斜計による比較觀測）　　萩原尊禮・中村宇之助・渡邊政雄

9. 高知縣須崎町に於ける津浪について　　高橋龍太郎・相田勇

第234回談話會（昭和22年5月20日）

1. 南海地震の餘震に就て　第一報　　淺田敏・鈴木次郎

（永田武氏紹介）

2. 南海地震の餘震觀測（續報）　　村内必典・山田重平

3. 南海大地震に依る地盤の昇降に就いて　　小向良七

4. 南海地震による地盤變化とその後の經過に就いて（第一報）　　河角廣・佐藤泰夫

5. 南海地震による須崎灣周邊及び高知市附近の地盤沈下　　河角廣・佐藤泰夫

6. 室戸岬における地表傾斜變化の觀測（續報）　　萩原尊禮・渡邊政雄

7. 南海大地震に依る津浪に就いて　　松崎卓一

8. 檢潮儀の記錄より求められる津浪の浪源の問題に就いて　　表俊一郎

9. 高知縣新宇佐町に於ける津浪の調査報告　　高橋龍太郎・相田勇・羽鳥德太郎

10. 南海地震津浪觀測資料　　河角廣・佐藤泰夫

11. 南海地震に於ける震度と震害　　同上

12. 高知縣における震害（其の二）　　森本良平・宮村攝三・西條八束・貝塚爽平

13. 餘震の地震動から觀た高知市內の地盤の震動性能　　水上武・佐久間修三

14. 高知縣中村町に於ける彈性波地下探査結果　　田中貞二・鈴木富三郎・金子重彦

15. 高知縣中村町に於ける地盤と震害との關係　　金井清

追　加

1. 南海地震に際しての角柱顚倒に對する考察　　池上良平・岸上冬彦

2. 高知縣須崎町に於ける驗潮儀による地盤沈下の測定豫報　　岸上冬彦

第235回談話會（昭和22年6月17日）

1. 往復機關による地盤震動防止についての一考察　　相田勇

2. 非常に厚い軟弱地盤に於ける地震動の卓越周期について　　高橋龍太郎

3. 能生谷村及び根知村地辷踏査報告　佐久間修三
4. ゴンドヮナの崩壊は火山噴火による間接の證明と中生代の氣候に就き　長岡半太郎
5. 南海地震に際しての角柱顚倒に對する考察（補遺）　池上良平・岸上冬彦
6. 地形的に見た四國足摺半島の動き　貝塚爽平
（森本所員紹介）
7. 南海地震に伴つた地殻變動について　永田武
8. 德島縣椿泊灣の津浪　力武常次・村内必典
9. 高知縣浦戸・種崎・久禮に於ける津波の狀況　那須信治・白井俊明・川島正治

第236回談話會（昭和22年7月15日）

1. 地震波速度の時間的變化　早川正巳
2. 地震探鑛に於ける火藥爆發の際の彈性波發生の有樣　早川正巳
3. 新發田附近で行つた地震探鑛　表俊一郎・山崎良雄
4. 南北アメリカの移動と大西洋の隆起　長岡半太郎
5. 海水面變化と地震との關係　山口生和
6. 地震にともなう諸現象の研究(1)地なりの方向性　佐藤泰夫
7. 地球内部の電氣的性質（其の五）地磁氣灣型變化に依る考察　力武常次
8. 半無限體上の表面層に於ける固體粘性と振動變位との關係　金井清
9. 堤の破壞について　那須信治
追加
1. 三河地震による三河灣海底沈下調査報告　水路部中山技官
2. 淺間山の近況に就いて　水上武・内堀貞雄

第237回談話會（昭和22年9月16日）

1. 地震による建物の損傷について（第二報）　金井清
2. 地球内部の電氣的性質（其の六）太陽面爆發に伴う地磁氣變化に依る考察および諸結果の比較檢討　力武常次
3. 四國足摺岬の花崗岩類について　森本良平
4. 櫻島の新噴出熔岩について　森本良平
5. 最近の淺間山の活動　水上武・佐久間修三・内堀貞雄
6. 北米の移動　長岡半太郎
7. 南北アメリカの間接なる移動證明　長岡半太郎
8. 水準改測によつて知られた日本の水準變化　宮部直巳

9. 東京における地盤沈下の研究（第八報）　宮部直巳
10. 新潟市沿岸の汀線移動と地盤沈降　河角廣
11. 富士山山麓に於ける地表傾斜の研究（昭和二十二年の水準測量）　萩原尊禮・表俊一郎・村内必典
12. 平均海水面變化と地震との關係（補遺）　山口生知

第238回談話會（昭和22年10月21日）

1. 堆積岩の內部構造の解析の可能性に就いて　村井勇（大塚所員紹介）
2. 岩手縣鉛・大澤・志戸平溫泉群の化學成分に就いて　野口喜三雄
3. 地震前後に於ける平均海水面變化に就いて　山口生知
4. 地質時代ゲオイドの形狀變化に依り生じたる裂罅と地震圈　長岡半太郎
5. 地震による建物の損傷について　金井清
6. 三河國西尾町附近に於ける脈動の比較觀測　岸上冬彥・宮村攝三・池上良平
7. 地震にともなう諸現象の研究　2. 地面の波狀運動に對する光學的說明の可能性　佐藤泰夫
8. 地震活動に就いて　坪井忠二

第239回談話會（昭和22年11月18日）

1. 岩手縣豐澤河水の增水に依る化學組成の變化　野口喜三雄
2. 地震による建物の損傷について（第四報）　金井清
3. 潮汐短期調和分解法について　河角廣・佐藤泰夫・關根彰
4. サンフランシスコ大地震、關東大地震、富士山の隆起、明の嘉靖三十四年黃河渭水合流點の大地震、其他の起因　長岡半太郎
5. 南海大地震の走時曲線と震原　吉山良一（河角所員紹介）
6. 南海地震餘震觀測（其の三）四國東部の地下構造　村內必典
7. 水管傾斜計遠隔測定裝置　力武常次・山田重平・萩原尊禮

第240回談話會（昭和22年12月16日）

1. 日立鑛山における電氣探鑛（第四報）　岸上冬彥・增田秀夫
2. 演算子法によつて解いた構造物の振動問題（補遺）　金井清
3. 木造家屋及び土藏の震害に關する二、三の統計　河角廣・佐藤泰夫
4. 地球內部の電氣的性質（其の七）電氣傳導度分布の第二近似　力武常次
5. 南北緯35°及び赤道附近の地震　長岡半太郎

6. 積分 $\int_a^b G(f) \begin{matrix}\cos\\ \sin\end{matrix} fx\, df$ の漸近展開　　佐藤泰夫

7. 表面層がある場合の彈性波の發生について　　佐藤泰夫

8. 重力の式　　坪井忠二・島津康男

追　加

1. 紀州沖地震の震源地附近の測深成果　　水路部千野技官

—— 終　り ——

BULLETIN
OF THE
EARTHQUAKE RESEARCH INSTITUTE
TOKYO UNIVERSITY

VOL. XXV

1947

東京大學
地震研究所彙報

第 25 號

昭和 22 年

Contents.

Vol. XXV.

Parts 1–4. January—December, 1947.

		Page
1.	R. TAKAHASI, Motion of the Bay Water caused by Seismic Sea Waves. (in English)	1
2.	R. TAKAHASI, On Seismic Sea Waves caused by Deformations of the Sea Bottom. The 3rd Report. The One-demensional Source. (in English)	5
3.	T. RIKITAKE, A Method for Studying the Relations between the Changes in Geomagnetism and Earth Current. (in English)	9
4.	S. OMOTE, On the Central Area of Seismic Sea Waves. (in English)	15
5.	T. RIKITAKE and S. MURAUCHI, Tsunami in Tsubaki-tomari Bay. (in English)	21
6.	T. HAGIWARA, Observation of Changes in the Inclination of the Earth's Surface at Mt. Tsukuba (Third Report). (in English)	27
7.	R. MORIMOTO, On the Modes of Occurrence of Cordierite from Sakkabira, Town Taru-mizu, Kimotsuki Province, Kagoshima Prefecture, Japan. (in English)	33
8.	Y. SATO, Possibility of Optical Explanation of Visible Wave-motion of Ground. (in English)	37
9.	F. KISHINOUYE and R. IKEGAMI, A Study of Microseisms after A. W. Lee's Method. (in English)	43
10.	R. IKEGAMI and F. KISHINOUYE, A Study on the Overturning of a Rectangular Columns in the Case of the Nankai Earthquake on December 21, 1946. (in English)	49
11.	N. NASU, Strong Motion Vibrograph. (in English)	57
12.	K. KANAI, On the Damages to Buildings due to Earthquakes. (in English)	61
13.	T. MINAKAMI, Recent Activities of Volcano Usu (I). (in English)	65
14.	T. MINAKAMI, Recent Activities of Volcano Usu (II). (in English)	71
15.	S. SAKUMA, Land-slides at Nodani and Nechj 1947. (in English)	77
16.	N. NASU and T. SHIRAI, Local Phenomena of Tsunami (Part 1) (in English)	81
17.	T. NAGATA and A. OKADA, Land Deformation of Muroto Point before and after the Nankaido Great Earthquake on Dec. 21, 1946. (in English)	85

目　次

第 25 號

第1～4册 (昭和22年1～12月)

目　次

論文及報告　　頁

1. 津浪による灣水の振動(英文) ……高橋龍太郎 1
2. 海底の變動に因る津浪の成生(第三報)一次元的浪源(英文)…高橋龍太郎 5
3. 地磁氣および地電流變化の關係を論ずる一方法(英文)……力武常次 9
4. 津浪の浪源について(英文)……表俊一郎 15
5. 德島縣椿泊灣の津浪(英文)……力武常次・村内必典 21
6. 筑波山に於ける土地傾斜變化の觀測(其の三)(英文)……萩原尊禮 27
7. 鹿兒島縣肝屬郡垂水町唉花平產蛍青石の產出狀態(英文)……森本良平 33
8. 地面の波狀運動に對する光學的說明の可能性(英文)……佐藤泰夫 37
9. A. W. Lee の方法による脈動の研究(英文)……岸上冬彥・池上良平 43
10. 1946年12月12日南海地震に際しての角柱轉倒の研究(英文)……池上良平・岸上冬彥 49
11. 强振動計(英文)……那須信治 57
12. 地震による建物の損傷について(英文)……金井清 61
13. 有珠火山の最近の活動(I)(英文)……水上武 65
14. 有珠火山の最近の活動(II)(英文)……水上武 71
15. 1947年の能生谷村及び根知村の地辷り(英文)……佐久間修三 77
16. 津浪の局部的現象(其一)(英文)……那須信治・白井俊明 81
17. 南海道大地震前後における室戸岬の地殼變動(英文)……永田武・岡田悖 85

所　報

Index to Vol. XXV.

Page

HAGIWARA, T., (6) Observation of Changes in the Inclination of the Earth's Surface at Mt. Tsukuba (Third Report). (in English) 27

IKEGAMI, R. and KISHINOUYE, F., (9) A Study of Microseisms after A. W. Lee's Method. (in English) 43

IKEGAMI, R. and KISHINOUYE, F., (10) A Study on the Overturning of Rectangular Columns in the case of the Nankai Earthquake on December 21, 1946. (in English) 49

KANAI, K., (12) On the Damages to Buildings due to Earthquakes. (in English) 61

KISHINOUYE, F. and IKEGAMI, R., (9) A Study of Microseisms after A. W. Lee's Method, (in English) 43

KISHINOUYE, F. and IKEGAMI, R., (10) A Study on the Overturning of Rectangular Columns in the case of the Nankai Earthquake on December 21, 1946. (in English) 49

MINAKAMI, T., (13) Recent Activities of Volcano Usu (I). (in English) 65

MINAKAMI. T., (14) Recent Activities of Volcano Usu (II). (in English) 71

MORIMOTO, R., (7) On the Modes of Occurrence of Cordierite from Sakkabira, Town Taru-mizu, Kimotsuki Province, Kagoshima Prefecture, Japan. (in English) 33

MURAUCHI, S. and RIKITAKE, T., (5) Tsunami in Tsubakitomari Bay, (in English) 21

NAGATA, T. and OKADA, A., (17) Land Deformation of Muroto Point before and after the Nankaido Great Earthquake on Dec. 21, 1946. (in English) 85

NASU, N., (11) Strong Motion Vibrograph. (in English). 57

NASU, N. and SHIRAI, T., (16) Local Phenomena of Tsunami (Part 1). (in English) 81

OKADA, A. and NAGATA, T., (17) Land Deformation of Muroto Point before and after the Nankaido Great Earthquake on Dec. 21, 1946. (in English) 85

OMOTE, S., (4) On the Central Area of Seismic Sea Waves. (in English)

RIKITAKE, T., (3) A Method for Studying the Relations between the Changes in Geomagnetism and Earth Current. (in English) . . 9

RIKITAKE, T. and MURAUCHI, S., (5) Tsunami in Tsubakitomari Bay. (in English) 21

SAKUMA, S., (15) Landslides at Nōdani and Nechi in 1947. (in English) 77

SATO, Y., (8) Possibility of Optical Explanation of Visible Wave-motion of Ground. (in English) 37

SHIRAI, T. and NASU, N., (16) Local Phenomena of Tsunami (Part 1). (in English) 81

TAKAHASI, R., (1) Motion of the Bay Water caused by Seismic Sea Waves. (in English) 1

TAKAHASI, R., (2) On Seismic Sea Waves caused by Deformations of the Sea Bottom. The 3rd Report. The One-dimensional Source. (in English) 5

第 24 號 索 引

頁

萩原尊禮 (6) 筑波山に於ける土地傾斜變化の觀測(其の三)(英文)… ……27

池上良平・岸上冬彦 (9) A. W. Lee の方法による脈動の研究(英文)……43

池上良平・岸上冬彦 (10) 1946年 2月12日南海地震に際しての角柱轉倒の研究(英文)……49

金井 清 (12) 地震による建物の損傷について(英文)……61

岸上冬彦・池上良平 (9) A. W. Lee の方法による脈動の研究(英文)……43

岸上冬彦・池上良平 (10) 1946年12月21日南海地震に際しての角柱轉倒の研究(英文)……49

水上 武 (13) 有珠火山の最近の活動(I)(英文)……65

水上 武 (14) 有珠火山の最近の活動(II)(英文)……71

森本良平 (7) 鹿兒島縣肝屬郡垂水町唉花平產蛍青石の產出狀態(英文)……33

村內必典・力武常次 (5) 德島縣椿泊灣の津浪(英文)……21

永田 武・岡田 惇 (17) 南海道大地震前後における室戸岬の地殼變動(英文)……85

那須信治 (11) 强振動計(英文)……57

那須信治・白井俊明 (16) 津浪の局部的現象(其一)(英文)……81

岡田 惇・永田 武 (17) 南海道大地震前後における室戸岬の地殼變動(英文)……85

表 俊一郎 (4) 津浪の浪源について(英文)……12

力武常次 (3) 地磁氣および地電流變化の關係を論ずる一方法(英文)…… 9

力武常次・村內必典 (5) 德島縣椿泊灣の津浪(英文)……21

佐久間修三 (15) 1947年の能生谷村及び根知村の地辷り(英文)……77

佐藤泰夫 (8) 地面の波狀運動に對する光學的說明の可能性(英文)……37

白井俊明・那須信治 (16) 津浪の局部的現象(其一)……81

高橋龍太郎 (1) 津浪による灣水の振動(英文)…… 1

高橋龍太郎 (2) 海底の變動に因る津浪の成生(第三報)一次元的浪源(英文)… 5

(終 り)

昭和24年3月10日印刷
昭和24年3月15日發行

編輯兼發行者　東京大學地震研究所

東京都中央區木挽町四丁目二番地
印刷者　小澤鐵太郎

東京都中央區木挽町四丁目二番地
印刷所　京屋出版印刷株式會社

岩波書店
東京都千代田區神田一ツ橋通町
賣捌所

丸善株式會社
東京都中央區日本橋通二丁目

Sold by

MARUZEN Co. Ltd.,

Chūō-ku, Nihonbasi, Tôkyô.

Price of this copy ; 314.87 Yen. (Postage exclusive.)

BULLETIN OF
THE EARTHQUAKE RESEARCH INSTITUTE
TOKYO UNIVERSITY

Vol. XXV, Parts 1—4. Jan.—Dec., 1947.

Contents.

Papers and Reports. Page

1. R. TAKAHASI, Motion of the Bay Water caused by Seismic Sea Waves. (in English) 1
2. R. TAKAHASI, On Seismic Sea Waves caused by Deformations of the Sea Bottom. The 3rd Report. The One-dimensional Source. (in English) 5
3. T. RIKITAKE, A Method for Studying the Relations between the Changes in Geomagnetism and Earth Current. (in English). 9
4. S. OMOTE, On the Central Area of Seismic Sea Waves. (in English) 15
5. T. RIKITAKE and S. MURAUCHI, Tsunami in Tsubaki-tomari Bay. (in English). 21
6. T. HAGIWARA, Observation of Changes in the Inclination of the Earth's Surface at Mt. Tsukuba (Third Report). (in English) 27
7. R. MORIMOTO, On the Modes of Occurrence of Cordierite from Sakkabira, Town Taru-mizu Kimotsuki Province, Kagoshima Prefecture, Japan. (in English) 33
8. Y. SATO, Possibility of Optical Explanation of Visible Wave-motion of Ground. (in English) 37
9. F. KISHINOUYE and R. IKEGAMI, A Study of Microseisms after A. W. Lee's Method. (in English) 43
10. R. IKEGAMI and F. KISHINOUYE, A Study on the Overturning of a Rectangular Columns in the Case of the Nankai Earthquake on December 21, 1946. (in English). 49
11. N. NASU, Strong Motion Vibrograph. (in English) 57
12. K. KANAI, On the Damages to Buildings due to Earthquakes. (in English). 61
13. T. MINAKAMI, Recent Activities of Volcano Usu (I). (in English) 65
14. T. MINAKAMI, Recent Activities of Volcano Usu (II). (in English) 71
15. S. SAKUMA, Land-slides at Nōdani and Nechi in 1947. (in English) 77
16. N. NASU and T. SHIRAI, Local Phenomena of Tsunami (Part 1) (in English). 81
17. T. NAGATA and A. OKADA, Land Deformation of Muroto Point before and after the Nankaido Great Earthquake on Dec. 21, 1946. (in English) 87

Institute Notes.